NASA-CR-54115

TWO STAGE POTASSIUM TEST TURBINE

QUARTERLY PROGRESS REPORT NO. 12
For Period : February 9, 1964 Thru May 8, 1964

EDITED BY E. SCHNETZER

prepared for
NATIONAL AERONAUTICS AND SPACE ADMINISTRATION
CONTRACT NAS 5-1143

SPACE POWER AND PROPULSION SECTION
MISSILE AND SPACE DIVISION
GENERAL ELECTRIC
CINCINNATI 15, OHIO

Requests for copies of this report should be referred to:

National Aeronautics and Space Administration
Office of Scientific and Technical Information
Washington 25, D.C.
Attention: AFSS-A

TWO STAGE POTASSIUM TEST TURBINE

QUARTERLY PROGRESS REPORT NO. 12

Covering the Period
February 8, 1964 through May 8, 1964

Edited By
E. Schnetzer, Manager
Development Engineering

NATIONAL AERONAUTICS AND SPACE ADMINISTRATION

Contract NAS 5-1143

Technical Management
NASA - Lewis Research Center
Nuclear Power Technology Branch
Joseph P. Joyce, Technical Manager

SPACE POWER AND PROPULSION SECTION
RE-ENTRY SYSTEMS DEPARTMENT
MISSILE AND SPACE DIVISION
GENERAL ELECTRIC COMPANY
CINCINNATI 15, OHIO
45215

TABLE OF CONTENTS

		Page No.
I.	SUMMARY, SCHEDULE AND FORECAST, by E. Schnetzer	1
II.	FLUID DYNAMIC TESTING, by R. J. Rossbach	6
	Turbine Test Preparation	6
	Converging-Diverging Nozzle Data Evaluation	17
III.	MECHANICAL DESIGN AND TESTING, by H. E. Nichols	24
	Pre-Potassium Test Turbine Check-Out	24
	Component Fabrication	25
	Experimental Casing	26
	Welded Turbine Casing	27
	Installation of Potassium Drain Manifold	28
	Leak Checking of the Turbine and Manifold	29
	Initial Turbine Run-Up	29
	Welding of the Turbine into the Facility	30
	Final Test Preparations	31
	Turbine Tare Loss Test	32
	Seal Malfunction	35
	Hydrodynamic Seal Test	36
IV.	3000 KW FACILITY, by S. E. Eckard	40
	Turbine Test Preparations	40
	Turbine Checkout Testing	44
V.	MATERIALS SUPPORT, by W. F. Zimmerman	47

TABLE OF CONTENTS

	Page No.
Metallurgical Evaluations of Pretest Buckets	47
Chemical Evaluation of Lube Oil	48
TABLES	53
FIGURES	69
APPENDIX A	133

LIST OF TABLES

Table Number		Page No.
I	Two-Stage Potassium Turbine Test Instrumentation	53
II	Turbine Test Conditions	59
III	Average Values of Effective Flow Area for Air	64
IV	Averaged Values of Converging-Diverging Nozzle Test Potassium Data and Probable Errors	65
V	Practice Casing, Internal Measurements	67
VI	Summary of Hydrodynamic Seal Tests in Air and Water	68

LIST OF FIGURES

Figure No.		Page No.
1	Program Schedule	69
2	Instrumentation Stations	70
3	Potassium Test Turbine Instrumentation Location	71
4	Potassium Test Turbine Instrumentation Location	72
5a	Average Inlet to Throat Polytropic Exponent Versus Inlet Quality. Inlet Throat Temperature, 1450°F.	73
5b	Average Inlet to Throat Polytropic Exponent Versus Inlet Quality. Inlet Total Temperature, 1500°F.	74
5c	Average Inlet to Throat Polytropic Exponent Versus Inlet Quality. Inlet Total Temperature, 1580°F.	75
6a	C-D Nozzle Critical Flow Versus Inlet Total Pressure. Inlet Quality, 99%.	76
6b	C-D Nozzle Critical Flow Versus Inlet Total Pressure. Inlet Quality, 95%.	77
6c	C-D Nozzle Critical Flow Versus Inlet Total Pressure. Inlet Quality, 90%.	78
6d	C-D Nozzle Critical Flow Versus Inlet Total Pressure. Inlet Quality, 85%.	79
7a	Electromagnetic Flowmeter Flow Versus Inlet Total Pressure. Inlet Quality, 99%.	80
7b	Electromagnetic Flowmeter Flow Versus Inlet Total Pressure. Inlet Quality, 95%.	81

LIST OF FIGURES (Continued)

Figure No.		Page No.
7c	Electromagnetic Flowmeter Flow Versus Inlet Total Pressure. Inlet Quality, 90%.	82
7d	Electromagnetic Flowmeter Flow Versus Inlet Total Pressure. Inlet Quality, 85%.	83
8a	Comparison of EMFM Flow and C-D Nozzle Critical Flow. Inlet Quality, 99%.	84
8b	Comparison of EMFM and C-D Nozzle Critical Flow. Inlet Quality, 95%.	85
8c	Comparison of EMFM Flow and C-D Nozzle Critical Flow. Inlet Quality, 90%.	86
8d	Comparison of EMFM Flow and C-D Nozzle Critical Flow. Inlet Quality, 85%.	87
9a	Variation of Average Inlet to Throat Polytropic Exponent with Static to Total Pressure Ratio	88
9b	Variation of Average Inlet to Throat Polytropic Exponent with Static to Total Pressure Ratio	89
10	Turbine Seen Installed in the Glove Box, for Pre-Potassium Check-Out Test.	90
11	Turbine Test Equipment and Instrumentation Installed in the Potassium Test Facility.	91
12	Stator Assembly with Thermocouple Wells Installed.	92
13	Outlet Guide Vane-Casing Assembly with Welded Pressure Taps Installed.	93
14	Casing Assembly with Welded Pressure Taps	94
15	Turbine Inlet Duct with Weld-Flange Blanks Attached.	95

LIST OF FIGURES (Continued)

Figure No.		Page No.
16	Turbine Inlet Duct with Machined Flanges and Welded Instrumentation Tubing.	96
17	Internal Diameter Measurements on Practice Weld Turbine Casing.	97
18	Turbine, Casing, Welding Sequence.	98
19	Turbine After Assembly.	99
20	View Looking Aft of Turbine After Being Welded into the 3000 KW Facility.	100
21	View Looking Forward of Turbine After Being Welded into the 3000 KW Facility.	101
22	View Looking Aft of Completed Turbine Installation.	102
23	View Looking Forward of Completed Turbine Installation.	103
24	Pad Bearing and Lube Oil Temperature During Mechanical Check-Out Test.	104
25	Torque Versus Speed for Various Values of Loop Pressure.	105
26	Hydrodynamic Seal Power Consumption Using Potassium as the Sealant.	106
27	Pad Bearing and Lube Oil Temperature During Turbine Tare Loss Tests.	107
28	Argon Temperature into Buffer Seal During Turbine Tare Loss Tests.	108
29	Assembly Drawing of the Two-Stage Turbine	109

LIST OF FIGURES (Continued)

Figure No.		Page No.
30	Original and Modified Assembly of the Lube Oil Seal Ring.	110
31	Hydrodynamic Seal Test Set-Up.	111
32	Sketch of Turbine Seal Assembly.	112
33	Turbine Seal Characteristics with All Flow Through Screw Seal. Rotative Speed, 5000 rpm, Water Flow, Zero.	113
34	Turbine Seal Characteristics Showing Argon-to-oil Sealing Capacity of Buffer Seal. Rotative Speed, 5000 rpm, Water Flow, Zero.	114
35	Turbine Seal Characteristics with Reduced Water Sump Manifold Pressure, Rotative Speed, 5000 rpm, Water Flow, Zero.	115
36	Turbine Seal Characteristics Showing Seal Cavity Pressure with Water Sump Outlet Manifold Pressure Relationship. Rotative Speed, 5000 rpm Water Flow, 8.5 ppm.	116
37	Turbine Seal Characteristics of the Seal Cavity Pressures and Water Sump Outlet Manifold. Rotative Speed, 5000 rpm, Water Flow, 13.5 ppm.	117
38	Turbine Seal Characteristics of the Seal Cavity and Water Sump Outlet Manifold Pressures. Rotative Speed, 5000 rpm, Water Flow, 16.2 ppm.	118
39	Hydrodynamic Seal Loop.	119
40	Potassium Turbine Main Lube System.	120
41	Starter Turbine and Water Brake Lube System.	121

LIST OF FIGURES (Continued)

Figure No.		Page No.
42	Control Panel.	122
43	Control Panel.	123
44	Turbine Installation.	124
45	Dynamometer Equipment Assembly	125
46	Dynamometer Equipment Assembly	126
47	Dynamometer Equipment Assembly	127
48	Dynamometer Equipment Assembly	128
49	View of the Assembled First and Second Stage Rotor Buckets.	129
50	Cold Flow Stage 3 Turbine Buckets Compared to Unused Buckets to Show Surface Pitting and Other Damage.	130
51	Comparison of the Specific Gravity of Lube Oil and Potassium as a Function of Temperature.	131

I. SUMMARY

The Re-Entry System Department of the General Electric Company has been under contract to the National Aeronautics and Space Administration since May 8, 1961, for the design and fabrication of a two-stage test turbine suitable for operation in saturated potassium vapor at 1600°F. The test turbine consists of stages three and four of a five-stage 500 KW turbine and is to have a design flow capacity of 2.8 pounds per second. The present sixteen-month phase of the contract covers assembly, test, and evaluation for the turbine and associated components.

The main objectives of this program are to study the effects of vapor wetness on performance, to study impingement damage and washing erosion with different blade materials, to study the phenomena of super-saturation and droplet formation, to establish the values of the polytropic exponent of potassium vapor as an improvement over General Electric's calculated Mollier diagrams, and finally, to establish accurate fluid flow design methods for potassium turbines operating in the wet vapor region. In addition an objective was to demonstrate interstage condensate extraction in steam. The test turbine runs on oil lubricated bearings. The test program anticipates 200 hours of performance testing, 1,000 hours endurance testing under design conditions at 19,200 rpm, and 1000 hours endurance testing under aggravated erosive conditions at 23,000 rpm.

The present report covers progress during the quarter ending May 8, 1964. The main events of this reporting period are:

Fluid Dynamic Testing

Turbine potassium test preparations during the quarter included the completion of the performance test plan including tolerances on test control variables, the check out of all data handling and reducing procedures and the completion of procedures for potassium performance prediction.

During the past quarter, evaluation of the converging-diverging nozzle data in potassium continued. The overall polytropic exponents between inlet and the throat were improved, resulting in trends with vapor quality which will be used in performance prediction and data evaluation. The potassium vapor mass flow values as measured with the facility electromagnetic flowmeter were composed with the critical mass flow values calculated from the average polytropic exponents. The variation in average polytropic exponent along the nozzle was also computed.

Mechanical Design and Testing

During the quarter the turbine, less the nozzle diaphragms and casing, was run up and then assembled for test. The assembly required welding of the casing and the bearing housing flanges in a carefully controlled

process which was developed with an experimental casing. Before welding the turbine into the facility, it was clamped in place and run up again to demonstrate that welding had not distorted the casing causing a rub. Next the turbine was welded into the facility and all final preparations for testing were completed. Turbine tare losses to establish the bearing and seal losses on the turbine shaft were carried out with the hydrodynamic seal operative. A scheduled shut down was carried out after this test. Attempts to restart the turbine failed because lube oil had entered the potassium seal loop. The quarter ended with the initiation of parallel programs to establish the cause of the oil leak. One program involved a modification of a shaft seal and the other, model testing in air and water.

3000 KW Facility

During the early part of this quarter, a General Electric Company sub-contractor completed all modifications and additions to the 3000 KW facility. The turbine bearing housing and support and the rotating parts of the turbine were installed and turbine auxiliary systems were checked and modified as required. The turbine was removed and reinstalled in the facility with the casing welded together. A rotating test to 17,000 rpm established that the casing had not distorted during welding. Then the turbine inlet and exit piping was welded into the facility. Hot flushing and hot trapping in the facility followed. A torque tare test on the turbine

resulted in small amounts of oil and potassium entering the slinger seal loop and lube system, respectively. The two affected subsystems were opened and cleaned. The facility is ready to proceed with testing.

Materials Support

The U-700 buckets for both stages of the turbine utilized during pretesting with air and steam were examined both metallographically and by hardness survey. The results of the examination revealed that all but three buckets are metallurgically suitable for further testing in potassium vapor and they are being held in reserve for endurance testing. The three rejected buckets can be replaced by available spares.

Subsequent to the leakage of lube oil into the slinger seal loop, an investigation was made to compare the degree of reaction of several lubricating oils with potassium as a function of temperature. The present oil, Mobil Oil Company, DTE 797, a mineral oil, was included and no reason for changing to a different oil was found.

Forecast

In Figure 1, the program schedule, the current turbine program status and future work to be completed is delineated.

In the fluid dynamics, the predicted performance of the two-stage turbine in terms of performance parameters corrected to design conditions will be completed for all data points in the test plan. Using the air-water

test data presented herein, analyses of the two-stage turbine seal will be carried out in an effort to identify the cause of the lube oil leak.

In mechanical design the turbine will be reassembled and run without the hydrodynamic seal being operative in a parallel attempt to establish the reason for the oil leak. In addition, procurement efforts will continue on the second set of hardware.

II. FLUID DYNAMIC TESTING

During the last quarter the effort was divided between turbine potassium performance test preparations and converging-diverging nozzle data evaluation.

Turbine Test Preparation

In Table I, the scanning sequence for the digital data handling system which permanently records turbine performance data during testing and the performance instrumentation is presented with all 40 efflux pressures along with 49 other instrumentation readings which will be recorded during each digital data scan. Figures 2, 3, and 4 show the location of the turbine performance instrumentation. Several instrumentation readings will be recorded more than once during each scan in order to obtain average values of important variables. These variables are reference pressure, which periodically measures Station #1 total pressure throughout a digital data scan, speed, main electromagnetic flowmeter reading and temperature, spray electromagnetic flowmeter reading and temperature, test turbine and starter turbine torques, and condenser vapor static pressure.

Condenser liquid level which was previously to be read several times during a digital data scan in order to correct main electromagnetic flowmeter reading was deleted because the application of this correction to the converging-

diverging nozzle data increased data scatter. Investigation of the condenser liquid level measuring system revealed that the time response of this instrument is so slow that the digital data scan reads a value that does not correspond to the remainder of the data taken. Although deleted from the digital data scanning sequence, condenser liquid level will remain on a Sanborn recorder channel for the purpose of controlling the test. This control will be exercised by specifying that the liquid level be held constant for sufficient time to allow for the time response prior to taking data.

Four important variables to be used as parameters on plots of turbine performance are turbine inlet temperature, turbine total-to-static pressure ratio, inlet vapor quality and corrected speed. In order to reduce the apparent data scatter, these quantities must be held to close tolerances during testing. As a result, tolerances have been established for the test control variables and made part ot the test plan.

The turbine inlet temperature tolerance will be $\pm$ 5°F for 1600, 15500, and 1450°F inlet temperature. In the event this tolerance cannot be held for 1450°F, which converging-diverging (C-D) nozzle tests in potassium indicated, the inlet temperature level will be increased until this tolerance can be held. The inlet temperature will establish an inlet total pressure. The tolerance on pressure ratio varies from $\pm$ 4.5 to 5.0 percent, permitting bounding values of turbine exit pressure to be calculated

in the control room. The tolerance on turbine rotative speed has been established at $\pm$ 200 rpm. Instead of specifying the tolerance on spray flowrate, which depends upon turbine vapor flow, electromagnetic flowmeter temperatures and spray liquid temperature for a given vapor quality, the spray flow will be determined using a prepared chart which incorporates compensations for these variables.

The above tolerances were established after giving consideration to the readability of the Sanborn recorders on which the control variables will be recorded, tolerances that could be held for the C-D nozzle tests and, in the case of speed, the tolerance that could be held in the steam pre-tests. In addition, consideration was given to the effect that errors in the four control variables would have on the value of efficiency. The observance of the tolerances delineated above will assure minimum data scatter due to variables that are to be used as plotting parameters deviating from the nominal values.

In Table II, the new test points are presented with tolerances on the control variables included. Testing will begin at 1450°F inlet temperature or increased until the $\pm$ 5°F tolerance can be held instead of 1400°F as specified in the previous test plan since the boiler was found to be somewhat unstable at 1400°F and 1450°F. The new test point schedule also includes a reduced number of low-quality points for inlet temperatures of 1450°F and

1550°F and no moisture extraction testing. Changes have also been made in the test values of rotative speed such that the following values of percent corrected speed can be obtained: 80, 90, 95, 100, 110, 120.

During the performance testing of the two-stage turbine in potassium, data will be recorded by means of the digital data handling system. This system records the 151 required bits of performance data from various sensors throughout the turbine and facility on a punched tape. Two means are provided for converting punched tape to digital computer input, namely a tape-to-card converter and the GE 225 computer which produces either punched cards or magnetic tape. Data reduction is to be accomplished on a specially prepared data reduction program.

This data reduction program accomplishes two specific tasks, namely, conversion of raw data to engineering units and the calculation of various performance parameters defined on page 14. The program is composed of 12 subroutines to facilitate program changes brought to light by use. It utilizes Battelle Memorial Institute (BMI) thermodynamic properties of potassium and incorporates calibration curves for the various instruments.

The data reduction procedure includes some time and space averages during each digital data scan along with some error detection methods to insure reliable data. Turbine inlet total pressure and temperature, inlet

total reference pressure, turbine rotative speed, water brake torque, starter turbine torque, main electromagnetic flowmeter reading and temperature, spray liquid electromagnetic flowmeter reading and temperature, and station 8 static pressure are reading more than once during each digital data scan and averaged. Error detection methods are incorporated in the program to reject erroneous data among various values to be averaged. Turbine inlet total average pressure, average reference total pressure, and the exit total pressure group average are compared with each individual respective group value. If each value is not within $\pm$ 7.0 psia of the average value, it is rejected and not included in the next averaging process which similarily rejects values within $\pm$ 2.0 psia before a final average is taken. For turbine inlet and exit, spray flowmeter, main flowmeter, and injector temperatures, a similar averaging process as used for inlet pressure averages is incorporated with $\pm$ 30°F and $\pm$ 10°F limits on respective temperature values before the final average is taken.

In the calculation procedure, Station #1 average total pressure is compared with the reference total pressure which is read periodically during each digital scan. If the reference pressure average is within $\pm$ 4.0 psia of the Station #1 average total pressure, it will be used to define the inlet pressure. If the average reference total pressure is not within

the 4.0 psia limit then the Station #1 average total pressure is used. This method will insure the deletion of reference pressure in the event it becomes plugged during testing.

Station #1 quality is determined from the inlet throttling calorimeter and is needed to accurately define turbine inlet conditions before liquid injection. The calorimeter temperature and pressure and the BMI superheated potassium properties permit Station #1 quality to be determined. However, if the condenser pressure is too high, the calorimeter will not give superheated conditions, as it should, because the calorimeter is vented to the condenser. In this event, an average inlet quality of .9925 obtained from the C-D nozzle tests in potassium is used. In order to determine which method is used to determine Station #1 quality, the calorimeter temperature is compared with the saturation temperature corresponding to the calorimeter pressure. If the calorimeter temperature is greater than the saturation temperature by 5.0°F, the inlet quality is calculated and if it is less than 5.0°F, the inlet quality is established as .9925, and Station #1 enthalpy is calculated using this quality.

Liquid injection rate and main flow rate are determined from the manufacturer flowmeter calibration curves which are included in the program. The calibration curves yield a gpm/mv value which can be converted to PPS since average flowmeter flow temperature, which defines liquid

density, and average flowmeter millivolt readings are known.

Since main and liquid injection flow, and liquid injection temperature are known, the turbine inlet enthalpy is found from a heat balance. (Symbols are listed in the Appendix A).

$$h_{m3} = \frac{W_{v1}h_1 + W_{12}h_{12}}{W_{12} + W_{v1}} \quad (1)$$

The turbine inlet quality is then found using BMI potassium properties as follows:

$$X_{t3} = \frac{h_{m3} - h_{s11}}{h_{fg1}} \quad (2)$$

The turbine specific work is calculated from the averaging torque reading plus the tare torque which is available in the program in the form of a table as a function of turbine speed. The turbine work is found as follows:

$$\Delta h_{act} = \frac{2\pi \bar{N} \bar{T}}{(7\,20)\, W_t J} \quad (3)$$

where average output torque and turbine flow are defined as

$$\bar{T} = \bar{T}_s + \bar{T}_m + \bar{T}_t \quad (4)$$

$$W_t = \bar{W}_m + \bar{W}_s - \bar{W}_c \quad (5)$$

The ideal enthalpy drop, needed for turbine efficiency, is determined from BMI "wet" properties. The efficiency, either total to total or total to static, is based on total turbine flow and is calculated as follows:

$$= \frac{h_{act}}{h_{ideal}} \tag{6}$$

The program then procedes to calculate corrected parameters, namely flow, speed, specific work, and power referenced to design inlet conditions of 1600°F, 92 percent quality and 19,200 rpm.

The corrected parameters are utilized for potassium vapor and based on dynamic similarity. It is assumed for dynamic similarity that the velocity diagrams normalized by the critical velocity of sound based on turbine inlet conditions correctly accounts for Mach number effect on losses and flow. The critical velocity of sound for a non-perfect gas is given by

$$a_{cr} = \frac{\sqrt{2 \gamma g P_t v_t}}{\gamma + 1} \tag{7}$$

For a perfect gas equation (7) becomes:

$$a_{cr} = \frac{\sqrt{2 \gamma g R T_t}}{\gamma + 1} \tag{8}$$

The substitution of equation (7) for equation (8) in Heaton et al* results in the following corrected parameters:

*Heaton, Thomas R.; Slivka, William R.; and Westra, Leonard F.: Cold-Air Investigation of a Turbine with Nontwisted Rotor Blades Suitable for Air Cooling. NACA RM E52A25, 1952.

Flow parameter:

$$W_c = W_t \frac{\left[\left(\frac{\gamma+1}{2}\right)^{\frac{\gamma+1}{\gamma-1}} v_t / P_t \gamma\right]^{1/2}_{\text{actual}}}{\left[\left(\frac{\gamma+1}{2}\right)^{\frac{\gamma+1}{\gamma-1}} v_t / P_t \gamma\right]^{1/2}_{\text{reference}}} \tag{9}$$

Speed parameter:

$$N_c = \bar{N} \frac{\left[\frac{\gamma+1}{\gamma} / P_t v_t\right]^{1/2}_{\text{actual}}}{\left[\frac{\gamma+1}{\gamma} / P_t v_t\right]^{1/2}_{\text{reference}}} \tag{10}$$

Specific work parameter:

$$\Delta h_c = \Delta h_{act} \frac{\left[\frac{\gamma+1}{\gamma} / P_t v_t\right]_{\text{actual}}}{\left[\frac{\gamma+1}{\gamma} / P_t v_t\right]_{\text{reference}}} \tag{11}$$

Horsepower parameter:

$$HP_c = 1.415 \ \Delta h_c W_c \tag{12}$$

Kilowatt parameter:

$$KW_c = 1.0555 \Delta h_c W_c \tag{13}$$

Values of polytropic exponent used in the corrected parameters were determined from the converging-diverging nozzle tests in potassium. Although no consistent correlation could be made with the experimental and BMI saturated polytropic exponents, a definite decreasing trend in polytropic exponent with vapor quality was noted. Using an average trend,

the inlet to throat average polytropic exponent for an inlet vapor quality, X, is found from equation (14) using a BMI saturated vapor polytropic exponent, γ_s, based on inlet total temperature.

$$\gamma = \gamma_s - 1.13\,(1-X) \tag{14}$$

The value -1.13 was found from the converging-diverging nozzle potassium test data.

The program continues by calculating individual stage hub and tip values of reaction and stage work split. Since the turbine inlet and exit total and static conditions are known (quality and enthalpy found from static and total pressures) and assuming a straight expansion line from inlet static and inlet total to exit static and exit total conditions respectively, the various interstage static enthalpies and qualities at hub and tip can be determined using geometric relationships and the static pressure values. The reaction at the hub of each stage is obtained from:

$$RX_1 = 1 - \frac{h_{m3} - h'_{s4}}{h_{m3} - h'_{s5}} \tag{15}$$

$$RX_2 = 1 - \frac{h_{t5} - h'_{s6}}{h_{t5} - h'_{s7}} \tag{16}$$

and the specific work for each stage is:

$$\Delta h_1 = h_{m3} - h_{t5} \tag{17}$$

$$\Delta h_2 = h_{t5} - h_{t7} \tag{18}$$

In order to obtain predicted performance for the two-stage potassium test turbine, an available combustion gas-turbine off-design computer program is being utilized. This program was modified slightly so as to incorporate reversion from supersaturated flow to equilibrium flow after each stage. Through the use of this program estimated turbine off-design performance will be obtained for all test conditions in the test plan. The results of this program are used as input for two other digital computer programs to obtain predicted values of torque, flow, efficiency, and the corrected parameters.

In the first program, turbine torque output and flow are determined. Turbine work is corrected for droplet drag losses which are determined by assuming that the moisture entering the stage must be accelerated to wheel speed upon entering the rotor. The calculation procedure used to determine droplet drag losses and turbine output torque are as follows:

$$\Delta h_d = \frac{(1-X_1)\, U_{p1}^2}{gJ} + \frac{(1-X_2)\, U_{p2}^2}{gJ} \qquad (19)$$

$$Q_t = \frac{720\, J\, W_t}{2\pi \bar{N}} \left[X_1 \Delta h_1 + X_2 \Delta h_2 - \Delta h_d \right] \qquad (20)$$

The second program is used to calculate efficiency corrected for droplet drag and the corrected parameters mentioned above. These parameters are obtained from equations 9, 10, 11, 12, and 13 and constitute

correction to design inlet conditions, namely, 1600°F and 92 percent vapor quality. The velocity ratio based on wet properties is also determined by this program.

Converging-Diverging Nozzle Data Evaluation

During the past quarter, evaluation of the converging-diverging (C-D) nozzle data has continued. The average values of polytropic exponent, n, reported in the February 8 Quarterly Report have been revised. The values of n reported therein were calculated from

$$\left(P_s/P_t\right)_{th} = \left(\frac{2}{n+1}\right)^{\frac{n}{n-1}} \qquad (21)$$

and required the use of the measured throat position to determine the throat pressure ratio from the pressure readings at taps on both sides of the throat (taps 12 and 13). Since the previously reported values of n were as much as 9.5 percent greater than the theoretical superheated value of the polytropic exponent at the saturation conditions, * an improvement in n was sought by improving the estimate of the throat critical pressure ratio from the experimental values of pressure ratio at the adjacent taps upstream and downstream of the throat.

The procedure for finding the critical pressure ratio was to determine the following parameters:

* Appendix Quarterly Number 10 - NAS 5-1143, November 8, 1963

$$C = \frac{\left(\frac{P_s}{P_t}\right)_{12} - \left(\frac{P_s}{P_t}\right)_{th}}{\left(\frac{P_s}{P_t}\right)_{12} - \left(\frac{P_s}{P_t}\right)_{13}} \qquad (22)$$

(where P_s and P_t are static and total pressures from taps 12, 13 and the throat) by iteration from supersaturated* properties of potassium vapor for temperatures of 1450, 1500, and 1580°F. The results are shown below.

Temperature, °F	C
1450	.733
1500	.7325
1580	.731
Average	.732

Since the variation of C with temperature was slight, the average value was used and the critical pressure ratio was found from the following equation:

$$\left(\frac{P_s}{P_t}\right)_{th} = \left(\frac{P_s}{P_t}\right)_{12} - C\left[\left(\frac{P_s}{P_t}\right)_{12} - \left(\frac{P_s}{P_t}\right)_{13}\right] \qquad (23)$$

using the experimental values of pressure ratio for the taps 12 and 13.

The experimental values of polytropic exponent calculated by the

---

* The supersaturated properties of potassium vapor were calculated from equations of the Appendix of Quarterly Report Number 10 - NAS 5-1143, November 8, 1963, using pressures higher than the saturated value.

above procedure, are plotted against inlet quality in Figure 5. The data has the same general trend as that previously reported. However, the values of exponent found by extrapolating straight lines through the data to the saturated vapor line are now 7.9, 4.3 and 3.4 percent greater than the theoretical saturated value at the temperatures of 1450, 1500 and 1580°F, respectively, compared to the 9.5, 8.0 and 5.0 percent values previously reported. Therefore, the data is seen to be somewhat improved, but the marked decrease in exponent with decrease in quality is still unexplainable.

In order to verify the potassium vapor mass flow as experimentally measured by the electromagnetic flowmeters, the nozzle critical mass flow was calculated by substituting the average polytropic exponent determined above into:

$$W_v^* = \left\{ ng \frac{P_t}{v_t} \left(\frac{2}{n+1} \right)^{\frac{n+1}{n-1}} \left(\frac{n+1}{n-1} \right) \right\}^{1/2} A^* \qquad (24)$$

Although flows with quality values less than unity are being dealt with, v_t has been shown to be the dry vapor specific volume rather than the wet value by comparisons with steam data on the same C-D nozzle.

The vapor specific volume, v_t, is calculated from the measured inlet total pressure and temperature substituted in the virial equation of

state. Equation (24) results in vapor flow only. The total flow (vapor and liquid) is found by dividing the vapor flow by the inlet vapor quality.

The inlet quality is determined as follows:

$$X = \frac{W_{v*}}{W_{v*} + W_l} \tag{25}$$

In Figure 6, the critical mass flow calculated from Equation (24) is plotted against inlet total pressure for the following values of nominal inlet vapor quality: 99, 95, 90 and 85 percent.

In Figure 7 is presented the total nozzle flow obtained from the sum of the main and spray electromagnetic flowmeters as a function of inlet total pressure. Shown in Figure 8 are lines representing the data of Figures 6 and 7 for each value of nominal quality. In general, the curves indicate that the electromagnetic flowmeter values are within approximately 3.9 percent of the C-D nozzle critical flow at low pressure (low vapor temperature) and high initial quality and within approximately 1.6 percent at high pressure (high vapor temperatures) and high initial quality. For the lower initial qualities, the difference between EM flowmeter flow and C-D nozzle critical flow increases for the low pressures and is as much as 16 percent for one case, but is generally only about 11 percent. For the high pressure data at the lower qualities, the difference remains at below 1.5 percent.

The polytropic exponent data presented above deals exclusively with the average polytropic exponent from the inlet to the throat. Of interest in turbine design and data evaluation is the variation of the polytropic exponent along the length of the nozzle. In the C-D nozzle test, the polytropic exponents are obtained from the continuity equation which can be written as follows:

$$\frac{W}{A_e}\sqrt{\frac{v_{t1}}{P_{t1}}} = \left\{\frac{2gn}{n-1}\left[\left(\frac{P_s}{P_{t1}}\right)^{\frac{2}{n}} - \left(\frac{P_s}{P_{t1}}\right)^{\frac{n+1}{n}}\right]\right\}^{1/2} \qquad (26)$$

For the case of the pressure ratio between inlet and the throat (the critical pressure ratio when the maximum flow passes through the C-D nozzle) the following is true:

$$\left(\frac{P_s}{P_t}\right)_{th} = \left(\frac{2}{n+1}\right)^{\frac{n}{n-1}} \qquad (27)$$

When equation (27) is substituted into equation (26), the following results

$$\frac{W}{A^*}\sqrt{\frac{v_{t1}}{P_{t1}}} = \left\{gn\left(\frac{2}{n+1}\right)^{\frac{n+1}{n-1}}\right\}^{1/2} \qquad (28)$$

Equation (27) was used to determine the values of polytropic exponent reported previously. The right hand side of equation (28) can be evaluated using the value of polytropic exponent found from equation (27) and using the experimental pressure ratio. The combining of equation (26) with (28) results in the following:

$$A_e \left\{ \frac{2g\bar{n}}{\bar{n}-1} \left[\left(\frac{P_s}{P_t}\right)^{\frac{2}{\bar{n}}} - \left(\frac{P_s}{P_t}\right)^{\frac{\bar{n}+1}{\bar{n}}} \right] \right\}^{1/2} = A^* \left\{ gn \left(\frac{2}{n+1}\right)^{\frac{n+1}{n-1}} \right\}^{1/2} \qquad (29)$$

where $\bar{n}$ is to be obtained and n is the value coming from equation (27). Shown in Table III are both A for all taps and A* which were determined experimentally in air. P_s/P_t is known experimentally for each pressure tap for a given set C-D nozzle potassium test condition. Using iteration, the average polytropic exponent between inlet and any tap may be determined from equation (29).

Shown in Figure 9 is the variation of average inlet to throat polytropic exponent from inlet to the several taps as a function of the measured pressure ratio. These data are for a nominal inlet temperature of 1580°F, the nominal condition where the least scatter was obtained. For clarity, the number of the tap from which the data was obtained is shown. The low-numbered taps are upstream of the throat and the high numbered values are downstream of the throat. The throat is between taps 12 and 13. The procedure breaks down for tap numbers lower than 10 because of random scatter. Reference to Figure 9a, which is for nominal vapor quality of 99 percent, indicates a slight increase in polytropic exponent as the flow proceeds through the nozzle. Certainly there is nothing to indicate reversion until tap 15 (downstream of the throat) is reached at which time the pressure

rises and the polytropic exponent decreases. However, the behavior of pressure ratio and polytropic exponent downstream of tap 14 is similar to that to be expected if reversion occurred.

Shown in Figure 9b is data for a nominal vapor quality of 85 percent. In contrast to the high-quality data (Figure 9a) for the low quality data, a reduction in polytropic exponent is indicated from tap 10 on. However, the same abrupt change in exponent is exhibited after tap 15, as is the case for the high-quality data. A possible explanation of the behavior of the low quality data in the region of taps 10 and 11 is that partial reversion is taking place.

To facilitate further evaluation of the 187 runs on the converging-diverging nozzle, the data (approximately 16 runs) for each nominal condition was averaged. The results are shown in Table IV. Shown also is the probable error computed as follows:

$$P.E. = 0.6745 \sqrt{\frac{y_1^2 + y_2^2 + \cdots + y_z^2}{z - 1}} \qquad (30)$$

No measurements exceeded 5 times P.E., therefore, all measurements were retained in the averages.

Reference to the table indicates that for the temperatures and flowrates the probable error rarely exceeded 1 percent. The maximum errors for the pressure measurements were larger than for the temperatures and flowrates.

III. MECHANICAL DESIGN AND TESTING

The major effort during this quarterly reporting period involved preparation and installation of the turbine into the potassium test facility, and checking mechanical performance of the assembled test rig. Tare loss tests were run on the turbine in the test facility, and additional testing of the labyrinth seal was performed on the plexiglass model of the turbine hydrodynamic seal in the hydraulics laboratory.

Pre-Potassium Test Turbine Check-Out

As indicated in the February 8 Quarterly Progress Report, the turbine was installed in the potassium facility for dynamic check-out. The casing and inlet duct were not welded on during this running, but instead, the turbine was run to speed on the steam starter turbine to check out facility instrumentation and control equipment, and system dynamics with other facility equipment running. The installation is shown in Figure 10 and 11. In Figure 11, the turbine can be seen in the glove box.

The turbine-dynamometer system had several modifications made for this installation. The water flow-line connnections to the water brake were modified to use flexible hoses to eliminate any water leaks. Also, the air-mist lubrication system on the brake bearings was replaced with a liquid lube system to eliminate the presence of oil mist in the test-cell

atmosphere. Shaft seals were added to both ends of the brake rotor to prevent oil leakage. All modifications to the brake worked satisfactorily during check-out testing.

Checks were made of the Berkley speed readout, Sanborn recorders, multipoint recorder, vibration readout instrumentation, and sensitivity and response of control valves. Linearity and operability of the torque meters and adequacy of the torque measuring system were checked. Bearing operating temperatures, vibrations, and flow requirements for this installation were observed. This was the first assembly of the turbine test rig in the potassium test facility (Building 318). The turbine was driven, in small speed increments, to 17,500 rpm. Beyond this speed, the steam turbine could no longer accelerate the system because of high bucket windage power consumption in the potassium turbine. In general, all test equipment and instrumentation functioned without any serious faults.

After completion of the check-out running, the turbine was removed from the facility for final assembly. An inspection showed that the labyrinth seal in the forward bearing housing had rubbed. A dimensional check revealed that the labyrinth seal had been machined undersized. It was remachined to the proper clearance, and the turbine was reassembled.

Component Fabrication

As stated in the previous quarterly, it was decided to incorporate

welded flanges on the turbine casing.

It was further decided to replace all brazed instrumentation joints with welded joints. From experience gained in heat transfer boiling experiments, it was decided to place the sheathed, end-welded thermocouples in wells rather than exposing them directly to alkali metal. The thermocouple wells used were 1/8 inch tubing and can be seen installed in the outlet guide vane and its casing in Figure 12. Shown in Figures 13 and 14 is the casing after completion of welding and leak-checking of the pressure instrumentation.

Shown in Figure 15 is the inlet duct (bullet nose) after the flange blanks were welded in place. Shown in Figure 16 is the same piece after the machining of the B flanges and installation of new instrumentation tubing. On all instrumentation for the casing and inlet duct, complete helium mass spectrometer leak checking was carried out.

Experimental Casing

Before proceeding with the assembly of the turbine by welding an experimental casing was welded. The original bolted casing was used for the experiment, which helped to establish the welding sequence so that the actual turbine could be welded with minimum and uniform distortion.

The scroll and the inlet duct were simulated, using low carbon

steel discs 2.5 inches thick machined with the required rabbet and joints designed for welding.

The components were held together with "C" clamps and internal diameter measurements were taken during the welding of the experimental casing to determine the movement resulting from welding. The locations of these measurements are shown in Figure 17.

The welding sequence is shown in Figure 18 and the inside diameter measurements of the experimental casing before, during, and after welding are shown in Table V. The internal diameters increased during welding except at the horizontal flanges. After welding, the maximum diameteral increase was 0.009 inches and the largest decreasewas 0.005 inches. The changes in dimensions from welding were within acceptable limits compatible with turbine seal running clearances.

Welded Turbine Casing

The actual turbine casing was fabricated using the same assembly, tacking, and welding sequence developed on the experimental casing. The turbine was positioned with its axis vertical. The casing halves were fitted together on the scroll rabbet and the inlet duct placed on top of the casing. The horizontal flanges were clamped together and the casing clamped to the scroll and the inlet duct.

The welded joint grooves were covered with glass tape to retain the argon gas backing of the weld joints. The argon backup gas was fed under the glass tape through a small diameter stainless steel tube. The tape was removed locally as tacking and welding progressed.

The assembly was tack-welded in the vertical position after which the clamps were removed. The turbine was then placed with the axis horizontal to permit welding in the flat position. The turbine was rotated as required during welding. Although it was not possible to nondestructively inspect the welded joints, the welding was done by an experienced welder, using procedures that are known to produce the highest possible weld quality. During welding, the turbine shaft was manually rotated with no indication of rubbing between the buckets and the rub seals. Shown in Figure 19 is a photograph of the turbine after assembly.

Installation of Potassium Drain Manifold

A drain manifold was installed at the rear of the bearing housing to collect potassium from six drain lines. The manifold was semi-circular in shape to form a yoke around the housing with a drain line coming off at its mid-point. The tubes emerging from the bearing housing were bent to the required positions to meet the manifold and sections of tubes added, where necessary. The connections were made in the required order to accomplish the welding. No difficulties were encountered with the assembly.

Leak Checking of the Turbine and Manifold

To insure that the turbine and manifold assembly was leak-tight, the turbine was pressurized with helium and checked for gas leaks, using a sniffer probe on a helium mass spectrometer. All inlet and exit entries on the turbine were sealed. The rear seal on the turbine shaft was tightened. The turbine was pressurized with helium to about 15 psi and all weld joints were checked with the spectrometer sniffer.

A leak was detected at the weld joint between a potassium drain line and the bearing housing. The leak was welded closed and the lines carefully checked again. No leaks were detected in any of the weld joints on the turbine.

Initial Turbine Run-Up

The turbine assembly was clamped in position in the 3000 KW facility, but instead of welding the turbine into the facility, it was closed with back-off plates and clamps. The water brake, starter turbine and strain gage torque meters were assembled to the turbine. Then, without attaching the potassium sealant loop, the turbine was run to 16,000 rpm. During this test, air instead of argon was used in the labyrinth seal. This test demonstrated that no rubs were being encountered between mating parts and that the torque meters, starter turbine and main lube supply system were functioning completely satisfactorily. In addition, the water brake which had been modified

to incorporate liquid-jet rather than oil-mist lubricant worked very well.

Welding of the Turbine into the Facility

Following the initial run-up, the turbine was connected to the facility. The turbine was aligned in position with the 8 inch inlet pipe so that the flanges to be welded together were parallel within .002 inches. The 10 inch discharge line into the condenser was aligned with the turbine exhaust scroll and flanges were clamped together. Due to the flexible joint in this line, a very accurate alignment of the welding flanges was not required. The 8 inch liquid metal spray nozzle section and pipe flange were inserted and clamped in position. The 8 inch flange was welded to the inlet line from the boiler. The joint between the turbine scroll and condenser line was welded next. The spray nozzle section was removed and the argon gas plug in the inlet 8 inch pipe removed. The spray nozzle section was placed in position and welded to the 8 inch pipe flange. Then the nozzle section was welded to the turbine inlet duct.

All flange welds were made with two passes that produced weld joints of adequate cross section. The joints were not filled to minimize distortion and stress on the turbine casing and scroll. The welds were not X-ray inspected because the mating flange faces would obscure the weld joint on the film.

Finally, the 1 inch liquid metal injector line to the spray nozzle was installed and the potassium slinger seal drain line from the manifold was connected to the facility. These joints were X-ray inspected and found to meet the welding specifications. After the completion of the installation welding, the turbine loading and the start-up equipment was assembled, maintaining an adequate axial clearance for the splined coupling (.060 inch to .090 inch) and at the starter turbine shaft and Bytrex torque-meter of about .060 inch.

The concentricity of the test rig equipment with the turbine shaft was checked at each component mounting flange. The maximum total run-out was less than one mil (.001) per one foot of the test rig length.

Shown in Figures 20 and 21 are photographs of the turbine after being welded into the 3000 KW facility and thermal insulation applied. Efflux system demister capsules and efflux lines are clearly visible in these figures. Lube and argon lines are visible in Figure 21.

Final Test Preparations

During the time the turbine was being welded into the facility, the water brake was fitted with new lube oil seals and bearings. This equipment was then reinstalled on the turbine.

A special test was made of the starter turbine in the Hydraulics

Laboratory. This turbine was run at low speed with varying lube oil flow. The test confirmed that the turbine internal labyrinth seal and external garter type shaft seal were sound and leak tight. This turbine was then installed on the potassium turbine shaft.

During the installation of the water brake and starter turbine all stack-up dimensions were measured and recorded.

Shown in Figures 22 and 23 is the turbine fully installed in the test facility.

Turbine Tare Loss Test

Upon completion of the test rig installation, a mechanical check-out run was made. The turbine was driven by the steam starter turbine while all turbine bearings had a normal lube oil flow. The main potassium loop was sealed off and argon was admitted to the turbine labyrinth seal, to prevent the lube oil leakage into the potassium seal cavity.

The lube oil pressure, temperature and the flow readings indicated that all test rig components were functioning well. The turbine pad bearing temperature and the lube oil temperatures are shown on Figure 24.

Before proceeding with the potassium performance testing, it was decided to make the turbine tare loss test. The main turbine was driven

during this test by the steam starter turbine, and all bearings lubrication system and seal argon loop were started as for normal turbine start-up procedure, described in the turbine test plan.

At about 7000 rpm, the liquid potassium was admitted to the rotating seal to establish a hydrodynamic seal between the seal argon cavity and the turbine exhaust. The main potassium loop was sealed off for this test and turbine housing and exhaust duct were pressurized with argon at 20 psia. The main loop argon pressure was gradually reduced during the test to about 6 psia.

The readings of the starter turbine torque, bearings temperature and the hydrodynamic seal flow and temperature were taken at several argon pressure levels in the turbine main loop.

The tare loss torque readings of this test are shown in Figure 25. During the tare torque test the steam turbine torquemeter was reading the sum of following torque values:

a) The potassium turbine bearings and seals

b) The potassium turbine rotor windage

c) The water brake bearings and seals

d) The water brake rotor windage

The turbine tare torque due to the high main loop pressure is shown to

increase about 12 percent for a 100 percent change in the main loop pressure, indicating very little of the tare loss is due to the test turbine blade and disc windage.

Shown in Figure 26 is the comparison of the experimental and theoretical power consumption of the hydrodynamic seal when using potassium as the sealant. The power loss was determined from the temperature rise and the liquid potassium flowrate through the seal. Reference to Figure 26 indicates a close agreement between the calculated and the test results, especially at the higher values of rotative speeds shown. At these high speeds the heat transfer from the heated bearing housing to the sealing fluid is at a lower rate due to the lower temperature difference.

The two-stage turbine, water brake and the starter turbine bearing temperatures were also recorded during the test. All bearing temperatures were within the expected range and there were no significant deviations in the test rig bearing performance characteristics from those previously reported. The turbine pad bearing temperature readings are shown on Figure 27 and the seal argon inlet temperature on Figure 28.

The turbine test facility was shutdown after the completion of this test.

Seal Malfunction

Several attempts were made to restart the potassium test facility for the turbine performance testing in potassium vapor, but without success. The EM pump in the potassium hydrodynamic seal loop could not be started. It was later discovered that lube oil had leaked into the liquid potassium of the seal loop and reacted with it forming a black residue that blocked the EM pump. Also, a certain amount of the potassium was found in the lube oil system, which rendered the lube oil pumps inoperative. The latter complication is believed to have occurred during the attempt to re-start the facility for potassium testing. Due to the difficulties, the test facility was shutdown for inspection and repair.

Shown in Figure 29 is the assembly drawing of the two-stage turbine with items germane to the discussion of the seal malfunction designated. Since the bearing housing flange as well as the turbine casing flanges, were welded, inspection had to be made by removal of the aft ball-thrust bearing. This permitted removal of the pivoted-pad bearing and the oil slinger but not the shaft nor the hydrodynamic seal. Inspection revealed particles of solidified potassium in the pad bearing cavities which apparently caused some damage to the bearing surface, requiring replating.

There are two possible means for the lube oil to enter the potassium

seal loop, namely, along the shaft past the "O" ring seal between the oil slinger and the oil labyrinth and the oil and potassium labyrinth seals. In order to determine whether oil could have passed through the labyrinth seals at some operating condition, a test program on the model of the turbine seal was initiated in the hydraulics laboratory. This series of tests is described in the next section. In order to prevent the leakage of oil along the shaft, a new nickel-plated stainless steel sealing ring was designed and fabricated for installation in the region of the "O" ring seal, shown on Figure 32, marked (A). The location of the ring on the turbine assembly is shown on Figure 29. This sealing ring required minor modifications to the adjacent parts, as shown on Figure 30.

After the facility was cleaned and repaired, the turbine was reassembled incorporating the seal ring modifications. At the end of the quarter, preparations were being made to run the turbine without establishing the hydrodynamic seal. The purpose of this test is to establish whether the leakage still occurs with the improved ring seal. If no leakage occurs, the possibility of oil leaking through the labyrinth can be excluded.

Hydrodynamic Seal Test

As stated above tests of the model of the two-stage turbine seal were scheduled in the hydraulics laboratory to establish, whether at some

operating condition oil could have leaked across the oil and potassium labyrinth seals and thus gotten into the potassium seal loop. The test set-up is shown in Figure 31 and a sketch of the seal is shown in Figure 32. In the sketch the pressures read are designed by a letter and numerals. The clearances of the screw and labyrinth seals and the sizes and number of the various pipes leading to and from seal cavities were the same as for the actual hardware with two exceptions. One of four of the oil return pipes (from P4 to P5) was utilized as a pressure lead and the close-gap seal near P6 was similated by openings in a cap having approximately 80 percent of the correct area. Air was introduced under pressure at P7 while P1, P5, P6, and P8 were atmospheric pressure throughout the tests unless sealed off. Water was introduced at the potassium inlet for some tests and both air and water were removed through the argon-potassium outlet manifold for these tests.

Shown in Table VI is a summary of the air-water tests on the seal. The ports that were closed for a specific test, the water flow rate and shaft speed are tabulated. The objective of the tests was to measure the flow and pressure drop along a single flow path for each test. The resistance across which the pressure drop was measured is also tabulated in Table VI along with the figure in which the test results are given. (Figures 33, 34, 35, 36, 37, and 38).

Present plans call for utilizing the test data presented above in an analysis of the two-stage turbine seal both with and without the hydrodynamic seal operative. In this analysis appropriate corrections will be made for slight area differences, temperature levels, and different fluids.

Back-Up Turbine Hardware for Potassium Testing

Of the several turbine components which have been ordered as replacement parts for the second and third turbine build-up, the status is as follows:

Component	Anticipated Delivery Date	Turbine Build-Up Set No.
1) Turbine Shaft	7-13-64	3rd set
2) Bearing Sleeve	7-13-64	3rd set
3) Jam Nut Revision 3	7-13-64	3rd set
4) Jam Nut	7-13-64	3rd set
5) Shaft Lock Nut	7-13-64	3rd set
6) Tie Bolt	available	3rd set
7) Hydrodynamic Seal	7-31-64	3rd set
8) Water Brake Shaft	available	3rd set
9) Steam Turbine Shaft	available	3rd set
10) Bearing Housing	out for manufacturing quotes	modified design

The turbine disks orders as part of the previously procurred

"second set of hardware" parts were delivered on May 27, 1964. These were the longest delivery items in the second set of hardware.

In addition to the above components procurred as part of the formal turbine build-up, a number of specialized components are being manufactured as necessary to solve the previously discussed oil leakage problems (Chevron seals, bellville springs, etc.).

IV. 3000 KW FACILITY

Turbine Test Preparations

During the early part of this quarter, a General Electric Company sub-contractor completed all modifications and additions to the 3000 KW facility that are necessary for potassium turbine testing. As in the past, all new welds in liquid metal piping have been radiographed and helium mass spectrometer leak checked. Repairs were made where necessary.

Particularly, the potassium turbine slinger seal loop was modified to circulate liquid potassium instead of NaK. One reason for the change from NaK to potassium in the turbine slinger seal resulted from observations made during pretest of the same seal. At the time water was used as the seal fluid. Water drops were observed to sporadically flow from the slinger seal cavity into what would be the potassium test facility. It is believed that Na from the NaK would dilute the potassium in the main loop, during long time operation, to the extent that thermodynamic properties of the potassium would be significantly altered. A second consideration which influenced the switch to potassium was the greater capacity of potassium to absorb oxygen contamination without causing plugging of the system. A third consideration is that make-up potassium for the slinger seal loop is easily obtainable from the main loop during operation of the facility. Some piping was rearranged, and heating elements and thermal insulation

was applied to the slinger seal loop to accomodate the potassium. Figure 39 shows the lower portion of the completed slinger seal loop. All heating elements and thermocouples were checked for operation and calibration.

Lubrication systems for the potassium turbine, steam turbine, and water brake were completely installed and checked for proper flow-pressure characteristics. Basically, the potassium turbine lube system can deliver 6 gpm at 200 psig. Normal requirement is 3.3 gpm at 80 psig. Oil flowrate to each turbine bearing is monitored and controlled separately. Flowrate measuring instrumentation was calibrated and was found to compare with the calibration flowmeter within 2 1/2 percent. All pressure transmitters and receiver gages for the potassium turbine lube system were calibrated. Thermocouples were installed, and thermocouple readout instrumentation was calibrated. Figure 40 shows the potassium turbine lube system completely installed.

The lube system for the steam starter turbine and water brake was also checked for proper operation. This system is capable of delivering 2 gpm at 80 psig. Normal requirements are 0.9 gpm at 50 psig. Although the steam turbine lube system is not as elaborate as the potassium turbine lube system, oil flowrate to each bearing can be controlled and measured independently. Oil pressure to each bearing is measured. Oil temperature to and from each bearing is measured. This

lube system is shown in Figure 41.

All facility control instrumentation had been installed and appropriately calibrated early this quarter. Figures 42 and 43 show the control panels exclusive of the Sanborn recorders which are also in the Control Room. The digital recorder is in a building next door to the test facility.

The 8.0 inch vapor shut-off valve which had been disassembled for repairs due to galling of the valve stem was completely rebuilt and checked for non-leakage and operation. Stellite inserts were applied to the area where galling had occurred. A new, slightly shorter, stem bellows was installed in the rebuilt valve. The bellows assembly was leak checked by the manufacturer and also by G. E. upon completion of assembly in the facility.

The argon reclamation system was checked for proper compressor operation and control valve action. It was found that additional oil vapor separation was required. Therefore, two additional Type 13X Linde Molecular sieves were installed in the argon reclamation system. Subsequent running of the system has shown that oil vapor has been kept below 5 ppm. An oil vapor detector has been installed in the argon reclamation system which has a calibrated sensitivity of 5 ppm. The detector is installed on the discharge of the argon compressor (also the inlet to the test turbine).

The detector is an American Instrument Company unit, Catalogue No. 47-16015.

During operation of the test turbine, an argon flowrate of 45 to 90 lb/hr has generally been circulated through the oil side of the test turbine labyrinth seal. This argon is laden with oil vapor and/or mist as it leaves the turbine. Separation of oil from the argon is accomplished by passing the argon-oil mixture through a number of demister type separators which removes most of the oil mist. Essentially all oil mist is finally removed by cooling the argon-oil mist to below $0^{\circ}F$ by flowing it through a liquid nitrogen cooled vapor trap. However, minute quantities of oil does get blown through the nitrogen cooled trap. A molecular sieve was installed to absorb this carry over of oil mist. The molecular sieves contain about 5 pounds of absorbent, and the absorbent can retain in the order of 1 lb of oil before the concentration of oil in the discharge argon becomes excessive. The present estimate is that the molecular sieves will be changed every 100 hours of operation.

During this reporting period, the turbine and all rotating equipment was completely assembled for testing with potassium vapor. Figures 22 and 23 show the turbine assembly essentially ready to run. Figures 20 and 21 show the turbine fully installed in the glove box with thermal insulation applied. Efflux demister capsules and efflux pressure sensing lines are clearly seen in these figures. Lube lines and argon lines are

shown in the rear view of the turbine.

Figures 44, 45, 46, 47 and 48 show the build-up sequence of the potassium turbine, water brake and steam turbine in the 3000 KW facility. Figure 49 is a view of the potassium turbine rotor showing the two stages of buckets.

Turbine Check-Out Testing

Early in March, the potassium turbine, without the guide vane casing and inlet bullet nose, was installed in the 3000 KW facility for preliminary check-out of the turbine and for check-out of various facility systems such as the steam control, water brake control, lube systems, oil-argon separation, etc. No liquid metal was involved.

Preliminary running of the turbine revealed that additional oil vapor-argon separation was required, that the main condenser blower transmitted 2 mil displacement vibration to the starter steam turbine, and that all other facility systems worked well. Consequently, the condenser blower speed has been reduced from 960 rpm to 850 rpm with only a 5 percent loss of air flowrate. Vibration was reduced to 0.5 mils. The loss of air flow is significant to condenser operation. As indicated above, two molecular sieves were installed for better oil vapor removal.

After the outer casing was welded to the turbine, the turbine was

again installed in the glove box without actually being welded in place. All loading and starter equipment was assembled, and the test turbine was rotated up to 17,000 rpm to make sure that weldings of the casing has not caused damaging distortion of the turbine assembly. Upon completion of this test, the turbine was welded into the facility with essentially no measurable distortion. During the welding process, the turbine shaft was turned by hand occasionally to make sure that internal parts were not binding. New welds were inspected by radiographing and/or helium mass spectrometer leak checking.

Following the above leak checking, the main loop and slinger seal loop was hot flushed with potassium at 250 - 500°F. 100 hours of hot trapping in the main loop dump tank followed. Oxygen concentration after hot flushing was about 5 ppm and was about 25 ppm after hot trapping.

Following the hot trapping, it was attempted to run the potassium turbine on potassium vapor. The initial test was to determine tare losses of the turbine with the main loop pressure below 1/2 psia. This test was conducted with the turbine slinger seal established and at a turbine speed up to 17,000 rpm. The test was successful in determining tare losses of the turbine. However, during this test a pressure differential between the turbine oil sump and the main loop caused oil to migrate past a defective shaft seal into the slinger seal loop. Consequently, oil mixed with the slinger

seal potassium. On the following day when an attempt was made to restart the slinger seal loop, the slinger seal E. M. pump would not function. Ultimately, it was discovered that oil had actually mixed with potassium. A black residue was found to be choking the E. M. pump. Most of the slinger seal loop piping was also coated with the residue. The presence of oil in the potassium was ultimately traced to a faulty shaft seal in the potassium turbine.

Removal of the potassium-oil compound from the slinger seal loop required the disassembly of the loop and mechanical cleaning of the various components and piping. Although several cleaning compounds have been tried, no cleaning solution other than wire brushing has been found which will satisfactorily remove the residue oil-potassium compound. The slinger seal loop has since been put back together and checked for proper operation.

During the attempts to start the slinger seal loop, following the tare test, a small quantity of potassium was inadvertently transferred to the lube oil system. Consequently, the lube oil system also had to be drained and cleaned. However, cleaning of this system was accomplished by pumping several changes of fresh oil through 5 micron filters. The small particles of potassium were collected on the filters. The oil system has been completely cleaned and put back into proper operation condition.

The facility is on standby until a new shaft seal is installed in the turbine.

V. MATERIALS SUPPORT

METALLURGICAL EVALUATION OF PRETEST BUCKETS

The U-700 stage 3 and 4 turbine buckets, which were exposed to steam and compressed air turbine test conditions at a maximum temperature of 350°F, were examined both metallographically and by hardness survey and were compared with unused buckets of the same manufactured lot. No difference was found in hardness or microstructure between the new and used buckets. These U-700 buckets were subjected to a grit blasting effect from rust particles which were dislodged from the compressed air lines during the pre-potassium tests. The rough surfaces of these buckets can be seen in Figure 50 as compared with the as-machined finish of unused buckets.

Both the stage 3 and the stage 4 buckets were electrolytically etched and Zyglo inspected. Two of the stage 3 buckets were found to have cracks in their leading edge located at dents which were caused by particle impact. Each bucket used in pre-testing was then visually inspected and categorized according to the degree of surface pits and leading edge damage. The following conclusions were drawn from this bucket inspection.

The turbine blade material (U-700) suffered no detrimental effects as a result of the particle impacts and operating conditions encountered

during pre-testing, and therefore, all of the buckets are metallurgically suitable for further use in potassium testing. None of the stage 4 buckets suffered the particle impacting to which the stage 3 buckets were subjected and accordingly the stage 4 blades are suitable for further use. Three of the stage 3 buckets have been rejected because of cracks and/or heavy dents in the leading edge, but these will be replaced with new blades which were procurred as replacement parts when the entire group of blades was purchased. All of these buckets used in pre-testing will be held in reserve for use in the second endurance test.

CHEMICAL EVALUATION OF LUBE OIL

Subsequent to the leakage of oil into the potassium of the slinger seal loop, an investigation was made of the oil used during test and three other possible lubricants. The purpose of the test was to determine degree of reaction of the oil with potassium as a function of temperature.

The lubricants examined were:

DTE-797: the mineral oil used in the April 13th test

LF-4095: a high molecular weight polybutene

OS-124: a high molecular weight polyphenyl ether

DuPont PR-143: a high molecular weight fluorocarbon polymer

All tests were made under argon in Pyrex apparatus with outgassed oils. The following tables show the results:

(1) DTE-797 (100 ml)

Temp. °F	Without Potassium	Remarks	With 0.1 gm of Potassium
260	Vaporizing		
290			Potassium appeared to flake
375	Clear condensate		
400			Beginning to darken
420	Cloudy due to precipitate		
550			Black
700	Boiling - no appreciable darkening		
Rm. T.			Carbonized product adheres to walls

With 1 ml. of oil and 1 gm. of potassium a black solid was obtained when heated. This material resembled the material obtained from the slinger seal loop.

(2) LF-4095 (100 ml)

Temp. °F	Without Potassium	Remarks	With 0.1 gm of Potassium
200	Vaporizing		
245	Clear condensate		
250			Beginning to darken
370			Black

515	Boiling - no appreciable darkening	
Rm. T.		Carbonized product stayed dispersed in oil

With 1 ml. of oil and 1 gm. of potassium a black solid was obtained on heating.

Less carbonized product as obtained with the LF-4095, but this is probably due to the fact that a greater quantity of oil was distilled off during heating.

The distillates from DTE-797 and LF-4095 were found to react with potassium in the same way as the original oils.

(3) OS-124

Temp. °F	Remarks With 0.1 gm. of Potassium
320	Beginning to darken
525	Black
Rm. T.	Black product adheres to walls

With 1 ml. of oil and 1 gm. of potassium much more carbonize product was obtained--more with OS-124 than with DTE-797 or LE-4095.

(4) DuPont PR-143

Temp. °F	Remarks With 0.1 gm. of Potassium
Rm. T.	Potassium becomes gray
300	Potassium becoming black
450	Non-condensible fumes appeared
Rm. T.	Liquid still water white

With 1 ml. of oil and 1 gm. of K, the potassium became gray at room temperature, and as the temperature rose, a thick carbon deposit formed on the potassium. At its melting point the potassium spread out and reacted in a similar manner. At 300°F the reaction speeded up. Sparking was seen and the heating was stopped at 370°F. The mixture then exploded violently and the temperature rose to above 700°F.

Shown in figure 51 is a comparison of the specific gravities of DTE-797, LF-4095, and potassium as a function of temperature. The specific gravity of potassium is lower than DTE-797 at temperatures below about 225°F and theoretically would float on the oil below this temperature.

There appeared to be no reason to change from DTE-797 to one of the other lubricants at this time. The LF-4095 might possible permit easier cleanup, but this is not known with certainty.

The black carbonaceous deposit which was removed from the potassium loop contained no free potassium when delivered to the chemistry laboratory. An alkaline cleaner which is commonly used to remove deposits from engine parts was tried as a solvent up to 200°F, but it had no effect. Trichloroethylene was also tried. It dissolved the tars and greases and permitted dispersal of the black, particulate material which formed the major part of the mixture.

One loop fitting which contained the carbonaceous deposit was heated to 1000°F in an oxidizing atmosphere. The black deposit was not visible after this treatment; however, a gritty deposit composed primarily of iron, chromium, nickel and potassium remained. The nature of this deposit has not yet been determined.

The 3000 kw loop dump tank was sampled for presence of hydrogen with negative results. A carbon alaysis is in process.

TABLE I

Two-Stage Potassium Turbine Test Instrumentation

Item Number	Parameter	Location	Sensor	Range	Accuracy (% of Full Scale)	Control Room Readout	Digital Channel Number
1	Vapor Total Temp	Sta. No. 1	T.C.	1400-1650°F	± 0.1%	Sanborn	
2	Vapor Total Temp	Sta. No. 1	T.C.	1400-1650°F	"	None	
3	Vapor Total Temp	Sta. No. 1	T.C.	1400-1650°F	"	Sanborn	
4	Vapor Total Temp	Sta. No. 1	T.C.	1400-1650°F	"	None	
5	Vapor Total Temp	Sta. No. 1	T.C.	1400-1650°F	"	None	
6	Vapor Total Press	Sta. No. 1	Efflux	0 - 50 psia	± 0.5%	Sanborn	
7	Vapor Total Press	Sta. No. 1	Efflux	0 - 50 psia	"	None	
8	Vapor Total Press	Sta. No. 1	Efflux	0 - 50 psia	"	Sanborn	
9	Vapor Total Press	Sta. No. 1	Efflux	0 - 50 psia	"	None	
10	Vapor Total Press	Sta. No. 1	Efflux	0 - 50 psia	"	None	
11	Vapor Static Press	Sta. No. 1	Efflux	0 - 50 psia	"	None	
12	Vapor Static Press	Sta. No. 1	Efflux	0 - 50 psia	"	None	
13	Calorimeter Temp	Sta. No. 1	T.C.	1400-1650°F	± 0.1%	Sanborn	
14	Calorimeter Press	Sta. No. 1	Efflux	0 - 50 psia	± 0.5%	Sanborn	
15	Spray Liquid Temp	Liquid Inj.	T.C.	1400-1650°F	± 0.1%	Sanborn	
16	Spray Liquid Press	Liquid Inj.		0 - 150 psia	"	Taylor Gauge	
17	Spray Liquid Flow	Liquid Inj.	EMFM	0 - .5 pps	± 0.5%	Sanborn	
18	Vapor Total Press	Sta. No. 3	Efflux	0 - 50 psia	"	None	
19	Vapor Total Press	Sta. No. 3	Efflux	0 - 50 psia	"	None	
20	Vapor Total Press	Sta. No. 3	Efflux	0 - 50 psia	"	None	
21	Vapor Total Press	Sta. No. 3	Efflux	0 - 50 psia	"	None	
22	Vapor Static Press	Sta. No. 3	Efflux	0 - 50 psia	"	None	
23	Vapor Static Press	Sta. No. 3	Efflux	0 - 50 psia	"	None	
24	Vapor Static Press	Sta. No. 3	Efflux	0 - 50 psia	"	None	
25	Vapor Static Press	Sta. No. 3	Efflux	0 - 50 psia	"	None	
26	Vapor Static Press	Sta. No. 4	Efflux	0 - 50 psia	"	None	
27	Vapor Static Press	Sta. No. 4	Efflux	0 - 50 psia	"	None	
28	Vapor Temp.	Sta. No. 4	T.C.	650-1650°F	± 0.1%	None	
29	Vapor Temp	Sta. No. 4	T.C.	650-1650°F	"	None	
30	Vapor Static Press	Sta. No. 5	Efflux	0 - 50 psia	± 0.5%	None	
31	Vapor Static Press	Sta. No. 5	Efflux	0 - 50 psia	"	None	
34	Vapor Static Press	Sta. No. 6	Efflux	0 - 20 psia	"	None	
35	Vapor Static Press	Sta. No. 6	Efflux	0 - 20 psia	"	None	
38	Vapor Total Press	Sta. No. 7	Efflux	0 - 20 psia	"	None	

TABLE I (Continued)

Item Number	Parameter	Location	Sensor	Range	Accuracy (% of Full Scale)	Control Room Readout	Digital Channel Number
39	Vapor Total Press	Sta. No. 7	Efflux	0 - 20 psia	± 0.5%	Sanborn	
40	Vapor Total Press	Sta. No. 7	Efflux	0 - 20 psia	"	None	
41	Vapor Total Press	Sta. No. 7	Efflux	0 - 20 psia	"	None	
42	Vapor Static Press	Sta. No. 7	Efflux	0 - 20 psia	"	None	
43	Vapor Static Press	Sta. No. 7	Efflux	0 - 20 psia	"	None	
44	Vapor Static Press	Sta. No. 7	Efflux	0 - 20 psia	"	None	
45	Vapor Static Press	Sta. No. 7	Efflux	0 - 20 psia	"	None	
46	Vapor Total Temp	Sta. No. 7	T.C.	1000-1500°F	± 0.1%	None	
47	Vapor Total Temp	Sta. No. 7	T.C.	1000-1500°F	"	None	
48	Vapor Total Temp	Sta. No. 7	T.C.	1000-1500°F	"	None	
49	Vapor Total Temp	Sta. No. 7	T.C.	1000-1500°F	"	None	
50	Vapor Total Temp	Sta. No. 7	T.C.	1000-1500°F	"	None	
51	Vapor Total Temp	Sta. No. 7	T.C.	1000-1500°F	"	None	
52	Vapor Total Temp	Sta. No. 8	T.C.	1000-1500°F	"	None	
53	Vapor Total Temp	Sta. No. 8	T.C.	1000-1500°F	"	None	
54	Vapor Total Temp	Sta. No. 8	T.C.	1000-1500°F	"	None	
55	Vapor Total Temp	Sta. No. 8	T.C.	1000-1500°F	± 0.1%	None	
56	Vapor Total Temp	Sta. No. 8	T.C.	1000-1500°F	"	None	
57	Vapor Total Press	Sta. No. 8	Efflux	0 - 20 psia	± 0.5%	None	
58	Vapor Total Press	Sta. No. 8	Efflux	0 - 20 psia	"	None	
59	Vapor Total Press	Sta. No. 8	Efflux	0 - 20 psia	"	None	
60	Vapor Total Press	Sta. No. 8	Efflux	0 - 20 psia	"	None	
61	Vapor Total Press	Sta. No. 8	Efflux	0 - 20 psia	"	None	
62	Vapor Static Press	Sta. No. 8		0 - 40 psia	± 0.1%	Sanborn & Taylor Gauge	
63	Vapor Static Press	Sta. No. 8	Efflux	0 - 20 psia	± 0.5%	None	
64	Vapor Static Press	Sta. No. 8	Efflux	0 - 20 psia	"	None	
65	Calorimeter Insulation Temp	Exit Superheater	T.C.	1150-1650°F	± 0.1%	None	
66	Calorimeter Insulation Temp	Exit Superheater	T.C.	1150-1650°F	"	None	
67	Calorimeter Insulation Temp	Exit Superheater	T.C.	1150-1650°F	"	None	
68	Calorimeter Insulation Temp	Exit Superheater	T.C.	1150-1650°F	"	None	
69	Calorimeter Insulation Temp	Exit Superheater	T.C.	1150-1650°F	"	None	

TABLE I (Continued)

Item Number	Parameter	Location	Sensor	Range	Accuracy (% of Full Scale)	Control Room Readout	Digital Channel Number
70	Calorimeter Insulation Temp	Exit Superheater	T.C.	1150-1650°F	± 0.1%	None	
71	Calorimeter Insulation Temp	Exit Superheater	T.C.	1150-1650°F	"	None	
72	Calorimeter Insulation Temp	Exit Superheater	T.C.	1150 - 1650°F	"	None	
73	Calorimeter Press	AFT Heater A	Efflux	0 - 20 psia	± 0.5%	None	
74	Calorimeter Press	Aft Heater B	Efflux	0 - 20 psia	"	None	
75	Calorimeter Temp	Aft Heater A	T.C.	650-1650°F	± 0.1%	None	
76	Calorimeter Temp	Aft Heater B	T.C.	650-1650°F	"	None	
77	Insulation Temp	Compensating Heater	T.C.	1150-1650°F	"	None	
78	Insulation Temp	Compensating Heater	T.C.	1150-1650°F	"	None	
79	Insulation Temp	Compensating Heater	T.C.	1150-1650°F	"	None	
80	Insulation Temp	Compensating Heater	T.C.	1150-1650°F	"	None	
81	Condenser Liquid Level	Condenser	Rad. Gage	0 - 6 inches	± 0.2%	Sanborn	
82	Main Condenser Flow	Main EMFM	EMFM	0 - 5 pps	± 0.1%	Sanborn	
83	Main Condenser Flow Temp	Main EMFM	T.C.	900-1400°F	"	Sanborn	
84	Spray EMFM Temp	Spray EMFM	T.C.	1400-1650°F	"	Sanborn	
85	Rotative Speed Potassium	Turbine	Magnet. Pickup	0-25000 rpm	"	Berkley & Sanborn	
87	Torque	Starter Turbine	Bytrex	0-200 in/lb	"	None	
88	Torque	Potassium Turbine	Strain Gage	0-2500 in/lb	"	None	
89	Condenser Liquid Temp.	Condenser	T.C.	300-1300°F	"	None	
95	Temp. Pad Bearing 1-L Upper	Potassium Turbine	CA T/C	250°F	± 0.25%	Multipt. Rec.	

TABLE I (Continued)

Item Number	Parameter	Location	Sensor	Range	Accuracy (% of Full Scale)	Control Room Readout	Digital Channel Number
96	Temp. Pad Bearing 2-L Upper	Potassium Turbine	CA T/C	250°F	± 0.25%	Multipt. Rec.	
97	Temp. Pad Bearing 3-C Pad Left	Potassium Turbine	CA T/C	250°F	"	Multipt.	
98	Temp. Pad Bearing 4-R Pad	Potassium Turbine	CA T/C	250°F	"	Sanborn Rec.	
99	Temp. 5 Pad Bearing Cavity	Potassium Turbine	CA T/C	250°F	"	Multipt.	
100	Pressure Pad Bearing Lube Inlet	Potassium Turbine	Gauge	200 psig	"	Visual & Wrng. Sig.	
101	Flow Pad Bearing Lube Inlet	Potassium Turbine	Transd. 3-15 psi	0-200"H_2O (3GPM)	"	Sanborn	
102	Temp. "K" Turbine Bearing Lube Out	Potassium Turbine	CA T/C	250°F	"	Multipt.	
103	Temp. "K" Turbine Lube In	Potassium Turbine	CA T/C	250°F	"	Multipt.	
104	Temp. Stab. Bearing Pad	Potassium Turbine	CA T/C	250°F	"	Multipt.	
	TURBINE BALL BEARING						
105	Temp. Ball Thrust Bearing 1	Potassium Turbine	CA T/C	250°F	± 0.2%	Sanborn Rec.	
106	Temp. Ball Thrust Bearing 2	Potassium Turbine	CA T/C	250°F	± 0.25%	Multipt.	
107	Pressure Ball Bearing Lube In	Potassium Turbine	Bourdon Gauge	200 psig	"	Visual & Wrng. Sig.	
108	Flow Ball Bearing Lube In	Potassium Turbine	Transd.	0-200"H_2O (2 GPM)	± 0.2%	Sanborn	
	STEAM TURBINE BEARING						
109	Temp. Steam Turbine Bearing Forward	Potassium Turbine	CA T/C	250°F	± .25%	Multipt. Rec.	
110	Temp. Steam Turbine Bearing Mid	Potassium Turbine	CA T/C	250°F	"	Multipt. Rec.	
111	Temp. Steam Turbine Bearing Aft.	Potassium Turbine	CA T/C	250°F	"	Multipt. Rec.	

TABLE I (Continued)

Item Number	Parameter	Location	Sensor	Range	Accuracy (% of Full Scale)	Control Room Readout	Digital Channel Number
112	Temp. Steam Turbine Lube In.	Potassium Turbine	CA T/C	200°F	± 0.25%	Multipt. Rec.	
113	Temp. Steam Turbine Lube Out	Potassium Turbine	CA T/C	200°F	"	P.B.	
114	Press. Steam Turbine Lube In (Located on the lube cart at present)	Potassium Turbine	Gauge	80 psig	± 0.2%	None	
115	Flow Steam Turbine Bearing Lube In	Potassium Turbine	Flow-rator in Test Cell	1 GPM	"	Low Flow Warning Light	
	WATER BRAKE						
116	Temp. H_2O Brake Inlet	Potassium Turbine	CA T/C	60°F	± 0.25%	Multipt.	
117	Temp. H_2O Brake Out	Potassium Turbine	CA T/C	150°F	"	Multipt.	
118	Temp. H_2O Brake Fwd Brg.	Potassium Turbine	CA T/C	180°F	"	Multipt. Rec.	
119	Temp. H_2O Brake Aft Brg.	Potassium Turbine	CA T/C	180°F	"	Multipt. Rec.	
120	Flow H_2O Brake-Water	Potassium Turbine	Millivolt	50 GPM	± 0.1%	Gauge	
121	Flow H_2O Brake-Lube	Potassium	Manual	1 GPM	"	Constant Flow Setting in Test Cell	
	VIBRATIONS						
122	Displ. Steam Turbine Aft. Bearing V.	Potassium Turbine	Vib P/V	0-5 mils	± 0.2%	Sanborn Rec.	
123	Displ. Steam Turbine Aft. Bearing H.	Potassium Turbine	Vib. P/V	0-5 mils	"	Sanborn Rec.	
124	Displ. Aft. K Turb V	Potassium Turbine	Vib. P/V	0-5 mils	"	Sanborn Rec.	

TABLE I (Continued)

Item Number	Parameter	Location	Sensor	Range	Accuracy (% of Full Scale)	Control Room Readout	Digital Channel Number
125	Displ. Aft K Turb. H	Potassium Turbine	Vib P/V	0-5 mils	± 0.2%	Sanborn Rec.	
126	Accel. Pad Brg. V	Potassium Turbine	Accelero-meter	0-10 G's	"	Visual	
127	Accel. Pad Brg. H	Potassium Turbine	Accelero-meter	0-10 G's	"	Visual	
	HYDRODYNAMIC SEAL						
128	Temp. Seal K In	Potassium Turbine	CA T/C	500°F	± 0.25%	Multip.	
129	Temp. Seal K Out	Potassium Turbine	CA T/C	1000°F	"	P.B.	
130	Pressure Seal K In	Potassium Turbine	3--15 psi	160 psig	± 0.2%	Visual	
131	Pressure Seal K Out	Potassium Turbine	3--15 psi	30 psig	"	Visual	
132	Flow Seal K Inlet	Potassium Turbine	EMFM	2 GPM	± 0.1%	Milli-Volt Rec.	
133	Temp. Argon Seal Inlet	Potassium Turbine	CA T/C	500°F	± 0.25%	Multip.	
134	Pressure Turbine Argon Inlet	Potassium Turbine	Gauge	100 psig	± 0.2%	Visual	
135	Temp. Bearing Sump Wall	Potassium Turbine	CA T/C	500°F	± 0.25%	Multipt.	
136	Pressure Lube Cart Out	Potassium Turbine	Gauge	200 psig	± 0.2%	Visual	
137	Pressure Stab. Brg. Lube In.	Potassium Turbine	Gauge	200 psig	± 0.2%	Visual	
138	Pressure Stab. Brg. Piston, Lube In.	Potassium Turbine	Gauge	200 psig	"	Visual	
139	Pressure Bearing Sump	Potassium Turbine	Gauge	50 psig	"	Visual	
140	Pressure Steam Turbine Lube In	Potassium Turbine	Gauge	80 psig	"	Visual	

TABLE II

TURBINE TEST CONDITIONS

Run	Point	Inlet Temp. °F	Nominal Inlet Pressure Psia	Nominal Inlet Percent Quality	Nominal* Spray Flow/ Main Flow	Pressure Ratio	Nominal Exit Pressure Psia	Speed rpm	Percent Corrected Speed
1	1	1450±10	19	99	.00255 ± .00008	2.0±.10	9.5	15,400±200	80
	2							17,320	90
	3							18,300	95
	4							19,280	100
	5							21,200	110
	6			99	.00255 ± .00008			23,110	120
	7			95	.0450 ± .00134			19,030	100
	8			92	.07780 ± .00236			18,910	100
	9			85	.163 ± .005			18,680	100
	10			85	.163 ± .005			22,240	120
2	11	1450±10	19	99	.00255 ± .00008	2.95±.15	6.44	15,400±200	80
	12							17,320	90
	13							18,300	95
	14							19,280	100
	15							21,200	110
	16			99	.00255 ± .00008			23,110	120
	17			95	.0450 ± .00134			19,030	100
	18			92	.07780 ± .00236			18,910	100
	19			85	.163 ± .005			18,680	100
	20			85	.163 ± .005			22,240	120
3	21	1450±10	19	99	.00255 ± .00008	4.0±.17	4.75	15,400±200	80
	22							17,320	90
	23							18,300	95
	24							19,280	100
	25							21,200	110
	26			99	.00255 ± .00008			23,110	120
	27			95	.0450 ± .00134			19,030	100
	28			92	.07780 ± .00236			18,910	100
	29			85	.163 ± .005			18,680	100
	30			85	.163 ± .005			22,240	120

TABLE II (Continued)

Run	Point	Inlet Temp. °F	Nominal Inlet Pressure Psia	Nominal Inlet Percent Quality	Nominal* Spray Flow/ Main Flow	Pressure Ratio	Nominal Exit Pressure Psia	Speed rpm	Percent Corrected Speed
4	31	1450±10	19	99	.00255 ± .00008	5.0±.19	3.80	15,400±200	80
	32							17,320	90
	33							18,300	95
	34							19,280	100
	35							21,200	110
	36			99	.00255 ± .00008			23,110	120
	37			95	.0450 ± .00134			19,030	100
	38			92	.07780 ± .00236			18,910	100
	39			85	.163 ± .005			18,680	100
	40			85	.163 ± .005			22,240	120
5	41	1450±10	19	99	.00255 ± .00008	6.0±.22	3.17	15,400±200	80
	42							17,320	90
	43							18,300	95
	44							19,280	100
	45							21,200	110
	46			99	.00255 ± .00008			23,110	120
	47			95	.0450 ± .00134			19,030	100
	48			92	.07780 ± .00236			18,910	100
	49			85	.163 ± .005			18,680	100
	50			85	.163 ± .005			22,240	120
6	51	1450±10	19	99	.00255 ± .00008	7.0±.27	2.72	15,400±200	80
	52							17,320	90
	53							18,300	95
	54							19,280	100
	55							21,200	110
	56			99	.00255 ± .00008			23,110	120
	57			95	.0450 ± .00134			19,030	100
	58			92	.07780 ± .00236			18,910	100
	59			85	.163 ± .005			18,680	100
	60			85	.163 ± .005			22,240	120

TABLE II (Continued)

Run	Point	Inlet Temp. °F	Nominal Inlet Pressure Psia	Nominal Inlet Percent Quality	Nominal* Spray Flow/ Main Flow	Pressure Ratio	Nominal Exit Pressure Psia	Speed rpm	Percent Corrected Speed
7	61	1550±5	30	99	.00255 ± .00008	2.95±.15	10.17	15,360±200	80
	62							17,290	90
	63							18,250	95
	64							19,210	100
	65							21,130	110
	66			99	.00255 ± .00008			23,050	120
	67			95	.0450 ± .00134			19,100	100
	68			92	.07740 ± .00236			19,030	100
	69			85	.162 ± .005			18,880	100
8	70	1550±10	30	99	.00255 ± .00008	4.0±.17	7.50	15,360±200	80
	71							17,290	90
	72							18,250	95
	73							19,210	100
	74							21,130	110
	75			99	.00255 ± .00008			23,050	120
	76			95	.0450 ± .00134			19,100	100
	77			92	.07740 ± .00236			19,030	100
	78			85	.162 ± .005			18,880	100
9	79	1550±10	30	99	.00255 ± .00008	5.0±.19	6.00	15,360±200	80
	80							17,290	90
	81							18,250	95
	82							19,210	100
	83							21,130	110
	84			99	.00255 ± .00008			23,050	120
	85			95	.0450 ± .00134			19,100	100
	86			92	.07740 ± .00236			19,030	100
	87			85	.162 ± .005			18,880	100

TABLE II (Continued)

Run	Point	Inlet Temp. °F	Nominal Inlet Pressure Psia	Nominal Inlet Percent Quality	Nominal* Spray Flow/ Main Flow	Pressure Ratio	Nominal Exit Pressure, Psia	Speed rpm	Percent Corrected Speed
10	88	1550±10	30	99	.00255 ± .00008	6.0±.22	5.00	15,360±200	80
	89							17,290	90
	90							18,250	95
	91							19,210	100
	92							21,130	110
	93			99	.00255 ± .00008			23,050	120
	94			95	.0450 ± .00134			19,100	100
	95			92	.07740 ± .00236			19,030	100
	96			85	.162 ± .005			18,880	100
11	97	1550±10	30	99	.00255 ± .00008	7.0±.27	4.25	15,360±200	80
	98							17,290	90
	99							18,250	95
	100							19,210	100
	101							21,130	110
	102			99	.00255 ± .00008			23,050	120
	103			95	.0450 ± .00134			19,100	100
	104			92	.07740 ± .00236			19,030	100
	105			85	.162 ± .005			18,880	100
12	106	1550±10	30	99	.00255 ± .00008	8.0±.36	3.75	15,360±200	80
	107							17,290	90
	108							18,250	95
	109							19,210	100
	110							21,130	110
	111			99	.00255 ± .00008			23,050	120
	112			95	.0450 ± .00134			19,100	100
	113			92	.07740 ± .00236			19,030	100
	114			85	.162 ± .005			18,880	100

TABLE II (Continued)

Run	Point	Inlet Temp. °F	Nominal Inlet Pressure Psia	Nominal Inlet Percent Quality	Nominal* Spray Flow/ Main Flow	Pressure Ratio	Nominal Exit Pressure, Psia	Speed rpm	Percent Corrected Speed
13**	115	1600±5	37	99	.00255 ± .00008	2.95±.15	12.85	19,330±200	100
	116	1600±5	37	92	.0770 ± .00236	2.95±.15	12.85	19,200±200	100
14**	117	1600±5	37	99	.00255 ± .00008	4.0±.17	9.25	19,330±200	100
	118	1600±5	37	92	.0770 ± .00236	4.0±.17	9.25	19,200±200	100
15**	119	1600±5	37	99	.00255 ± .00008	5.0±.19	7.40	19,330±200	100
	120	1600±5	37	92	.0770 ± .00236	5.0±.19	7.40	19,200±200	100
16**	121	1600±5	37	99	.00255 ± .00008	6.0±.22	6.16	19,330±200	100
	122	1600±5	37	92	.0770 ± .00236	6.0±.22	6.16	19,200±200	100
17**	123	1600±5	37	99	.00255 ± .00008	7.0±.27	5.29	19,330±200	100
	124	1600±5	37	92	.0770 ± .00236	7.0±.27	5.29	19,200±200	100
18**	125	1600±5	37	99	.00255 ± .00008	8.0±.36	4.63	19,330±200	100
	126	1600±5	37	92	.0770 ± .00236	8.0±.36	4.63	19,200±200	100

*Flow ratio is correct only if ΔT between spray flow temperature and main flow temperature does not exceed 50°F.

**In runs number 13 - 18, the following test points shall be run first: 116, 118, 120, 122, 124 and 126. Only those of the remaining runs which can be accomplished before the facility has been operated at 1600°F for eight hours shall be run.

TABLE III

AVERAGE VALUES OF
EFFECTIVE FLOW AREA FOR AIR

Tap Number	Effective Area (Sq. Inches)	Actual Area (Sq. Inches)
1	20.669	20.173
2	16.346	16.529
3	13.066	13.422
4	11.319	11.154
5	9.144	9.327
6	7.859	8.116
7	7.075	7.154
8	6.541	6.710
9	6.033	6.158
10	5.538	5.645
11	4.996	5.086
12	4.899	4.980
13	4.886	4.932
14	4.968	5.035
15	5.145	5.285
17	5.525	5.692
18	5.524	5.800
Throat Area	4.884	4.906

TABLE IV

AVERAGED VALUES OF CONVERGING-DIVERGING NOZZLE TEST POTASSIUM DATA AND PROBABLE ERRORS

Nominal Temperature, °F	1450								1500								1580							
Nominal Quality, %	99		95		90		85		99		95		90		85		99		95		90		85	
Average Value	*		*		*		*		*		*		*		*		*		*		*		*	
Probable Error		*		*		*		*		*		*		*		*		*		*		*		*
Inlet Total Pressure, Psia	17.95	.4029	18.35	.4280	18.65	.4878	19.57	.4827	25.23	.2811	24.94	.2975	24.14	.2884	26.59	.4872	34.08	.0986	34.74	.1570	35.04	.1224	35.34	.1846
Inlet Total Temperature, °F	1443	2.653	1447	5.705	1446	4.254	1453	3.991	1506	1.032	1502	2.073	1496	2.155	1517	4.045	1578	1.208	1582	.9946	1585	.9519	1587	1.027
Main EMFM Temperature, °F	439.6	2.515	458.5	2.416	453.6	1.783	471.3	3.006	778.7	7.762	545.3	2.872	485.3	7.035	841.1	4.964	762.5	2.730	727.6	1.785	768.1	7.425	735.3	2.866
Spray EMFM Temperature, °F	566.4	1.110	479.4	1.870	465.7	1.513	481.5	3.451	622.1	2.655	571.7	5.491	532.6	3.770	794.1	5.622	488.2	1.186	748.3	1.509	774.9	8.726	752.3	3.354
Main EMFM Flow, pps	1.423	.0168	1.533	.0207	1.652	.0105	1.579	.0127	1.844	.0108	1.896	.0129	1.781	.0197	2.013	.0279	2.466	.0333	2.586	.0229	2.500	.0103	2.426	.2021
Spray EMFM Flow, pps	None	None	.0669	.0048	.1526	.0043	.2622	.0057	None	None	.0818	.0040	.1533	.0050	.2374	.0079	None	None	.1502	.0195	.2863	.0108	.5087	.0144
Pressure, Tap 1, Psia	17.57	.4989	18.16	.5028	18.25	.6249	19.47	.3582	24.93	.1962	24.59	.3262	23.74	.2423	26.36	.4544	33.59	.1086	34.30	.1866	34.58	.1178	34.93	.1659
Pressure, Tap 2, Psia	17.28	.5192	17.80	.5945	17.98	.6261	19.26	.3632	24.64	.1901	24.31	.3247	23.53	1.101	26.08	.4397	33.16	.1122	33.80	.1866	34.05	.1176	34.45	.1556
Pressure, Tap 3, Psia	17.23	.5378	17.83	.5554	17.91	.6134	19.13	.3816	24.43	.1708	24.11	.3300	23.30	.2262	25.70	1.048	33.16	.0947	33.91	.1612	34.22	.1137	34.61	.1387
Pressure, Tap 4, Psia	16.95	.5330	17.65	.4783	17.64	.5432	18.89	.4009	24.19	.1697	23.80	.3462	23.10	.2217	25.56	.4727	32.54	.0155	33.25	.1586	33.63	.1294	34.01	.1435
Pressure, Tap 5, Psia	16.34	.5005	17.13	.4652	17.09	.5815	18.30	.8042	23.48	.1568	23.08	.3381	22.47	.3041	24.88	.4799	31.42	1.366	32.24	.1381	32.65	.1455	32.96	.1444
Pressure, Tap 6, Psia	16.15	.4900	16.99	.4776	17.09	.4976	18.04	.3814	23.10	.1389	22.63	.3469	22.12	.2232	24.42	.4875	31.20	.1642	31.96	.1492	32.42	.1368	32.77	.1525
Pressure, Tap 7, Psia	15.59	.4334	16.37	.4763	16.56	.5523	17.45	.3736	22.28	.1355	21.89	.3286	21.38	.2132	23.64	.4989	30.03	.1595	30.74	.1570	31.22	.1281	31.57	.1643

TABLE IV (continued)

Nominal Temperature, °F	1450								1500								1580							
Nominal Quality, %	99		95		90		85		99		95		90		85		99		95		90		85	
Average Value	*		*		*		*		*		*		*		*		*		*		*		*	
Probable Error		*		*		*		*		*		*		*		*		*		*		*		*
Pressure, Tap 8, Psia	15.26	.3108	15.77	.4440	16.11	.4084	16.91	.3787	21.60	.1324	21.22	.2477	20.83	.2818	22.90	.4499	29.11	.1546	29.87	.1345	30.34	.0842	30.77	.1866
Pressure, Tap 9, Psia	14.46	.3648	15.16	.4679	15.49	.5273	16.21	.3384	20.67	.1214	20.28	.3055	19.86	.2252	21.99	.4596	27.75	.1419	28.43	.1469	28.87	.1092	29.27	.1554
Pressure, Tap 10, Psia	13.21	.3084	13.79	.4033	14.21	.3734	14.97	.3550	18.72	.1333	18.61	.2233	18.32	.2481	20.22	.3977	25.25	.1388	26.28	.1134	26.80	.0606	27.24	.1497
Pressure, Tap 11, Psia	11.20	.2906	11.62	.3483	12.06	.3848	12.63	.2999	15.86	.1400	15.76	.2213	15.54	.3099	17.07	.3457	21.35	.1149	21.96	.1038	22.38	.0533	22.84	.1503
Pressure, Tap 12, Psia	9.911	.2675	10.34	.3238	10.93	.5911	11.27	.2968	13.97	.1090	14.09	.2885	13.86	.3454	15.28	.3124	10.09	.1322	19.79	.1008	20.31	.0721	20.70	.1190
Pressure, Tap 13, Psia	9.072	.2533	9.439	.2592	9.847	.3947	10.30	.2586	12.93	.1207	12.90	.3012	12.79	.3954	14.05	.2834	17.44	.1109	17.86	.0889	18.27	.0487	18.75	.1330
Pressure, Tap 14, Psia	7.366	.2351	7.919	.2660	8.675	.7709	9.004	.3019	10.30	.1125	10.82	.2984	10.66	.1787	12.05	.2816	13.98	.1386	15.36	.1223	16.08	.0834	16.66	.1434
Pressure, Tap 15, Psia	6.982	.1878	7.292	.2821	8.157	.9057	8.297	.3944	9.857	.1246	10.00	.2840	9.869	.1461	11.24	.3285	13.43	.1302	13.99	.1434	14.66	.0887	15.30	.1895
Pressure, Tap 16, Psia	5.809	.2420	6.224	.3439	7.112	1.044	7.517	.4838	8.519	.1633	8.509	.2699	8.517	.1717	10.09	.3797	15.11	.4587	14.56	.1982	15.20	.0715	15.34	.0983
Pressure, Tap 17, Psia	7.800	.4868	7.263	.6297	7.568	.7193	8.377	.4938	13.08	.3810	12.01	.2437	11.12	.1928	12.37	.3085	16.79	.2351	16.71	.2110	16.69	.1138	16.32	.1192
Pressure, Tap 18, Psia	9.045	.2997	8.311	.7068	8.165	.5199	8.691	.3183	12.38	.1329	12.24	.1216	11.51	.1632	12.36	.2615	15.98	.1620	16.23	.1121	16.38	.0953	16.03	.1078

TABLE V

PRACTICE CASING, INTERNAL MEASUREMENTS

Location	Dimension Position	As Clamped, Inch	Dimensional Change, Inch x 10^3						
			After Tack Welds 1 through 6	After Tack Welding Welding	After Welds 1, 2, 3, and 4	After Welds 5, 6, 7, and 8	After Welds 9 and 10	Final Dimensions After Welding	After 16 hours
A	1	11.570	+5	+2	+3	+2	--	+5	+3
	2	11.570	+5	+3	+4	+4	--	+9	+7
	3	11.569	+1	+4	-1	-2	+4	+3	0
	4	11.570	+4	+3	+4	+4	--	+8	+1
B	1	10.284	+8	+3	+4	+4	+3	+5	+3
	2	10.284	+3	+2	+4	+4	+5	+7	+6
	3	10.282	-10	+1	-5	-5	-1	-2	-4
	4	10.283	+4	+2	+3	+4	+3	+7	+5
C	1	10.292	+6	+2	+3	+3	--	+2	+1
	2	10.292	+2	+1	+2	+3	--	+5	+4
	3	10.289	-6	0	-3	-4	-1	-4	-5
	4	10.289	+4	+2	+3	+4	--	+5	+4

TABLE VI

SUMMARY OF HYDRODYNAMIC SEAL TESTS IN AIR AND WATER

Item	Pressure P1 psia	Pressure P5, P6 psia	Pressure P8 psia	Water flow ppm	Speed rpm	Resistance of	Figure
1.	14.7	sealed	sealed	0	5000	Screw seal	33
2.	sealed	14.7	sealed	0	5000	Oil labyrinth, lube outlet pipes and close-gap seal	34
3.	sealed	sealed	14.7	0	5000	Argon inlet manifold, potassium labyrinth, argon-potassium outlet manifold	35
4.	sealed	sealed	14.7	8.5	5000	Argon-potassium outlet manifold	36
5.	sealed	sealed	14.7	13.5	5000	Argon-potassium outlet manifold	37
6.	sealed	sealed	14.7	16.2	5000	Argon-potassium outlet manifold	38

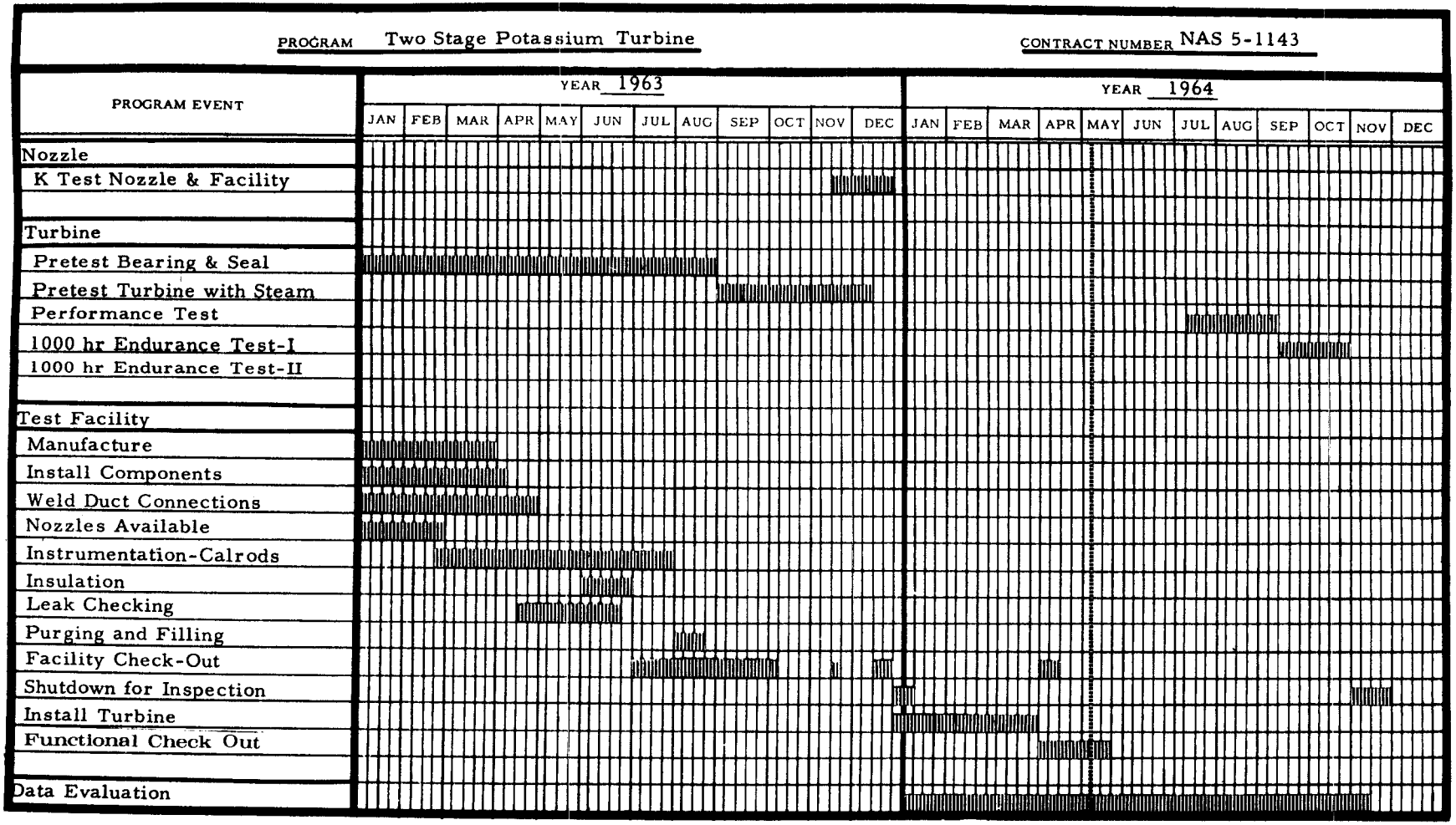

Figure 1. Program Schedule

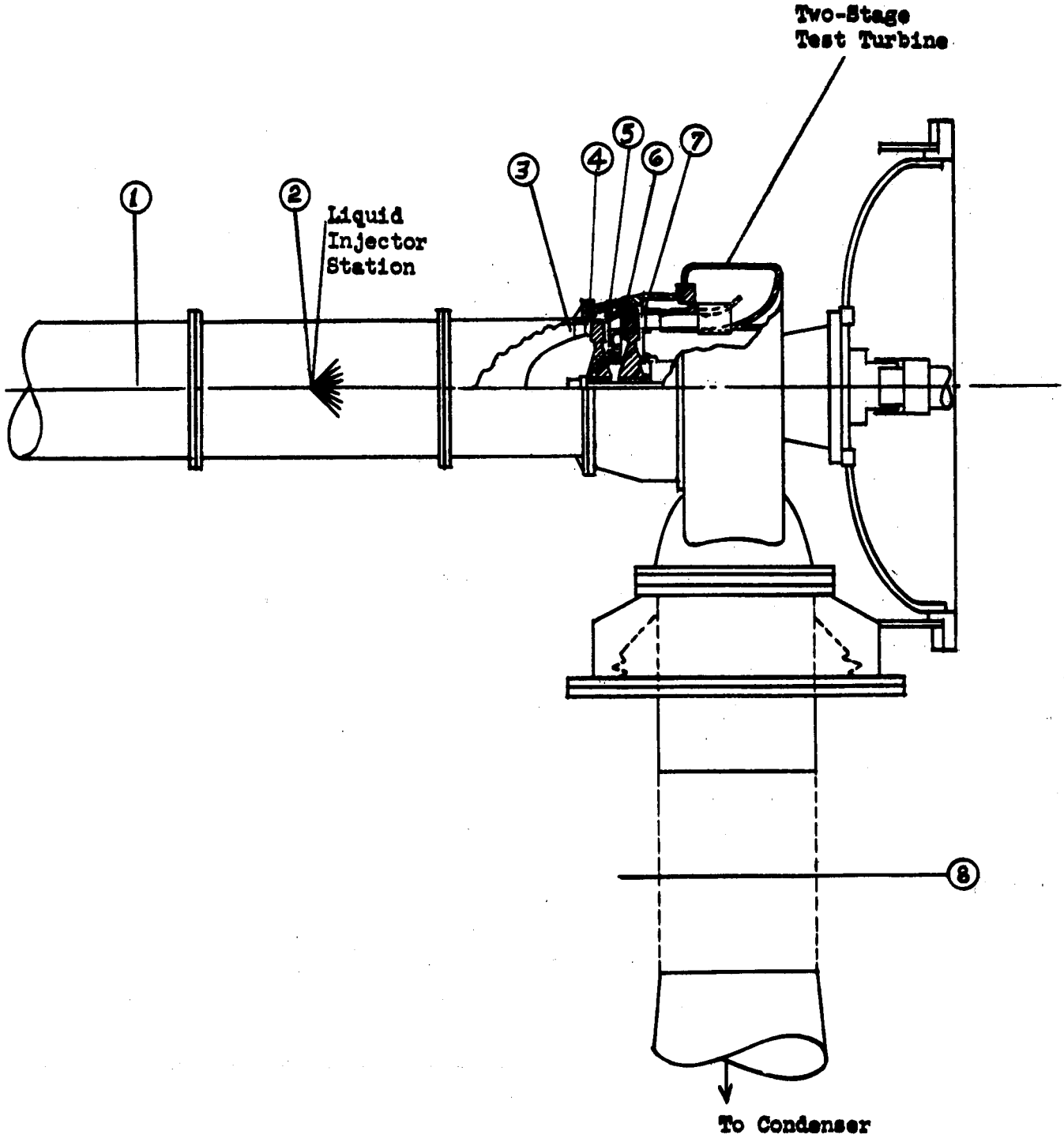

Figure 2. Instrumentation Stations

Note: All total pressure and total temperature sensors arranged in equal area annuli.

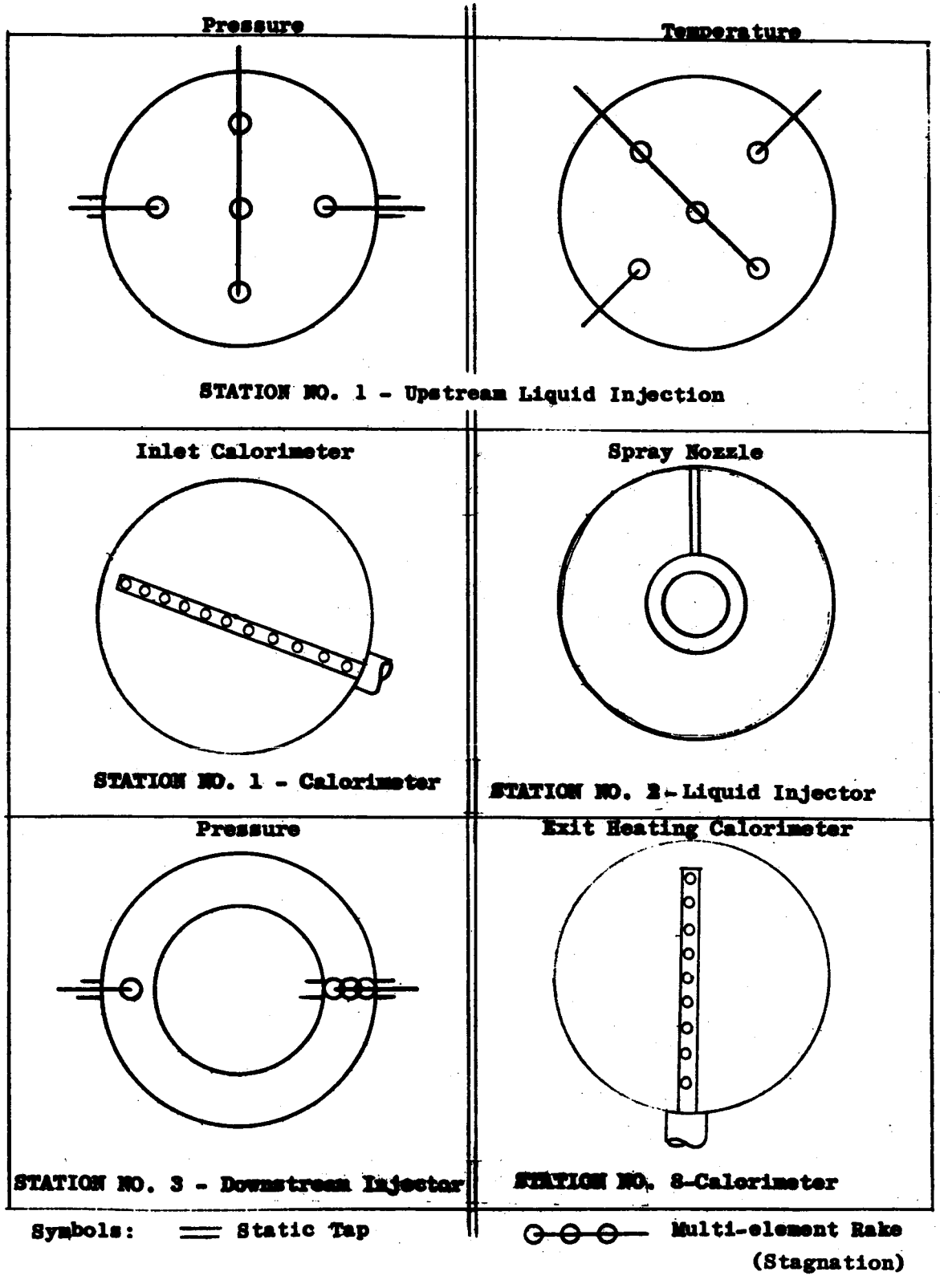

Figure 3. Potassium Test Turbine Instrumentation Location

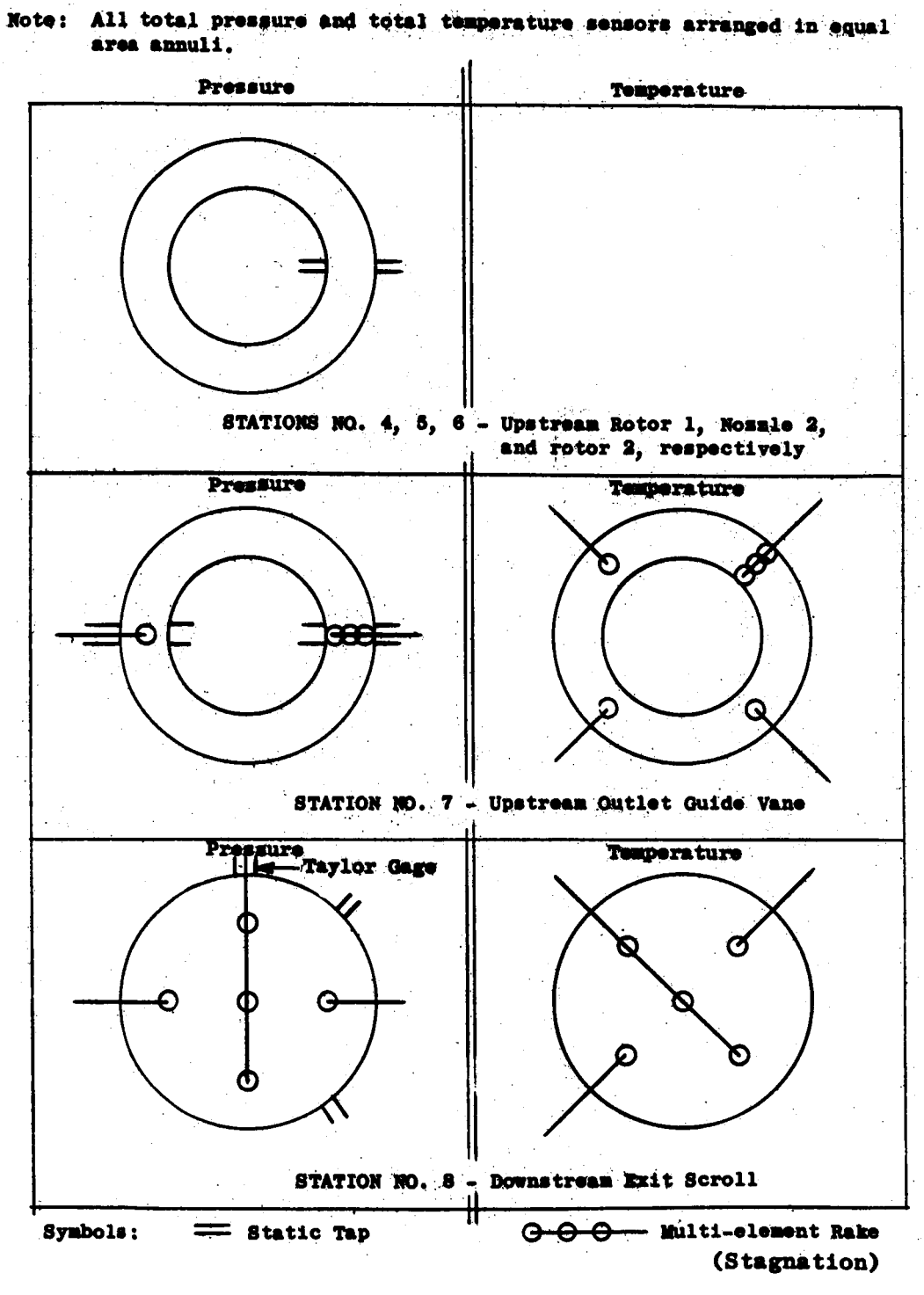

Figure 4. Potassium Test Turbine Insturmentation Location

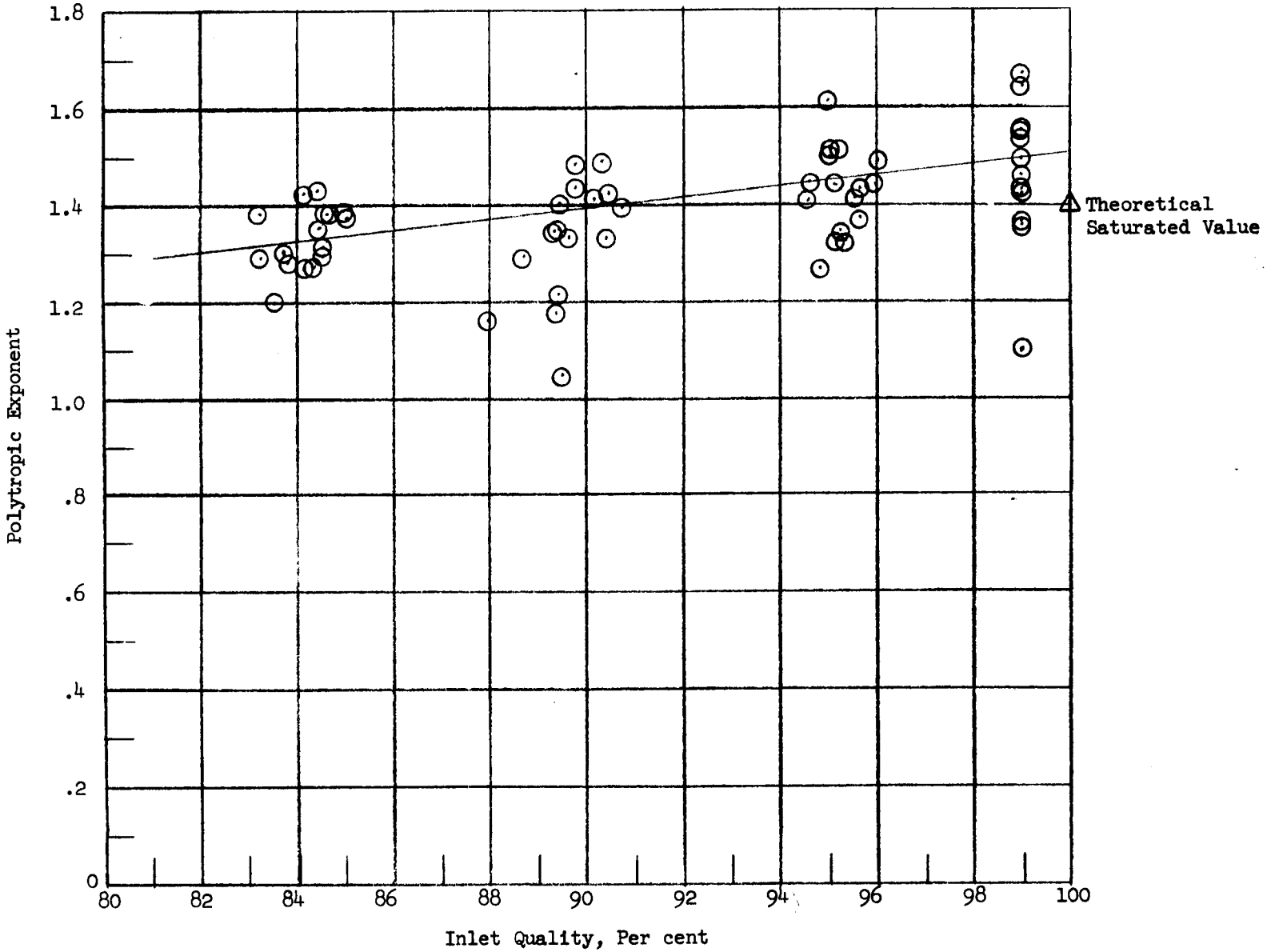

Figure 5a. Average Inlet to Throat Polytropic Exponent Versus Inlet Quality. Inlet Throat Temperature, 1450°F.

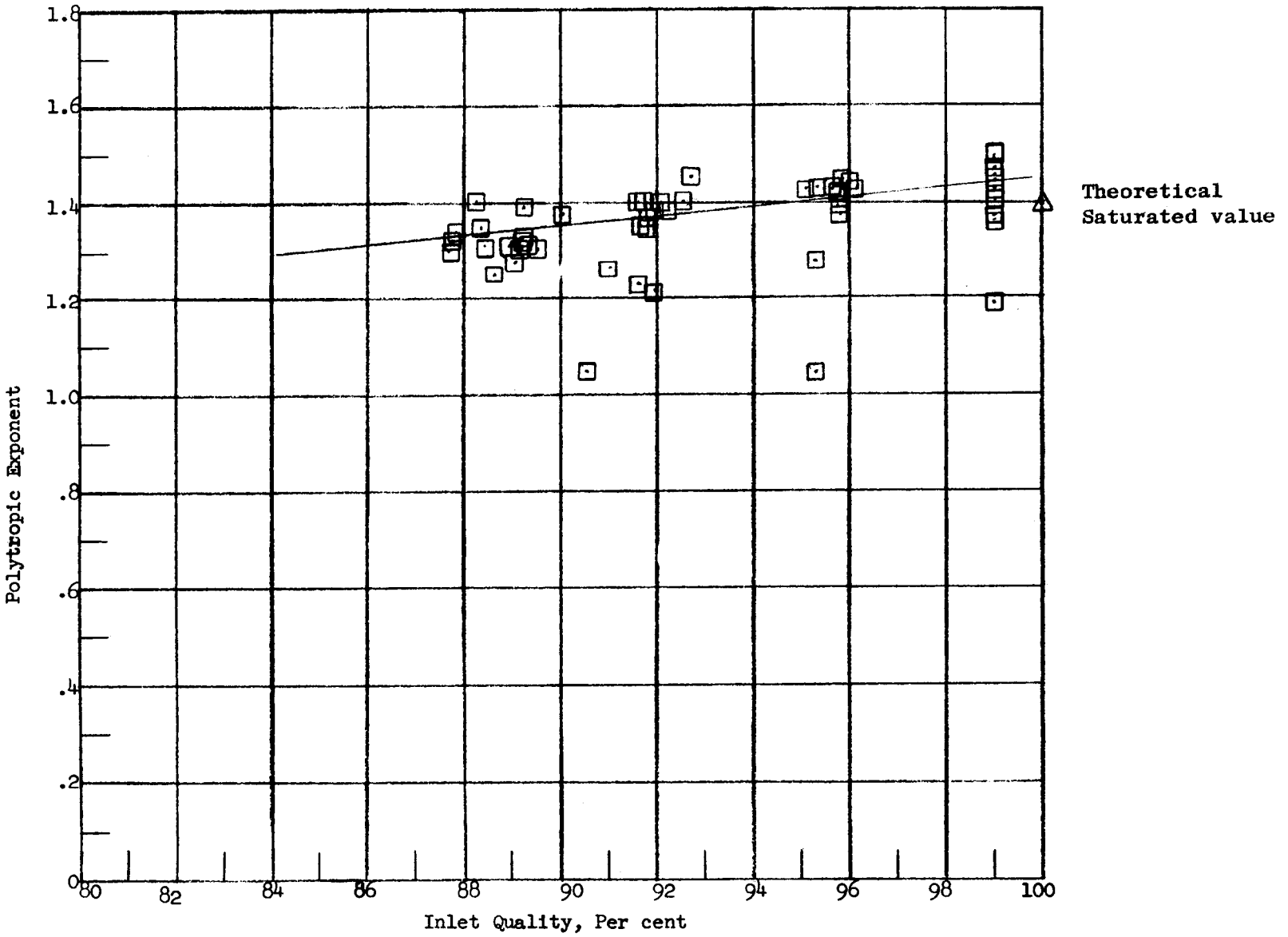

Figure 5b. Average Inlet to Throat Polytropic Exponent Versus Inlet Quality. Inlet Total Temperature, 1500°F.

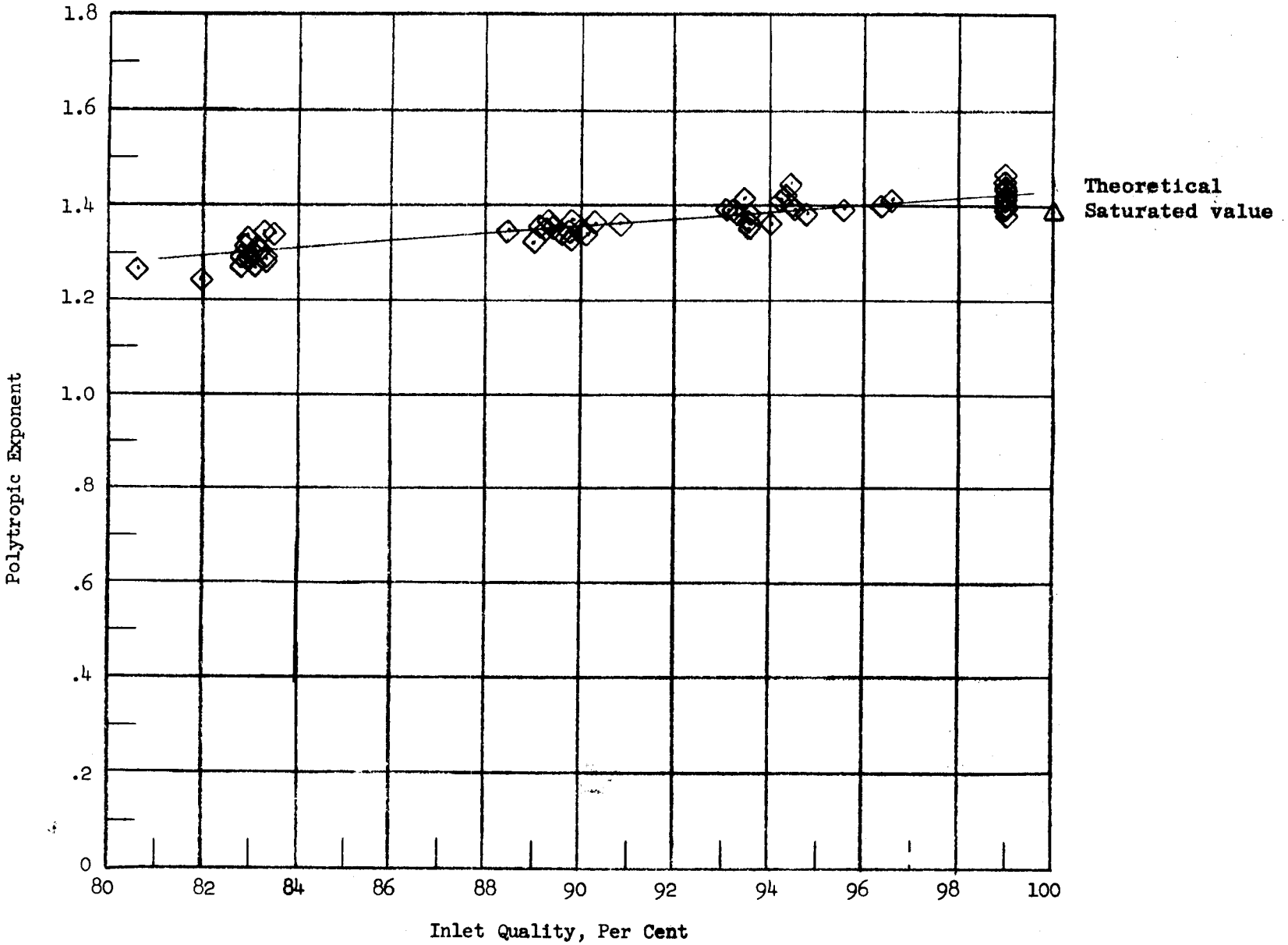

Figure 5c. Average Inlet to Throat Polytropic Exponent Versus Inlet Quality. Inlet Total Temperature, 1580°F.

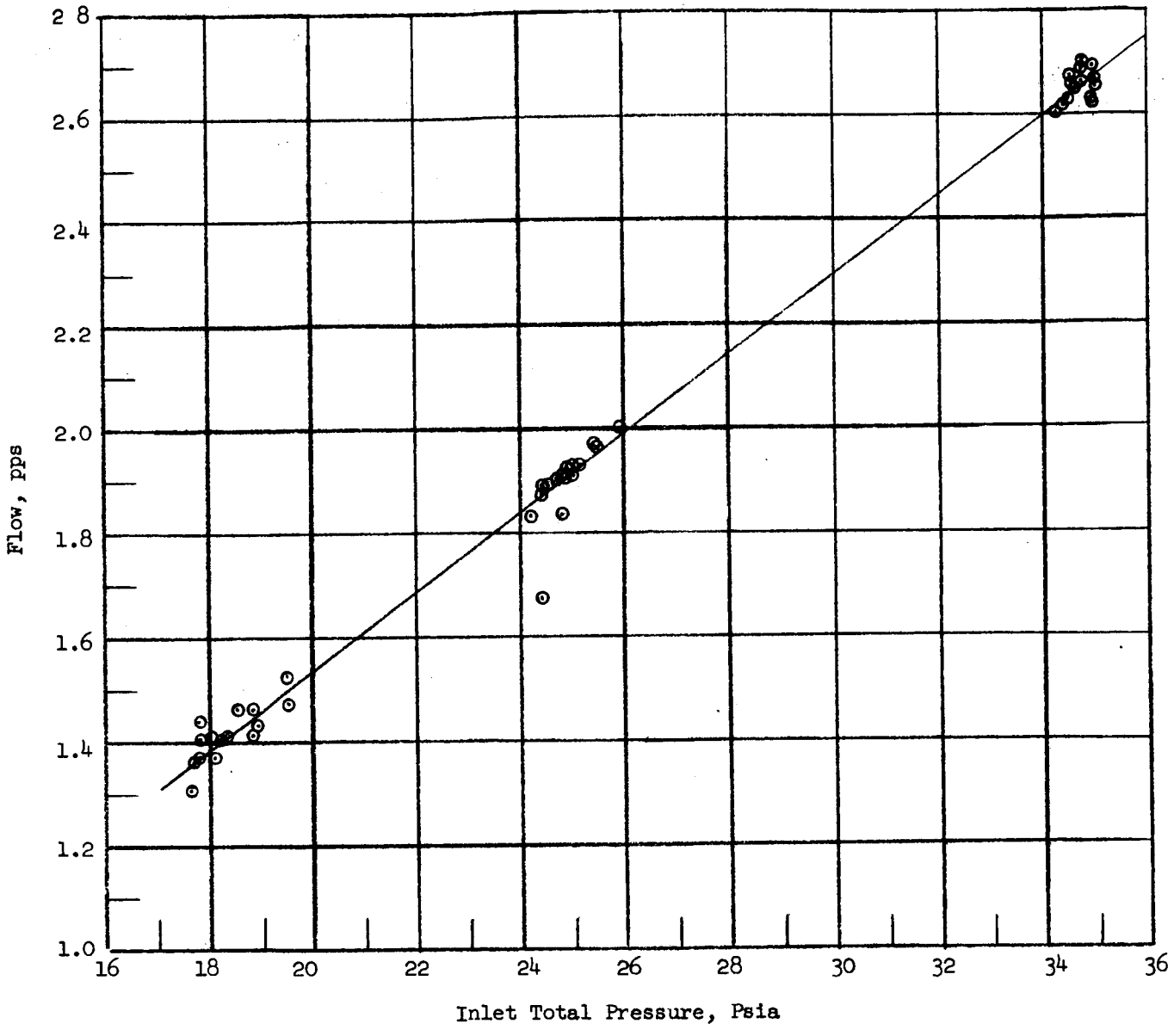

Figure 6a. C-D Nozzle Critical Flow Versus Inlet Total Pressure. Inlet Quality, 99%.

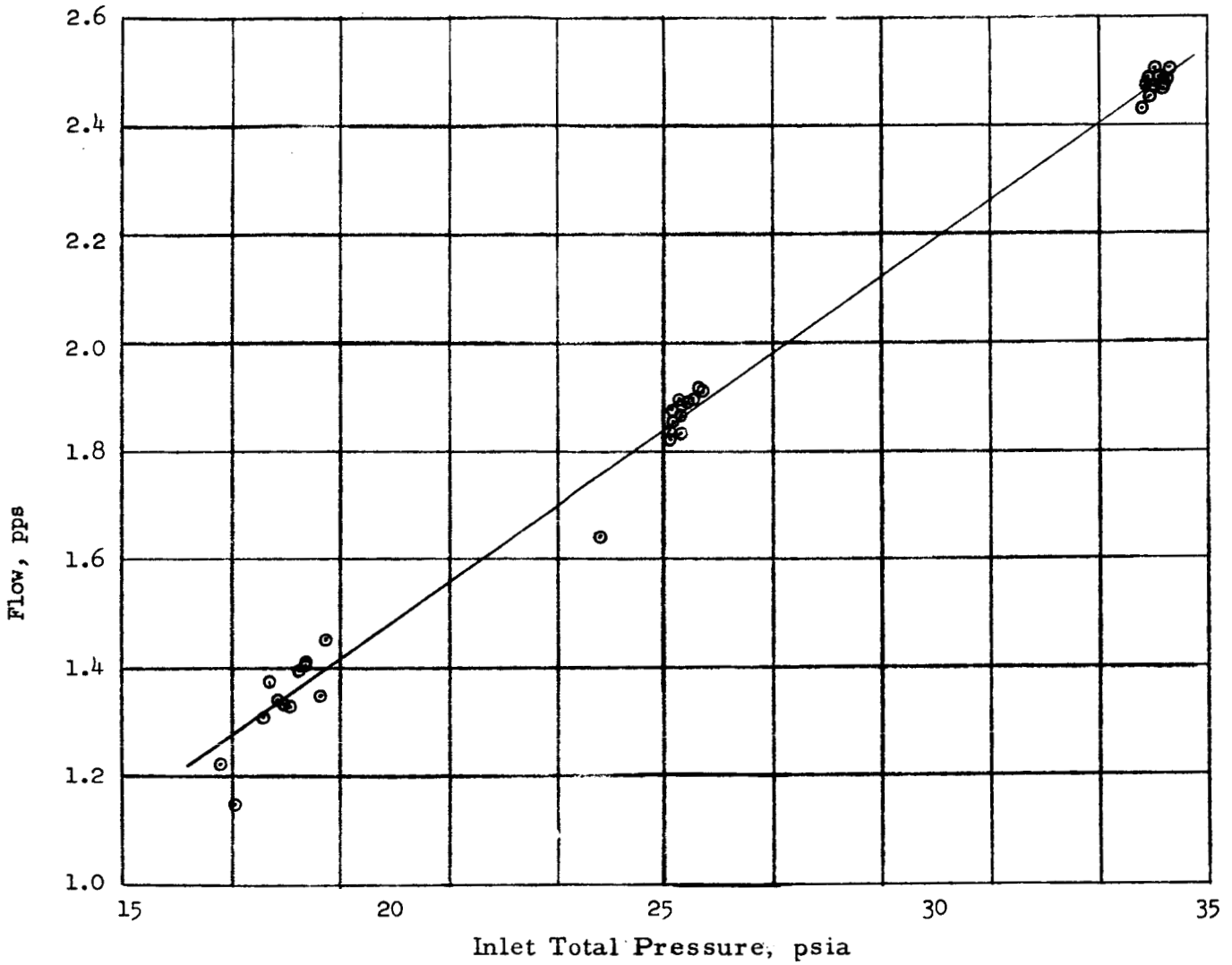

Figure 6b. C-D Nozzle Critical Flow Versus Inlet Total Pressure. Inlet Quality, 95%.

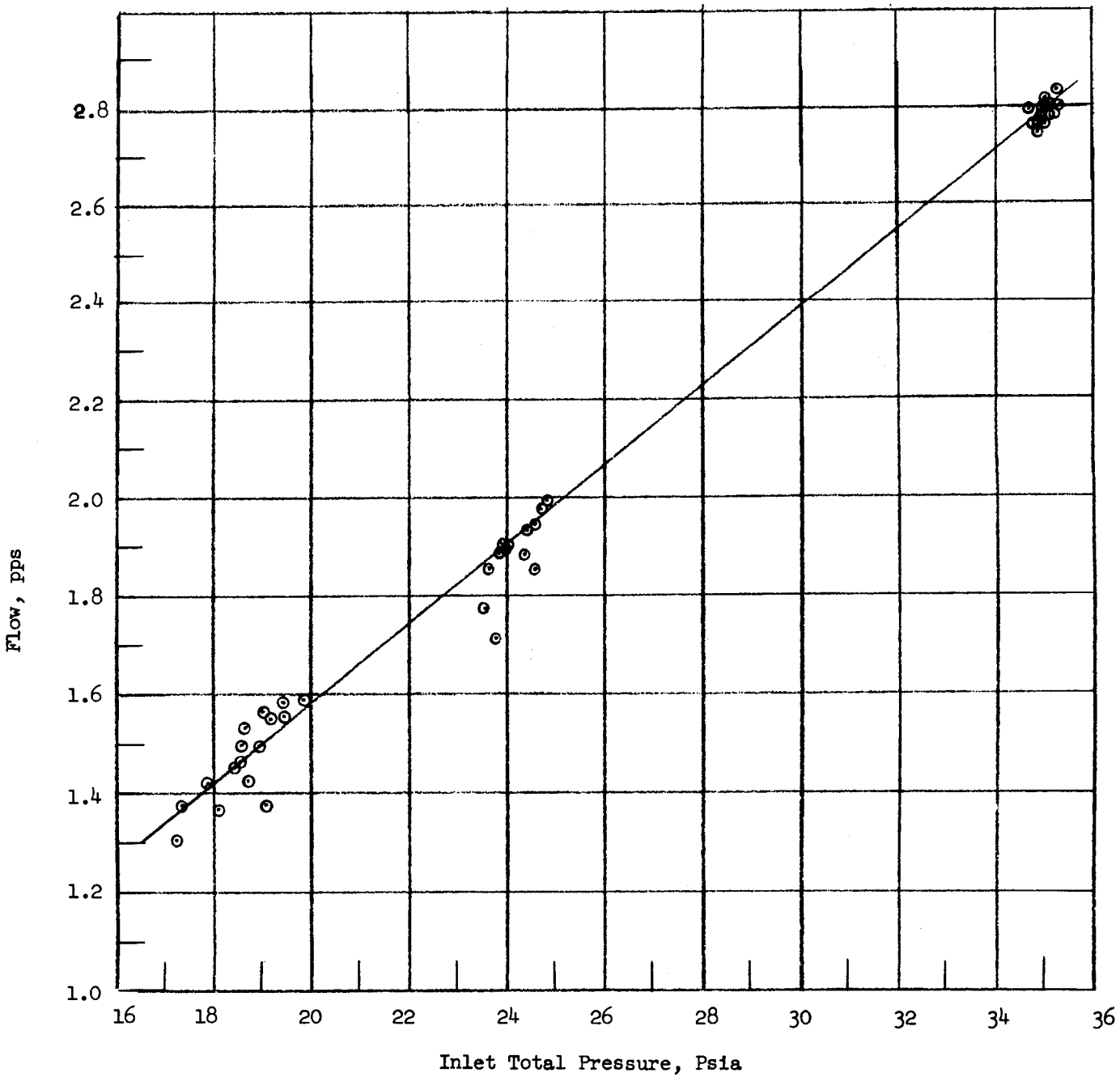

Figure 6c. C-D Nozzle Critical Flow Versus Inlet Total Pressure. Inlet Quality, 90%.

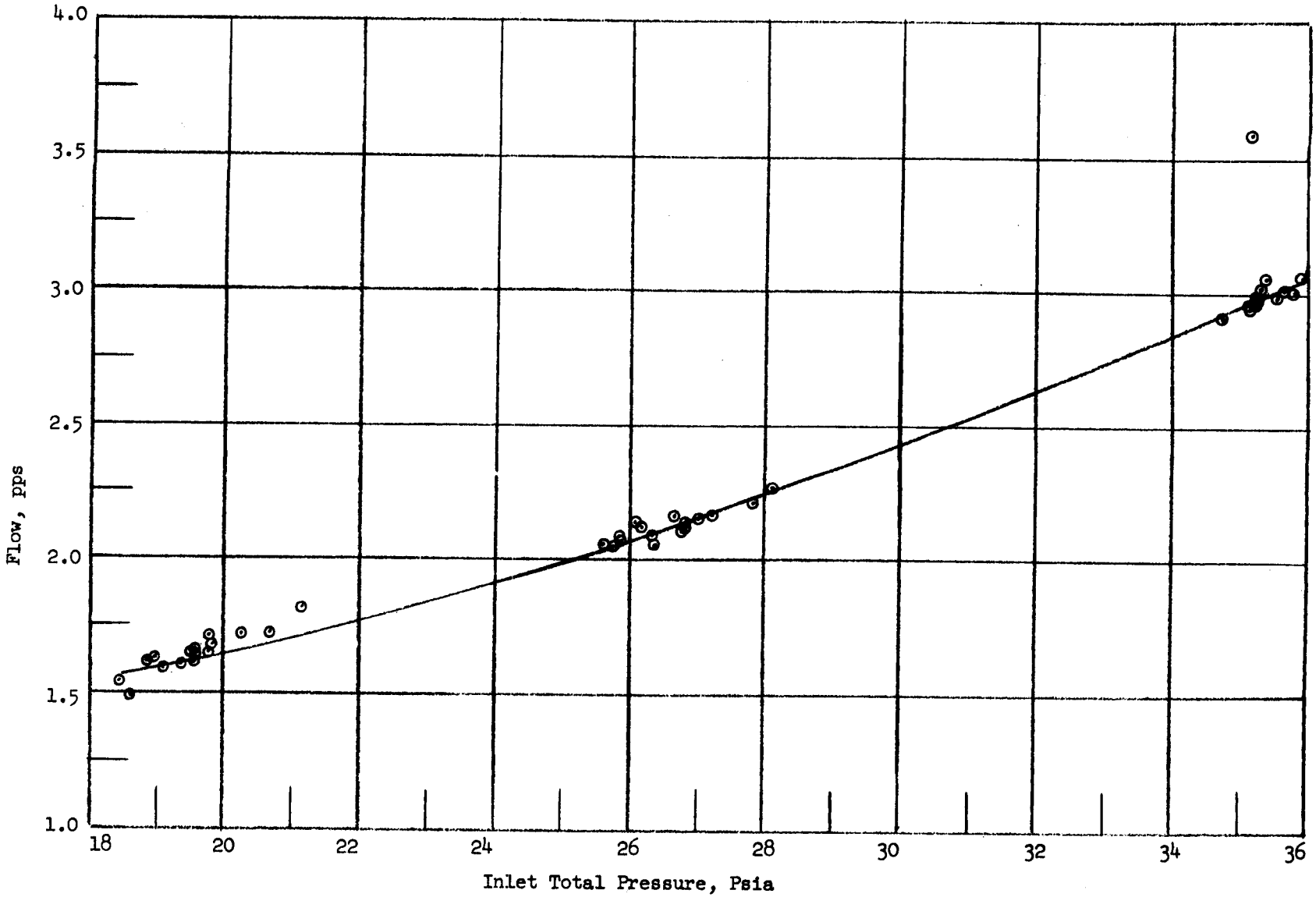

Figure 6d. C-D Nozzle Critical Flow Versus Inlet Total Pressure. Inlet Quality, 85%.

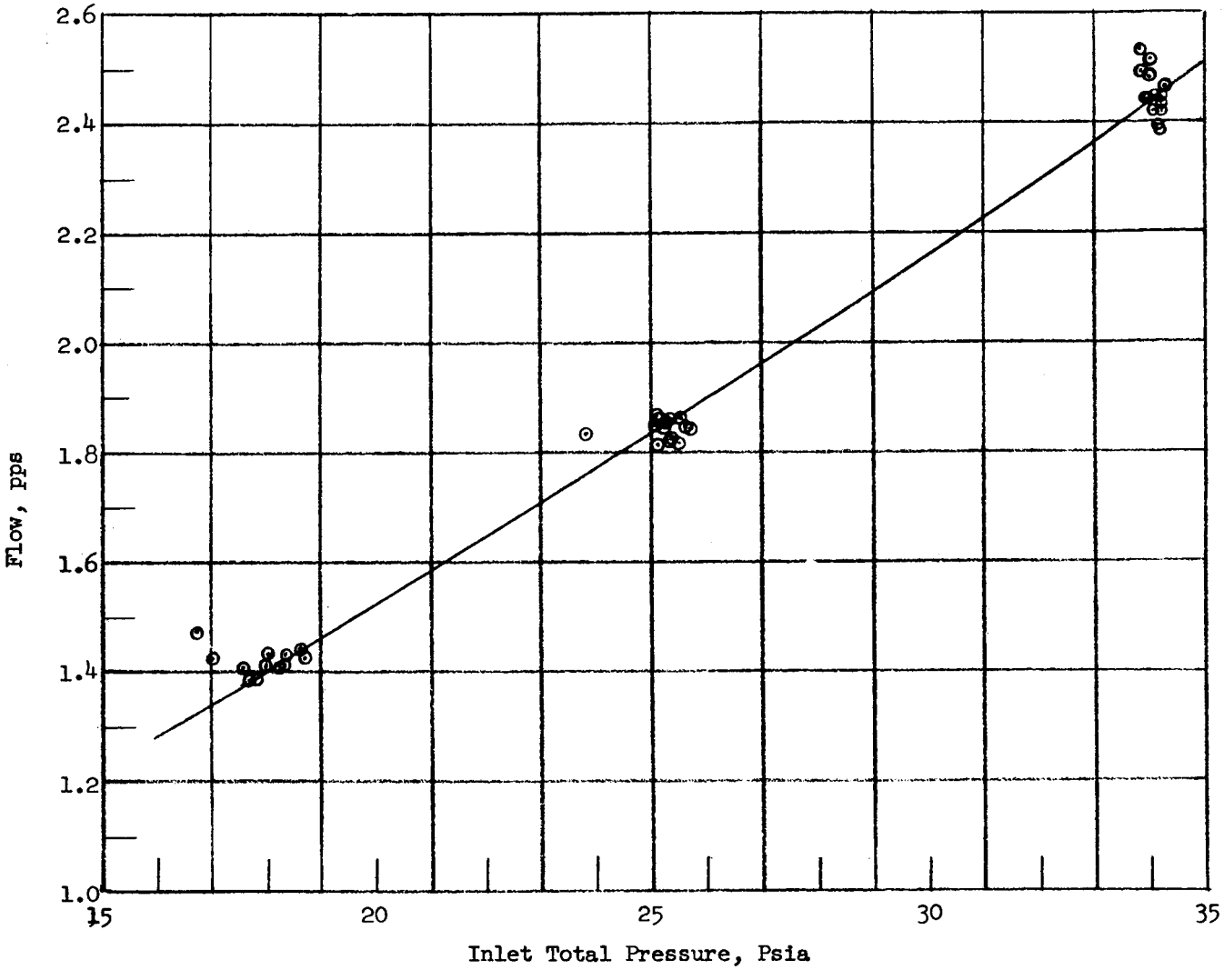

Figure 7a. Electromagnetic Flowmeter Flow Versus Inlet Total Pressure. Inlet Quality, 99%.

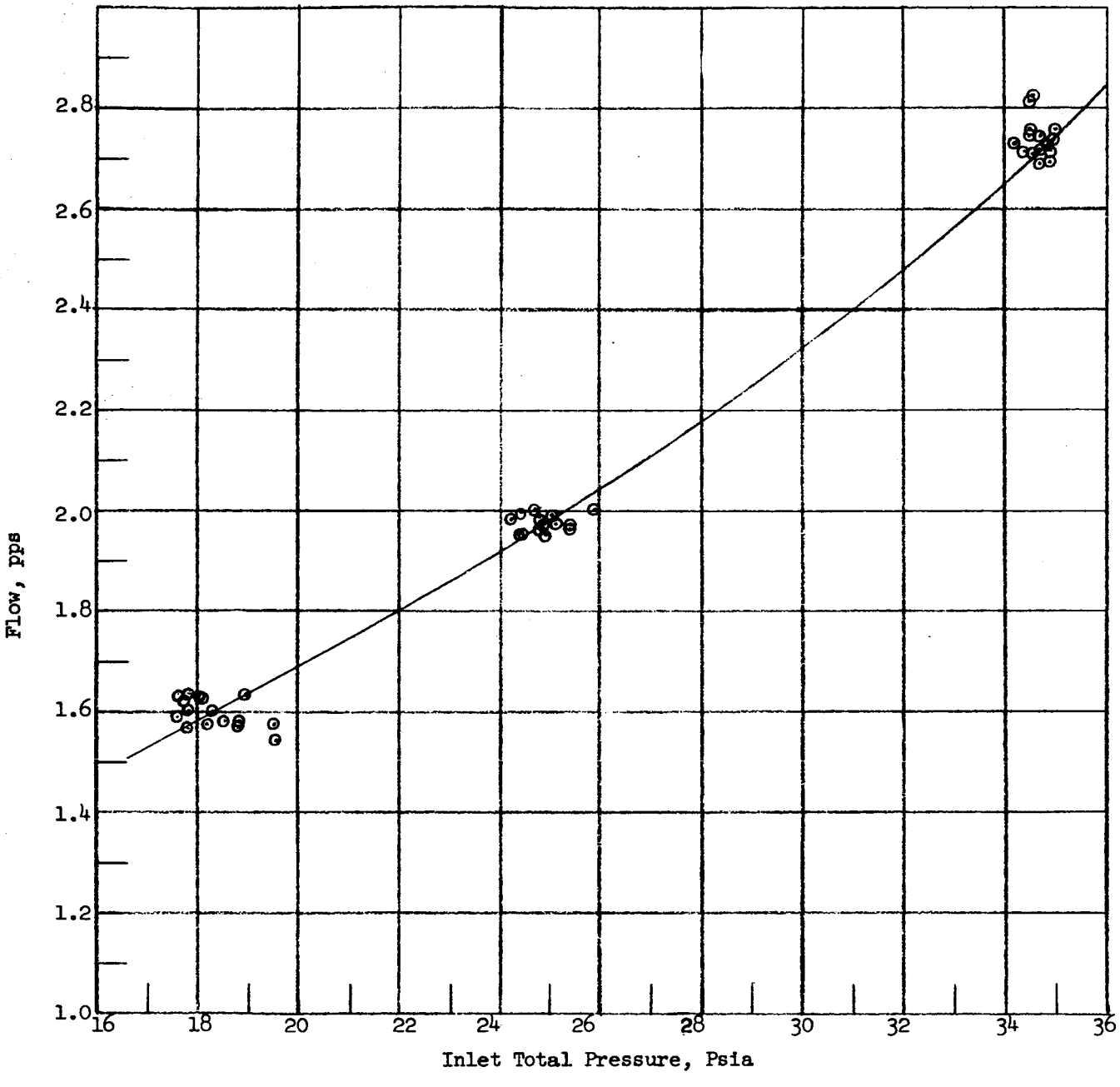

Figure 7b, Electromagnetic Flowmeter Flow Versus Inlet Total Pressure. Inlet Quality, 95%.

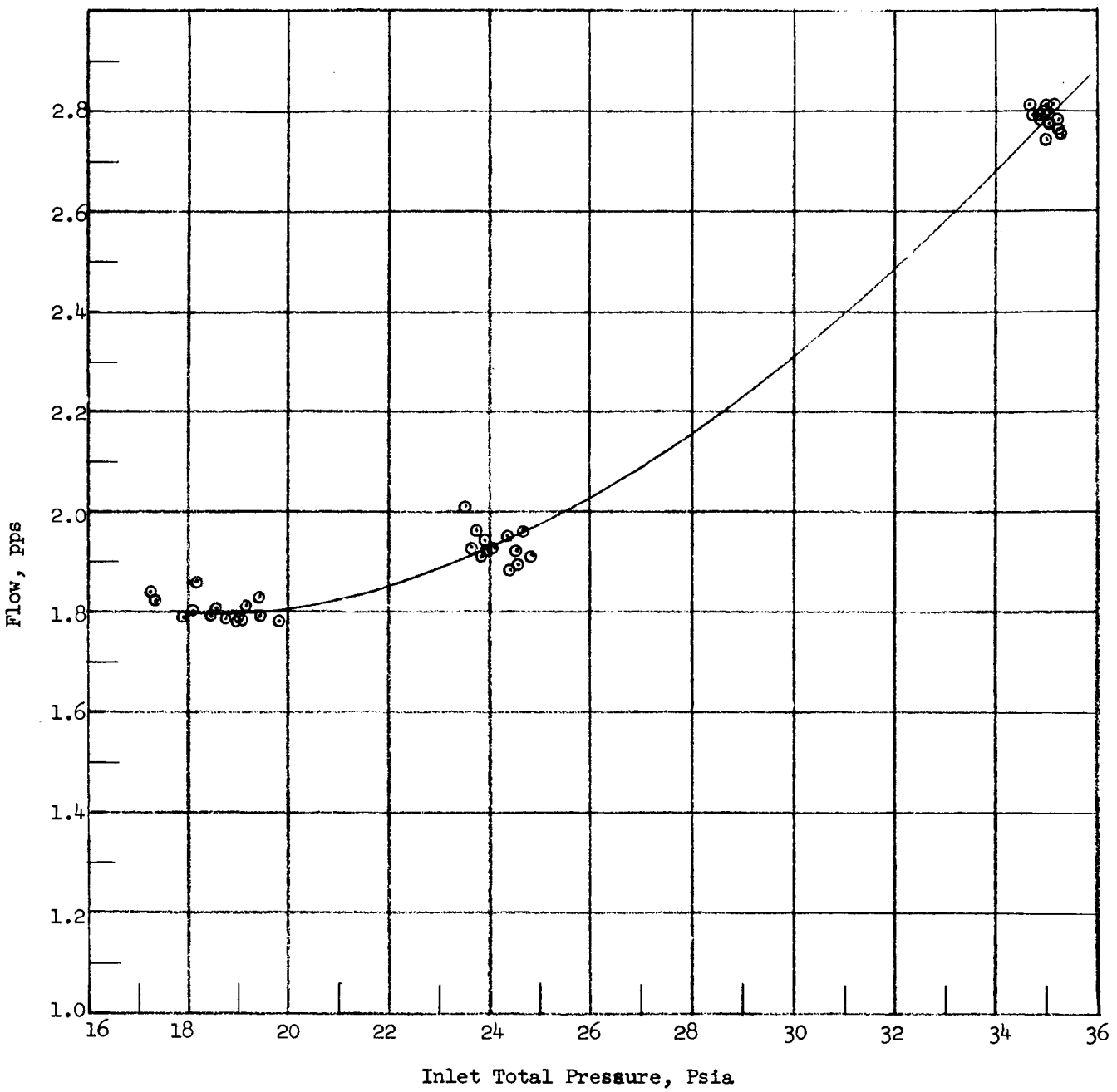

Figure 7c. Electromagnetic Flowmeter Flow Versus Inlet Total Pressure. Inlet Quality, 90%.

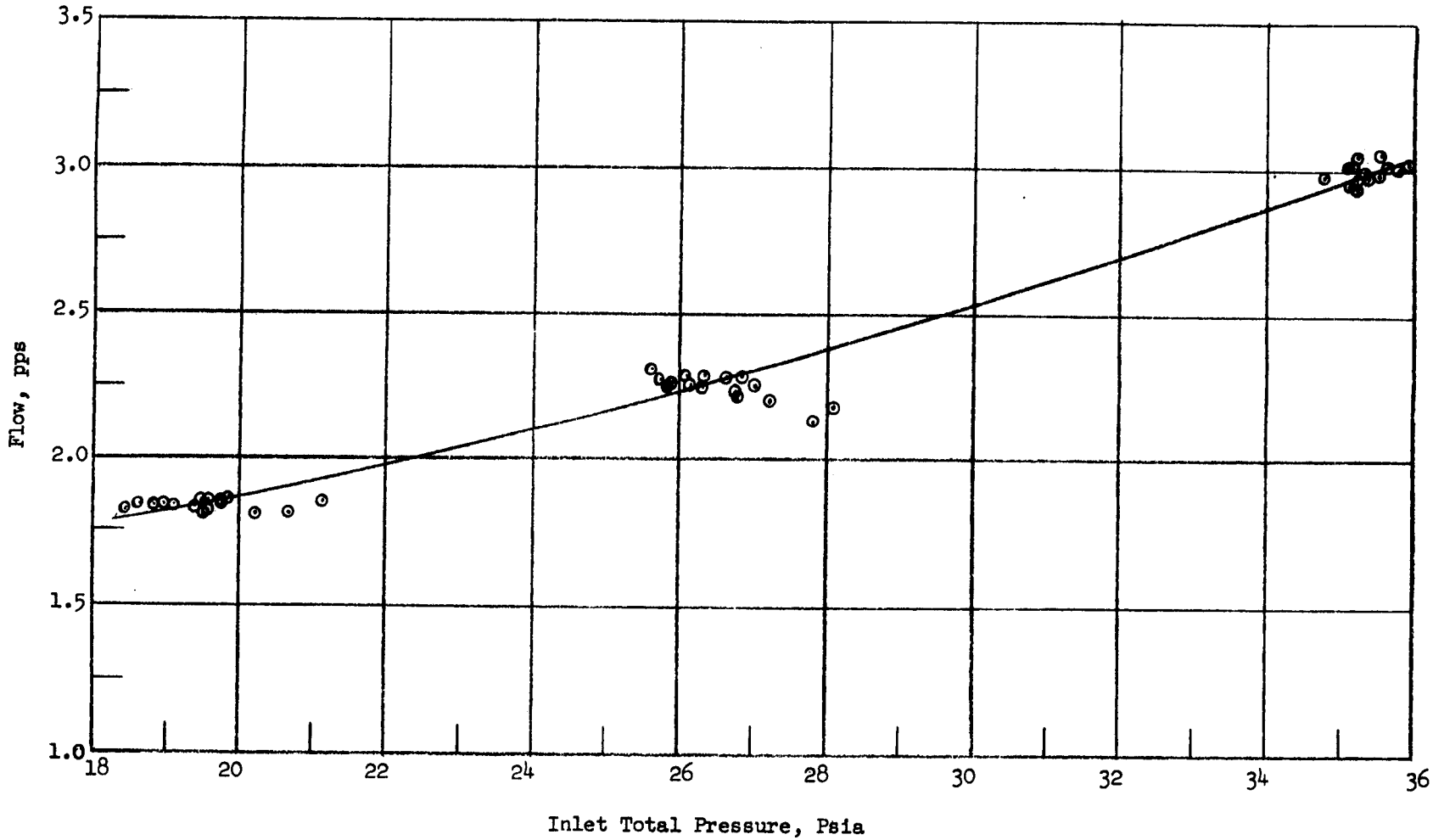

Figure 7d. Electromagnetic Flowmeter Flow Versus Inlet Total Pressure. Inlet Quality, 85%.

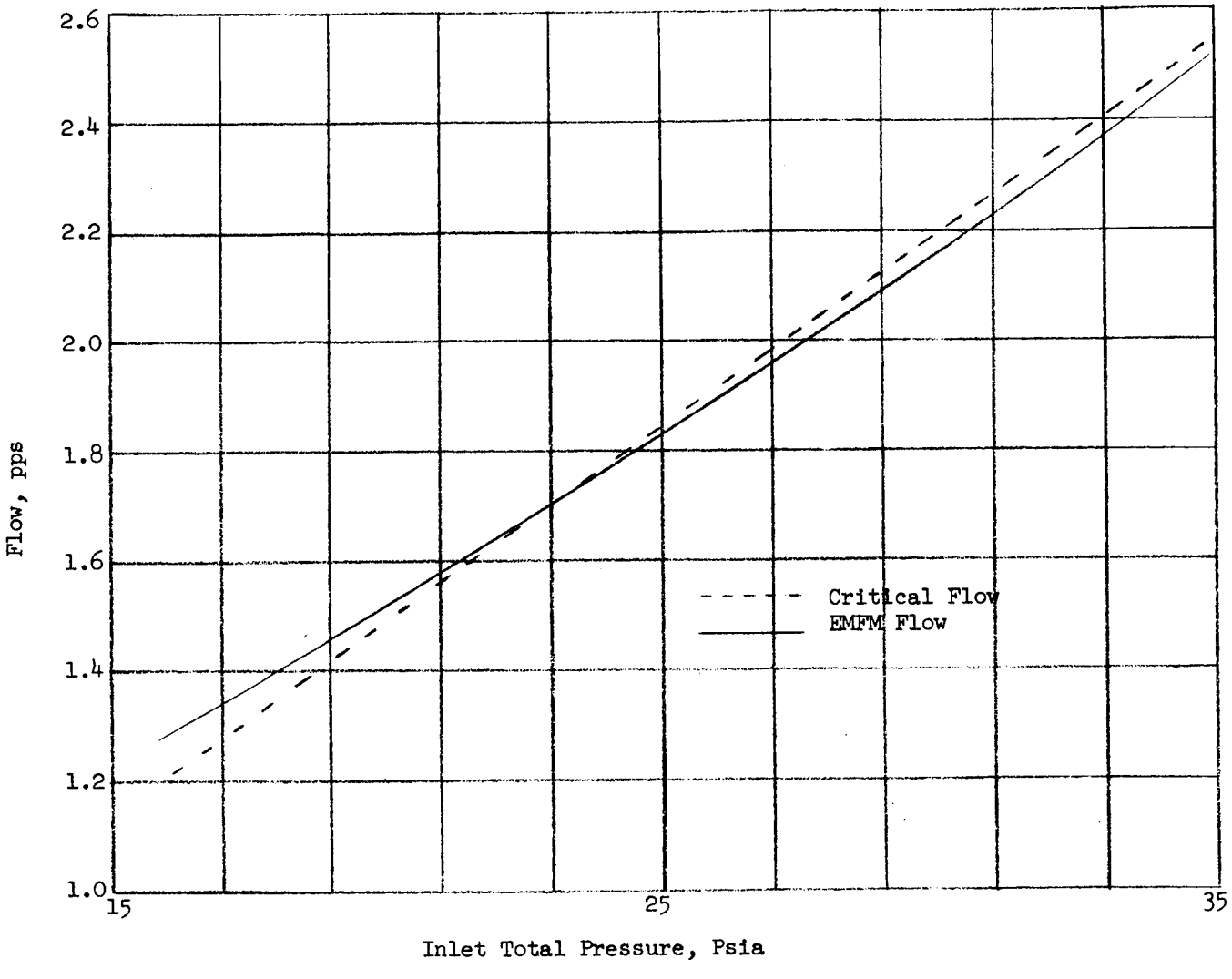

Figure 8a. Comparison of EMFM Flow and C-D Nozzle Critical Flow. Inlet Quality, 99%.

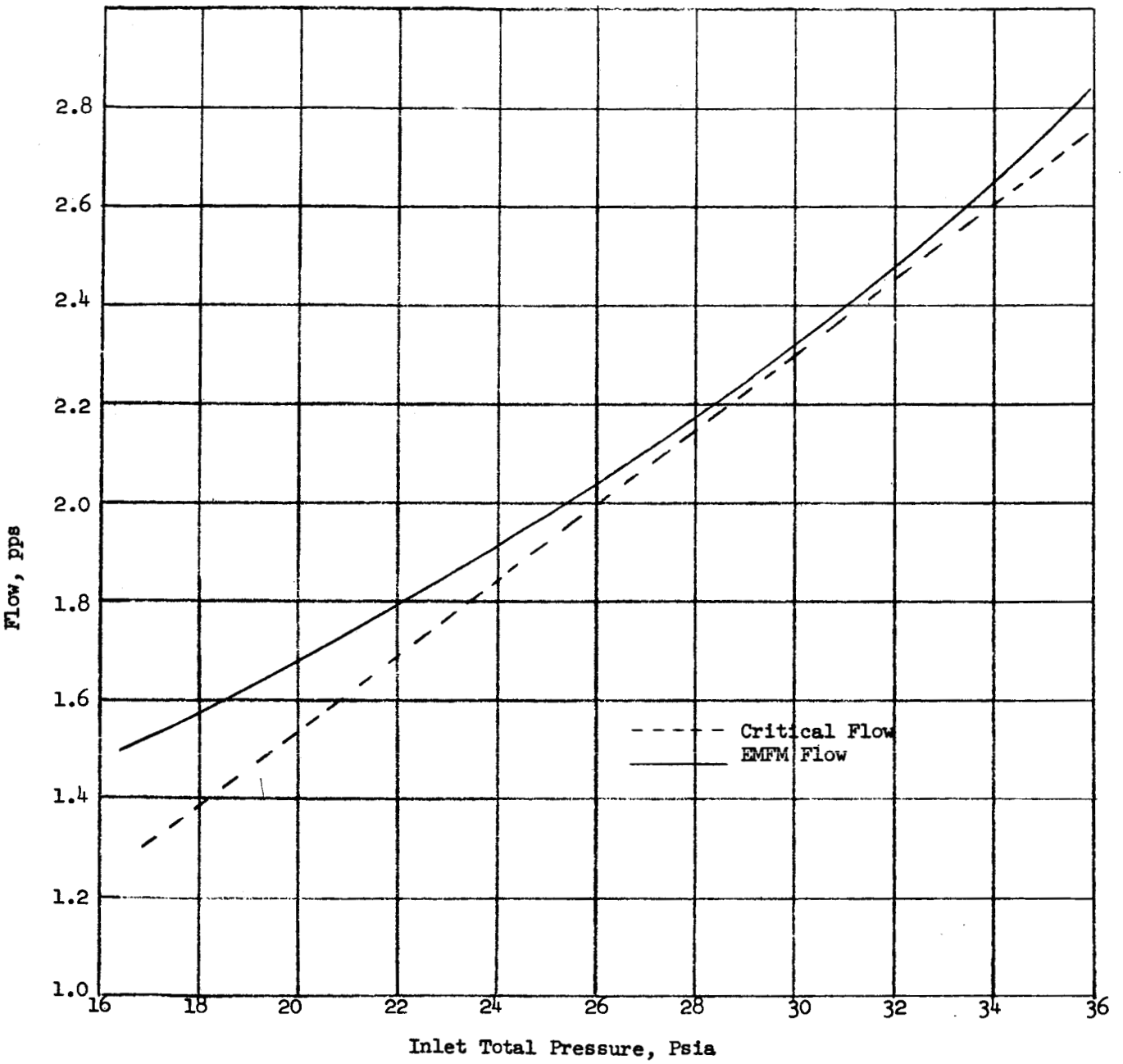

Figure 8b. Comparison of EMFM and C-D Nozzle Critical Flow. Inlet Quality, 95%.

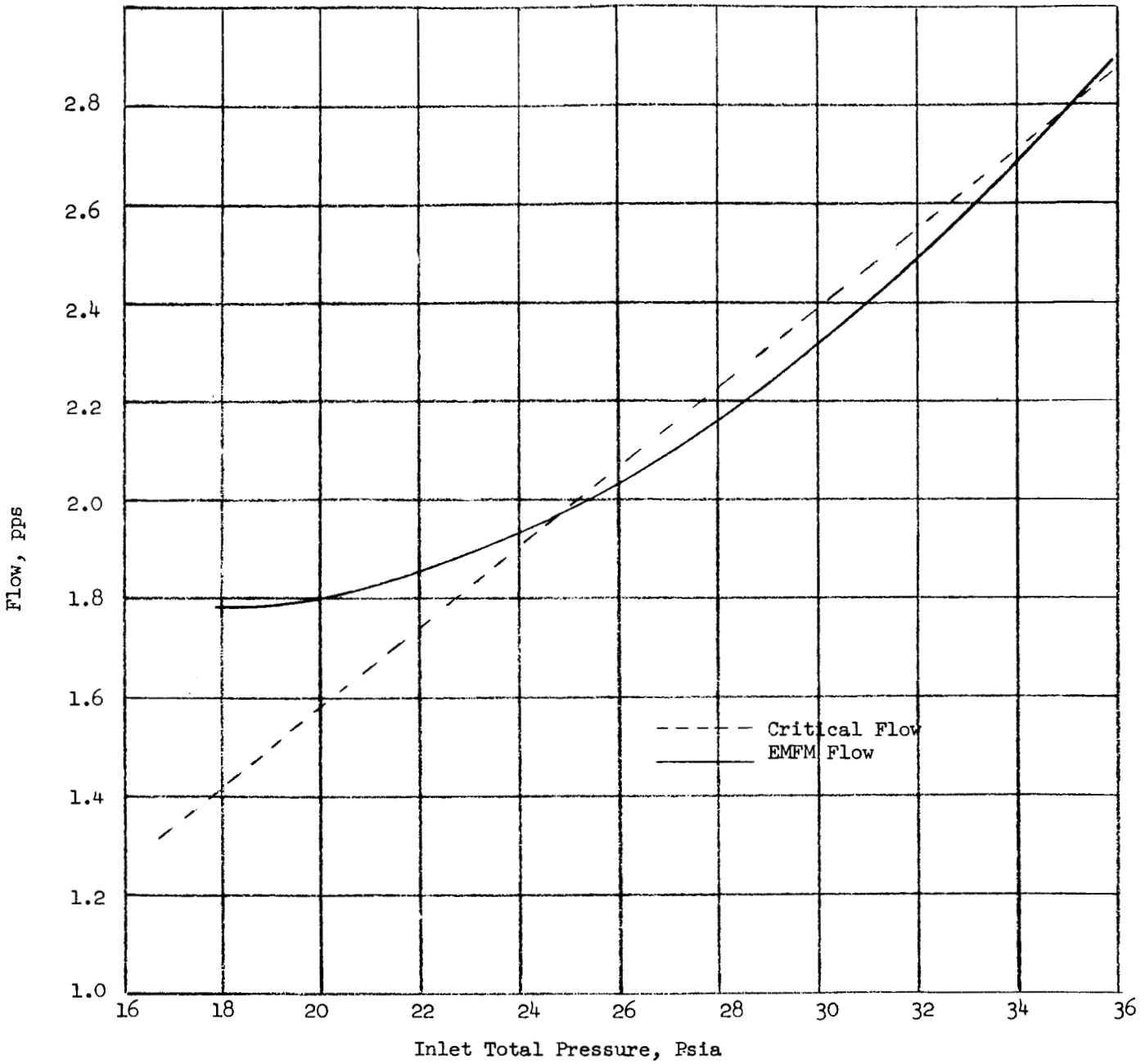

Figure 8c. Comparison of EMFM Flow and C-D Nozzle Critical Flow. Inlet Quality, 90%

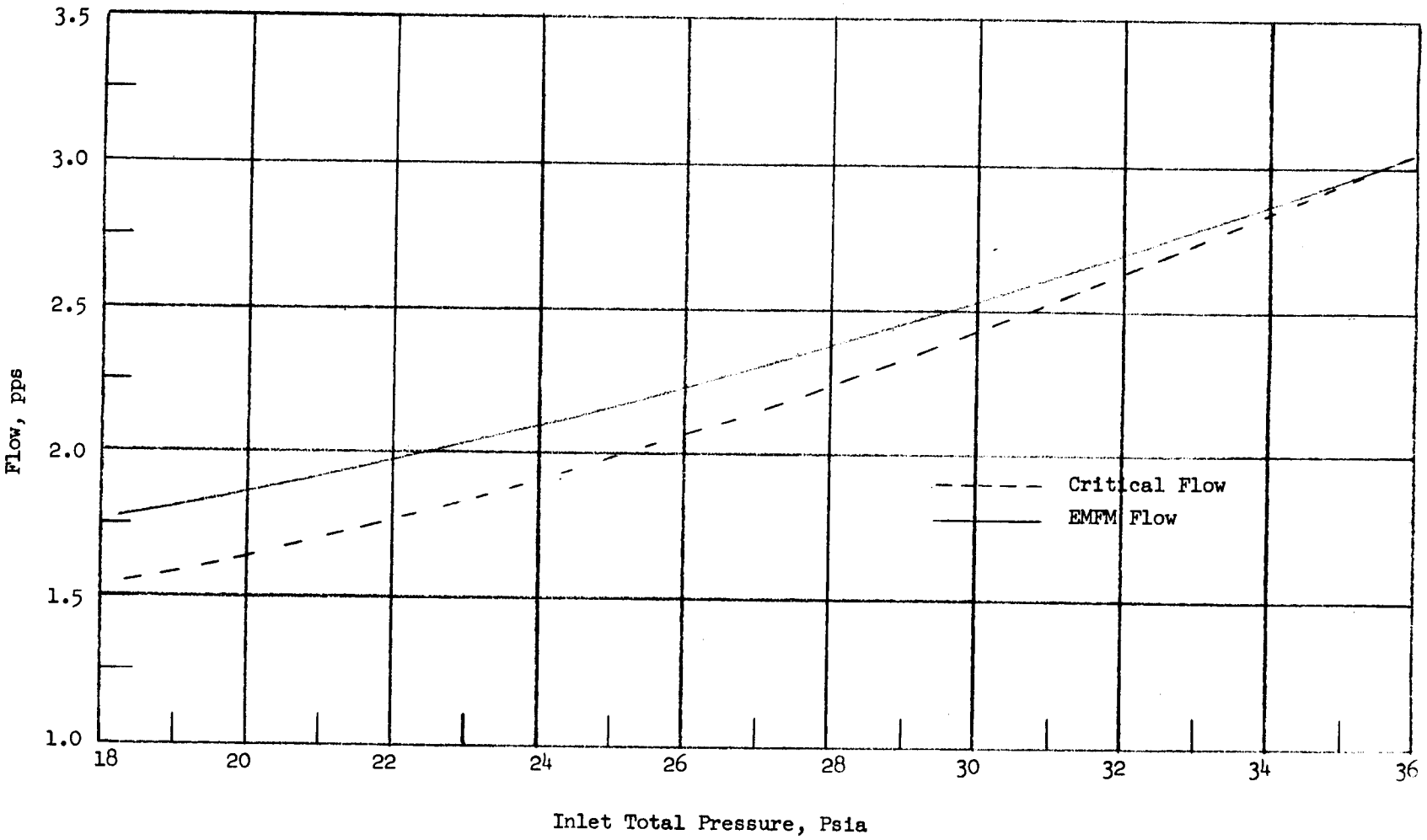

Figure 8d. Comparison of EMFM Flow and C-D Nozzle Critical Flow. Inlet Quality, 85%.

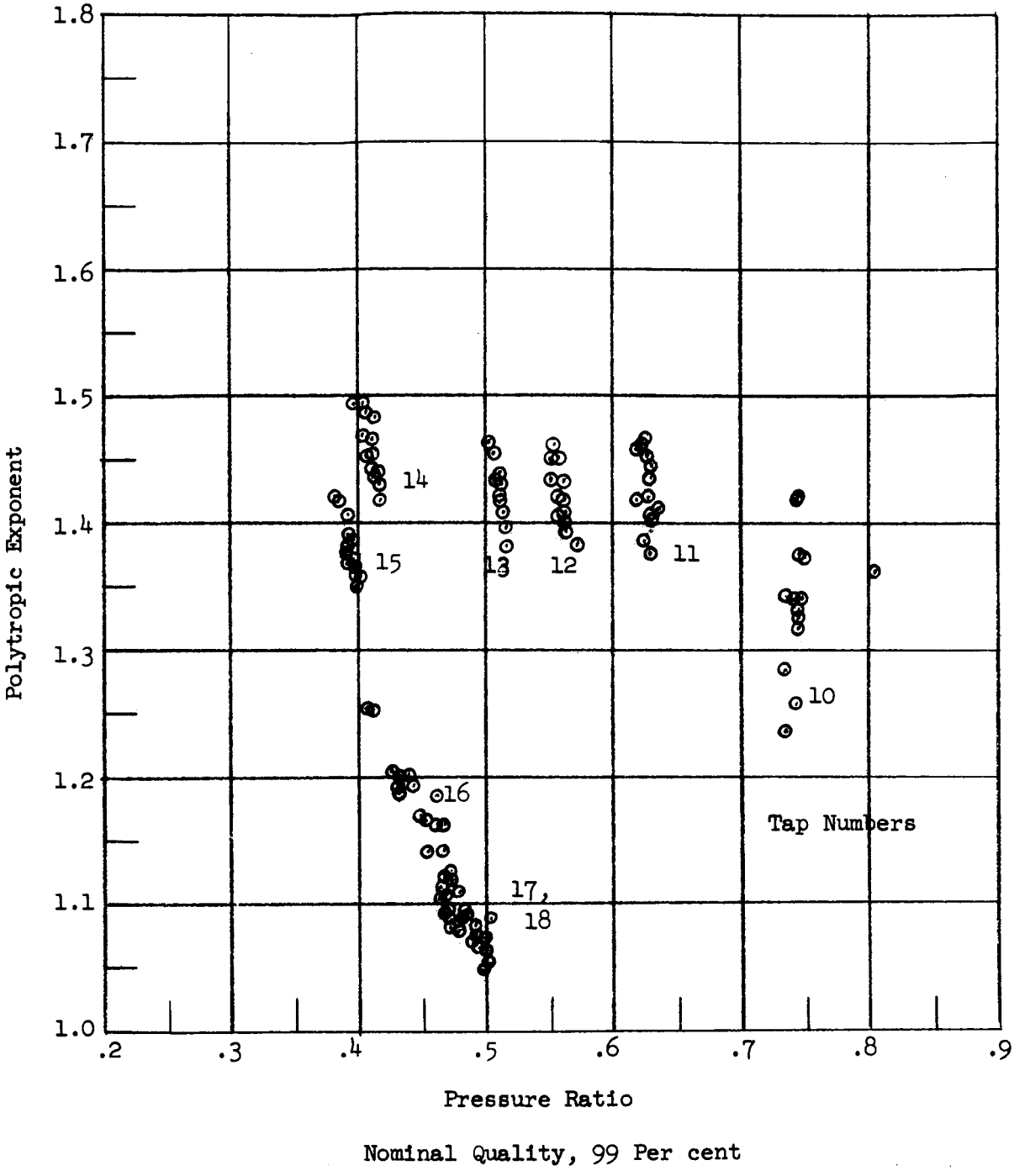

Figure 9a. Variation of Average Inlet to Throat Polytropic Exponent With Static to Total Pressure Ratio

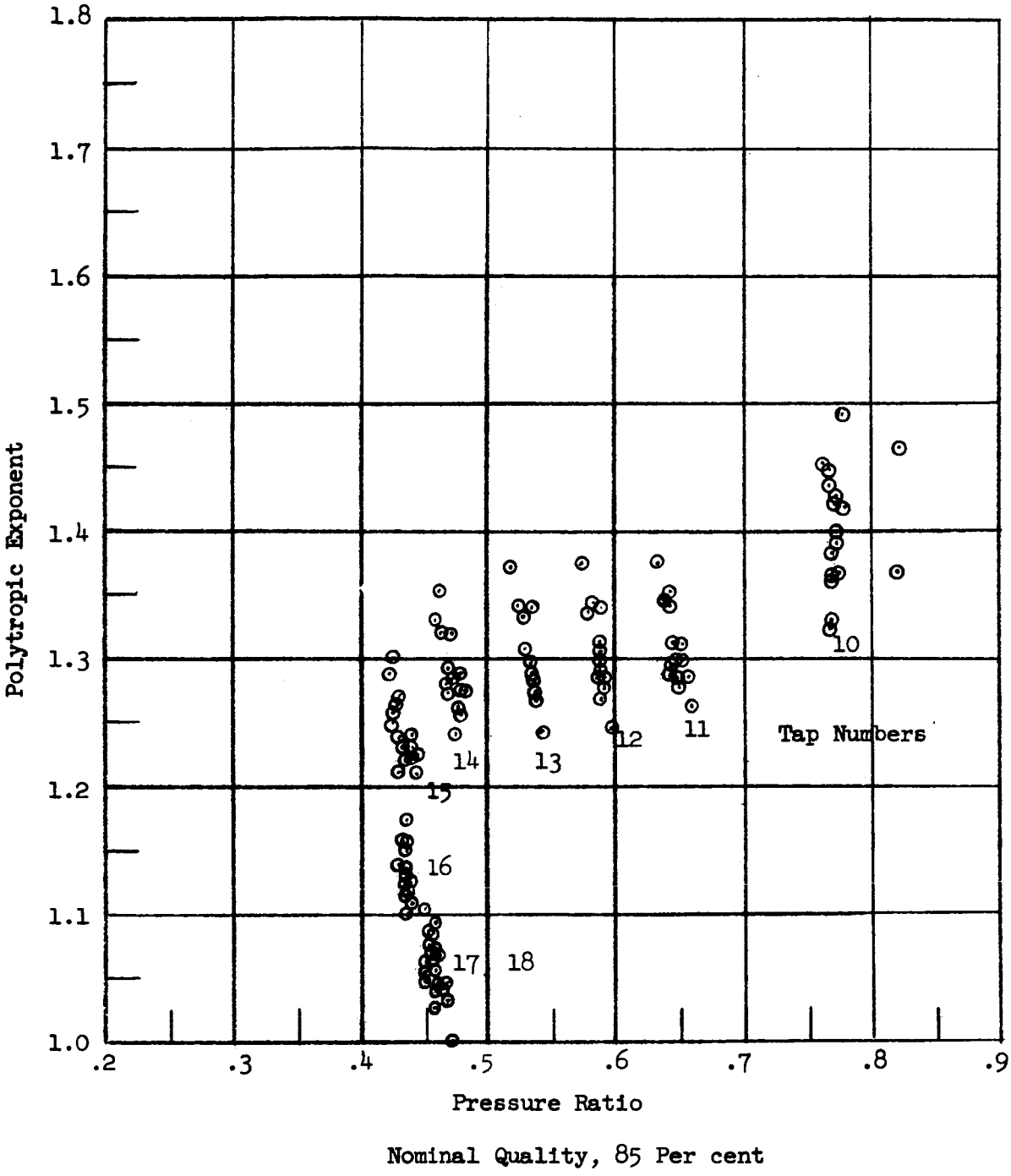

Figure 9b. Variation of Average Inlet to Throat Polytropic Exponent with Static to Total Pressure Ratio

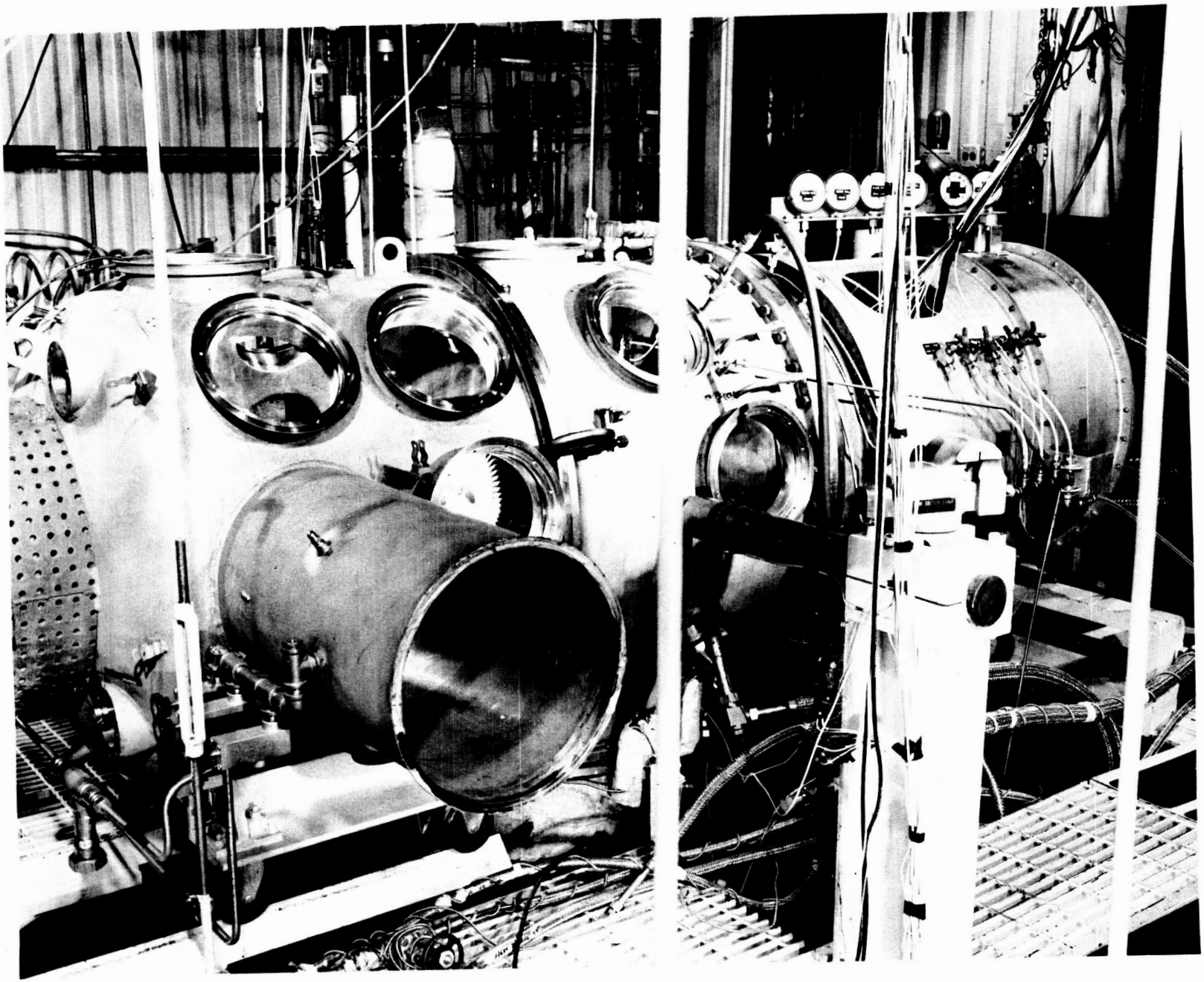

Figure 10. Turbine Seen Installed in the Glove Box, for Pre-Potassium Check-Out Test.

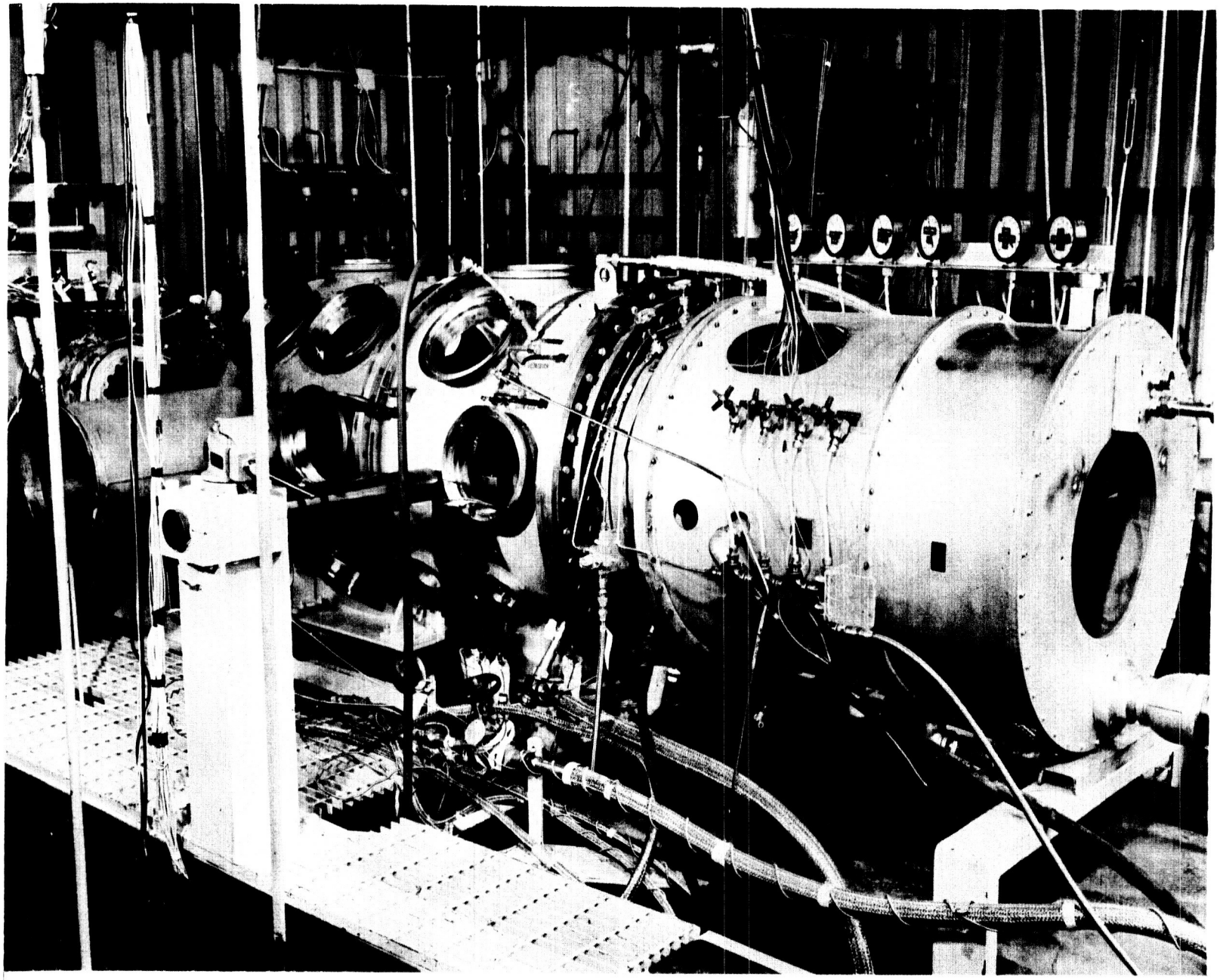

Figure 11. Turbine Test Equipment and Instrumentation Installed in the Potassium Test Facility.

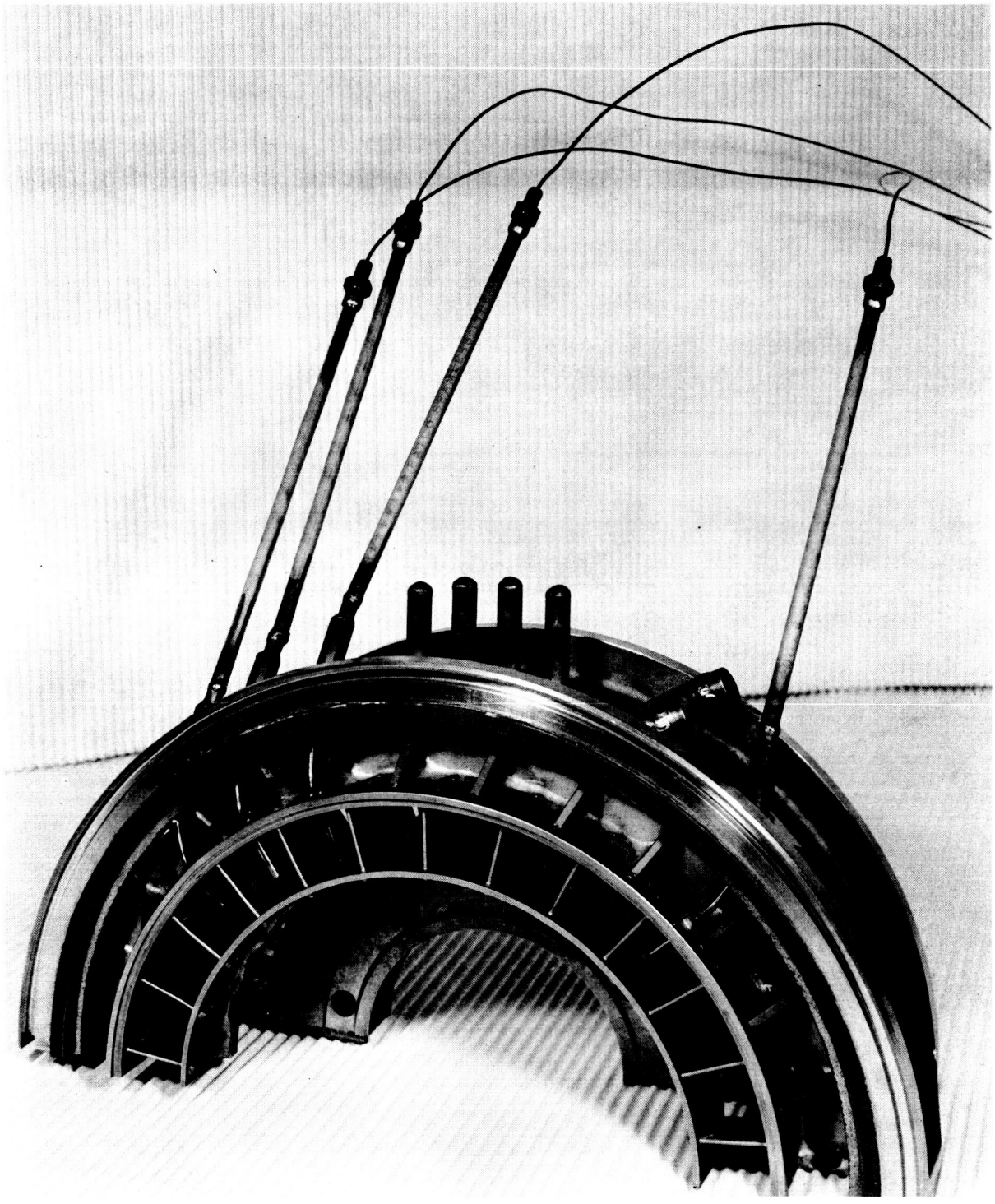

Figure 12. Stator Assembly with Thermocouple Wells Installed.

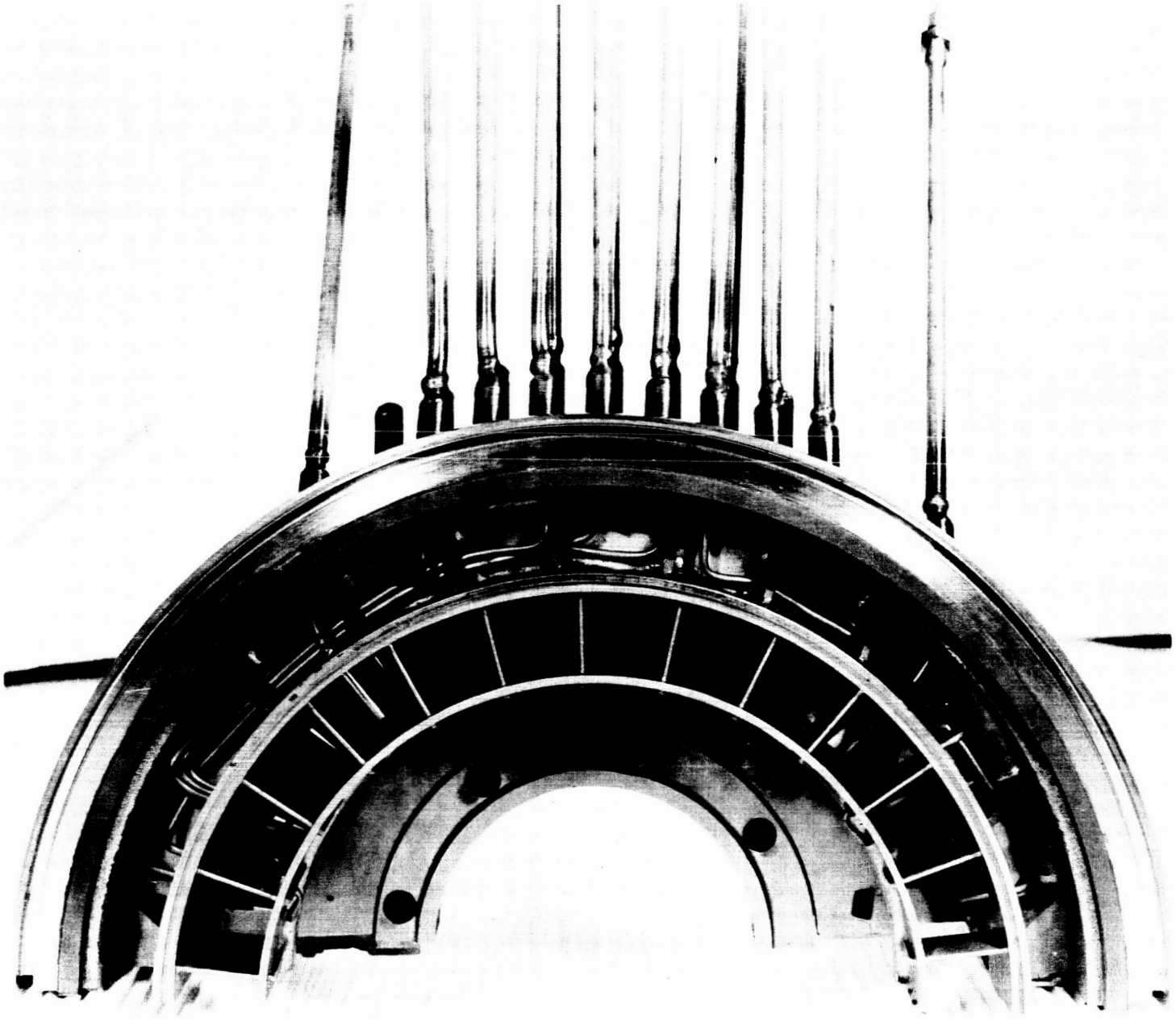

Figure 13. Outlet Guide Vane-Casing Assembly with Welded Pressure Taps Installed.

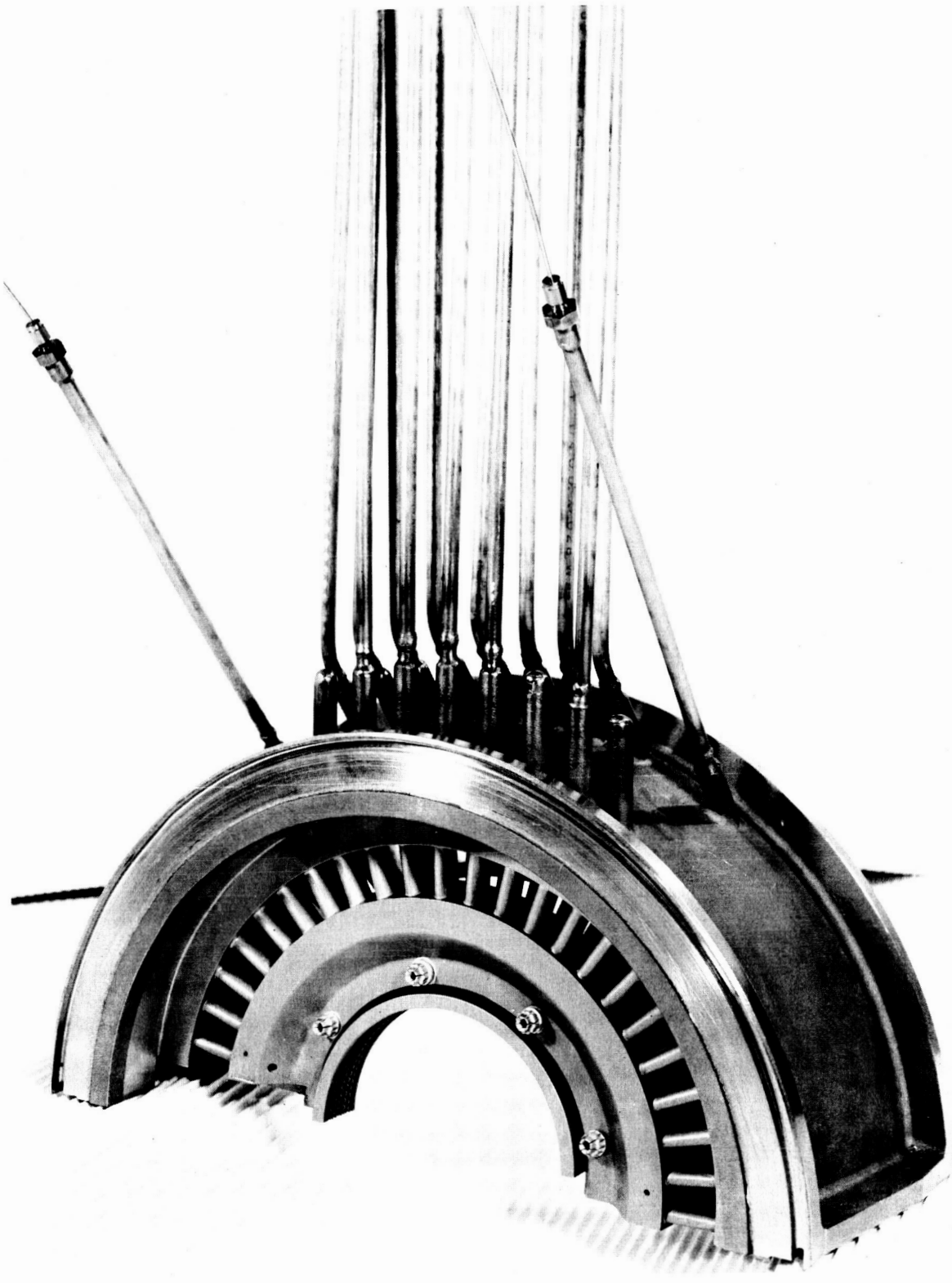

Figure 14. Casing Assembly with Welded Pressure Taps.

Figure 15. Turbine Inlet Duct with Weld-Flange Blanks Attached.

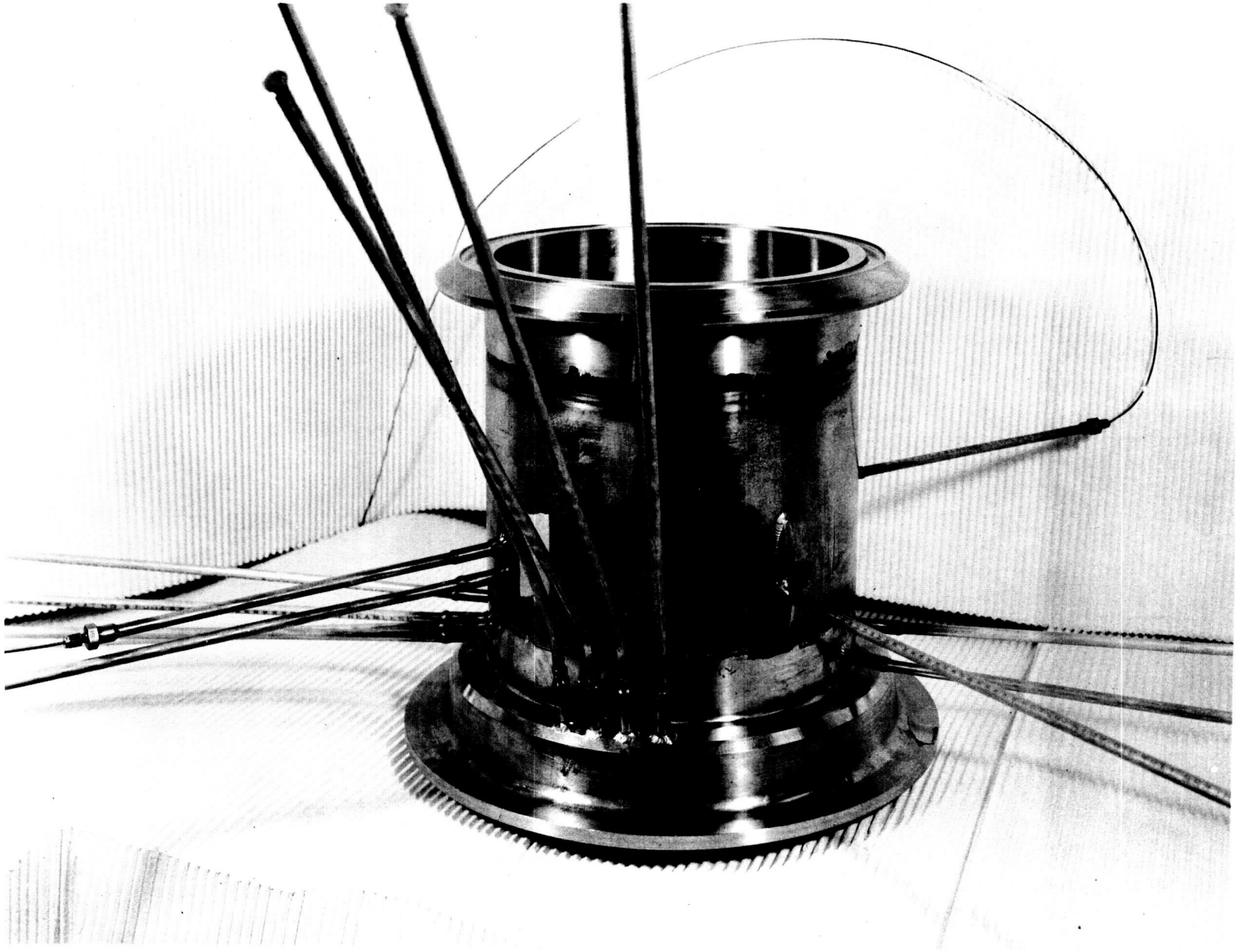

Figure 16. Turbine Inlet Duct with Machined Flanges and Welded Instrumentation Tubing.

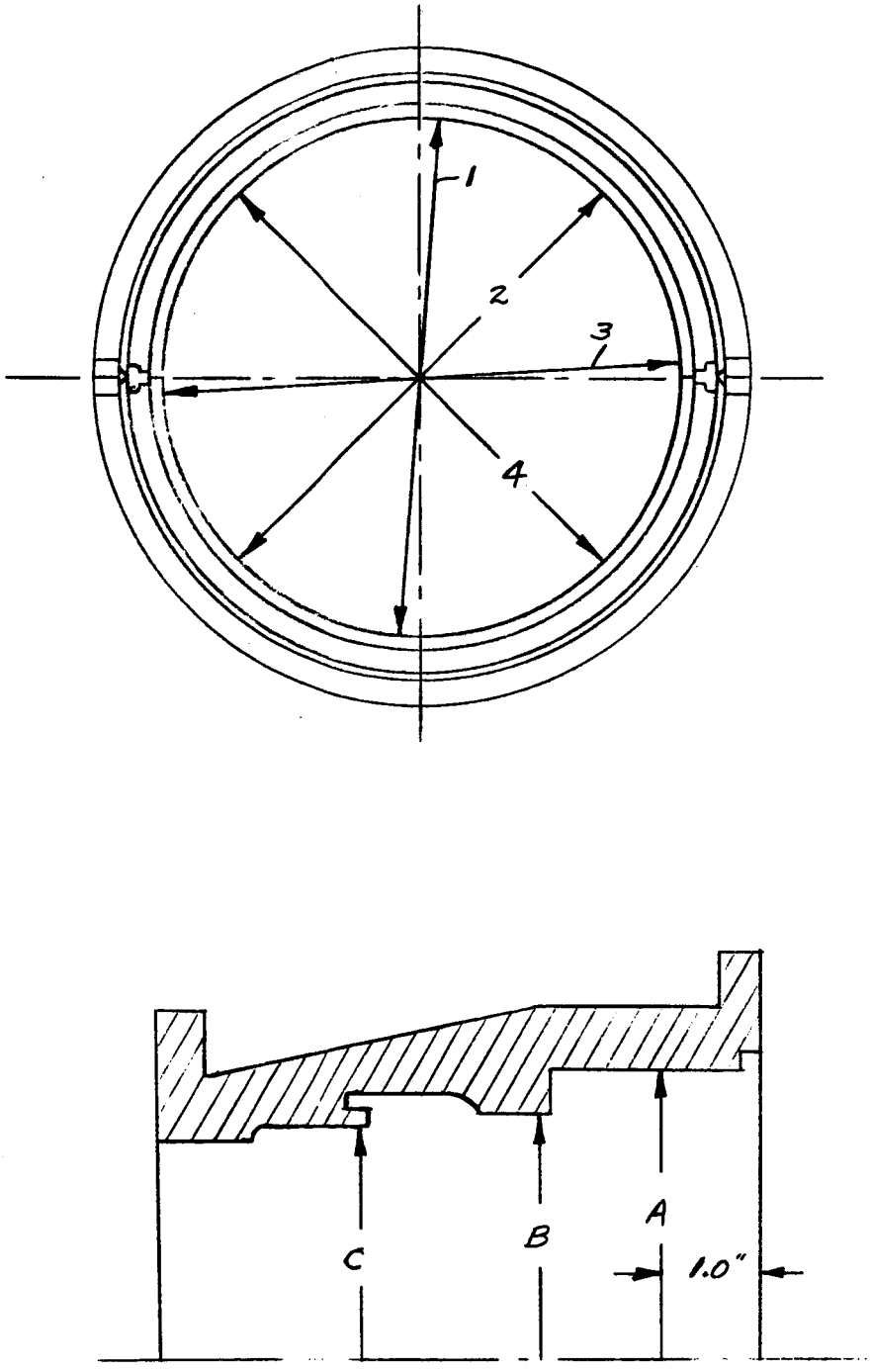

Figure 17. Internal Diameter Measurements On Practice Weld Turbine Casing

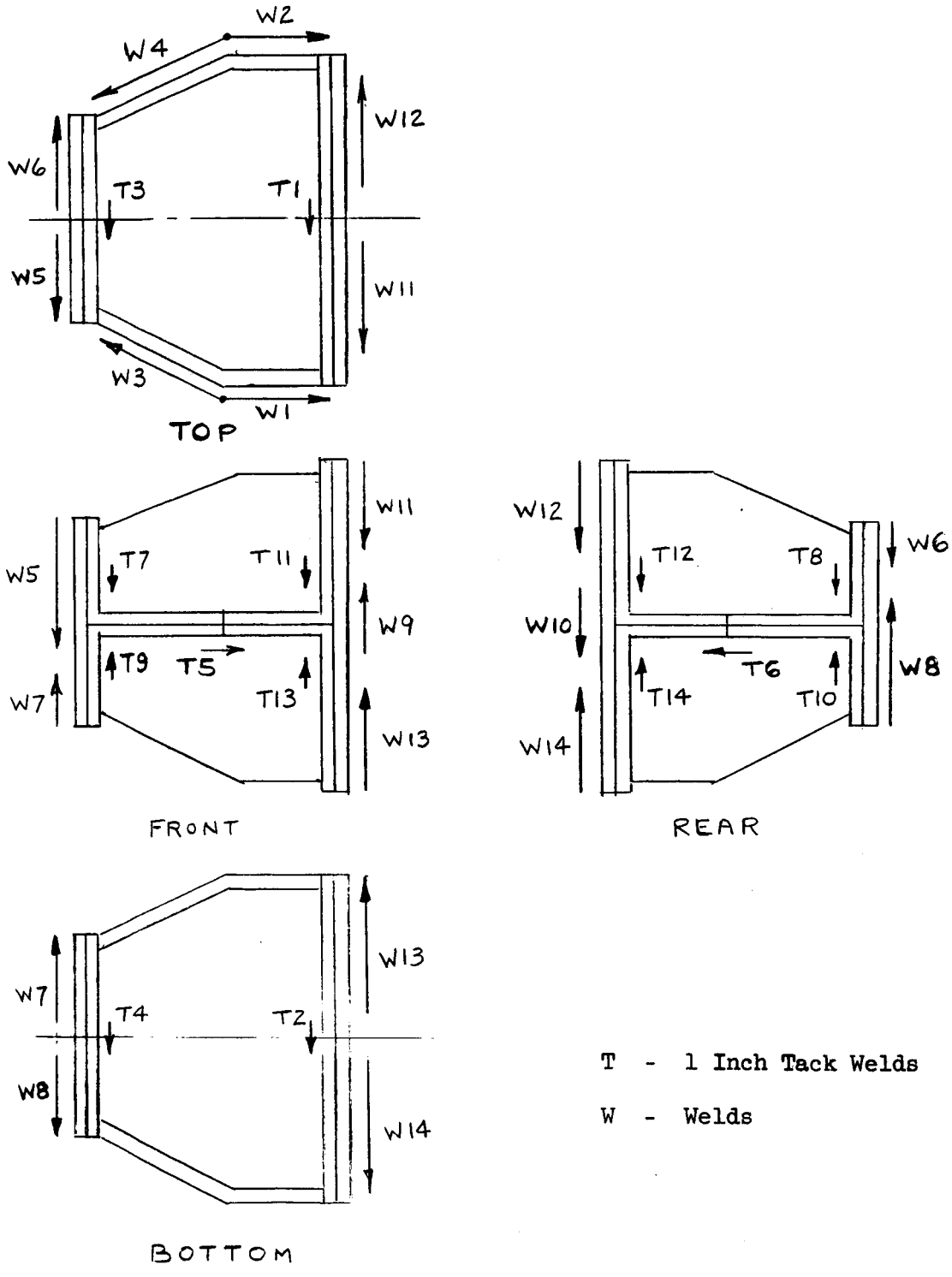

Figure 18.. Turbine Casing, Welding Sequence

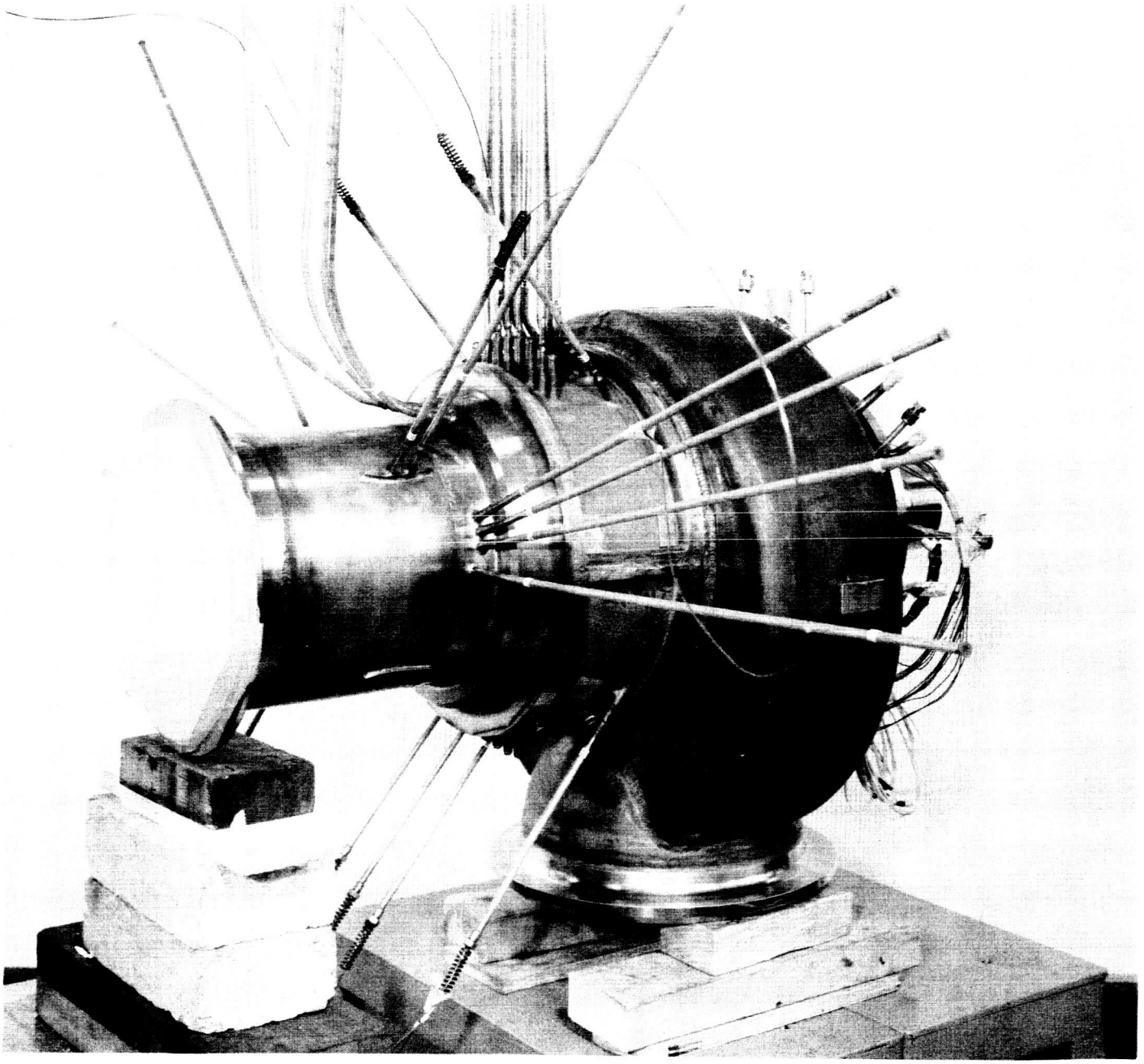

Figure 19. Turbine After Assembly

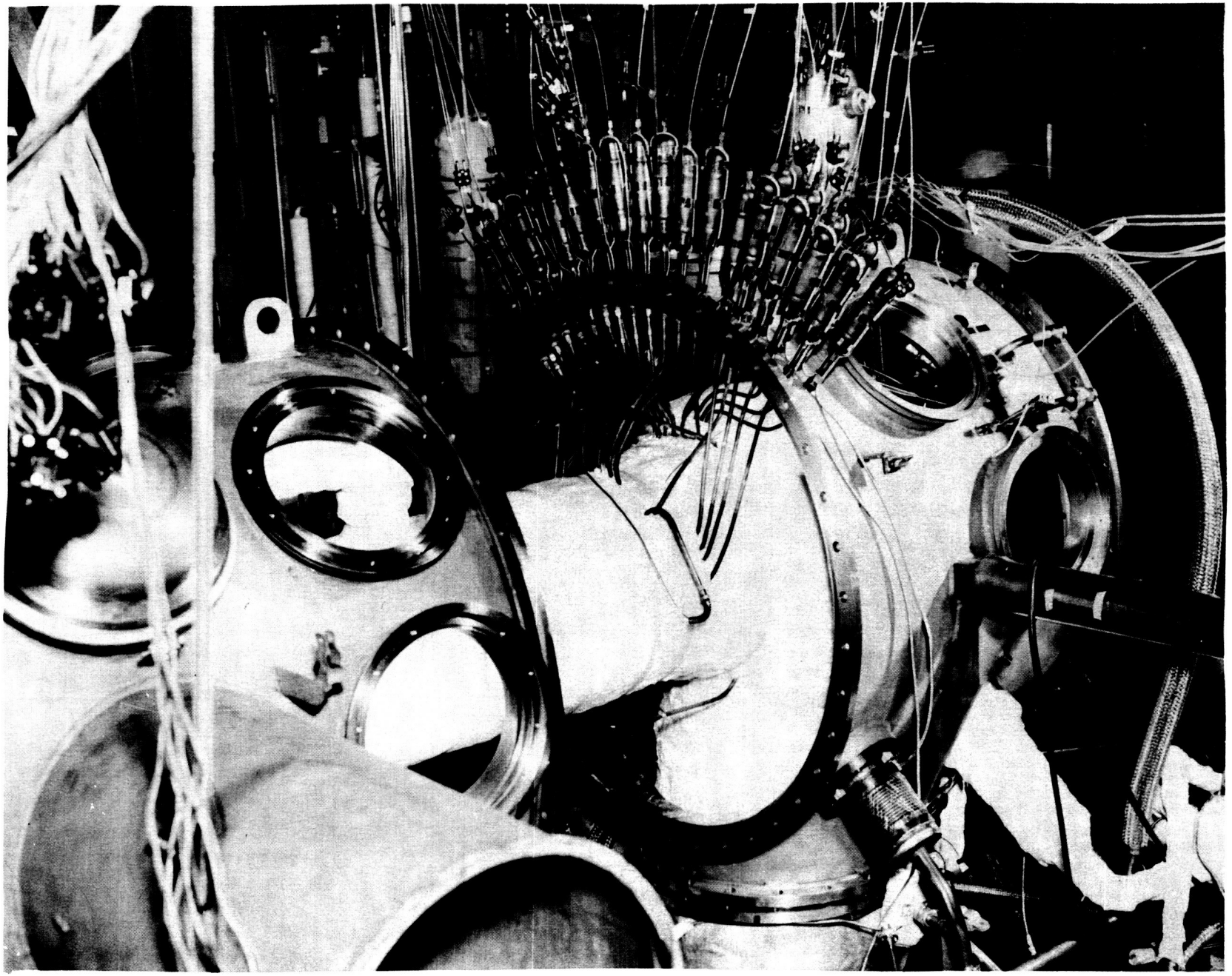

Figure 20. View Looking Aft of Turbine After Being Welded Into The 3000 KW Facility

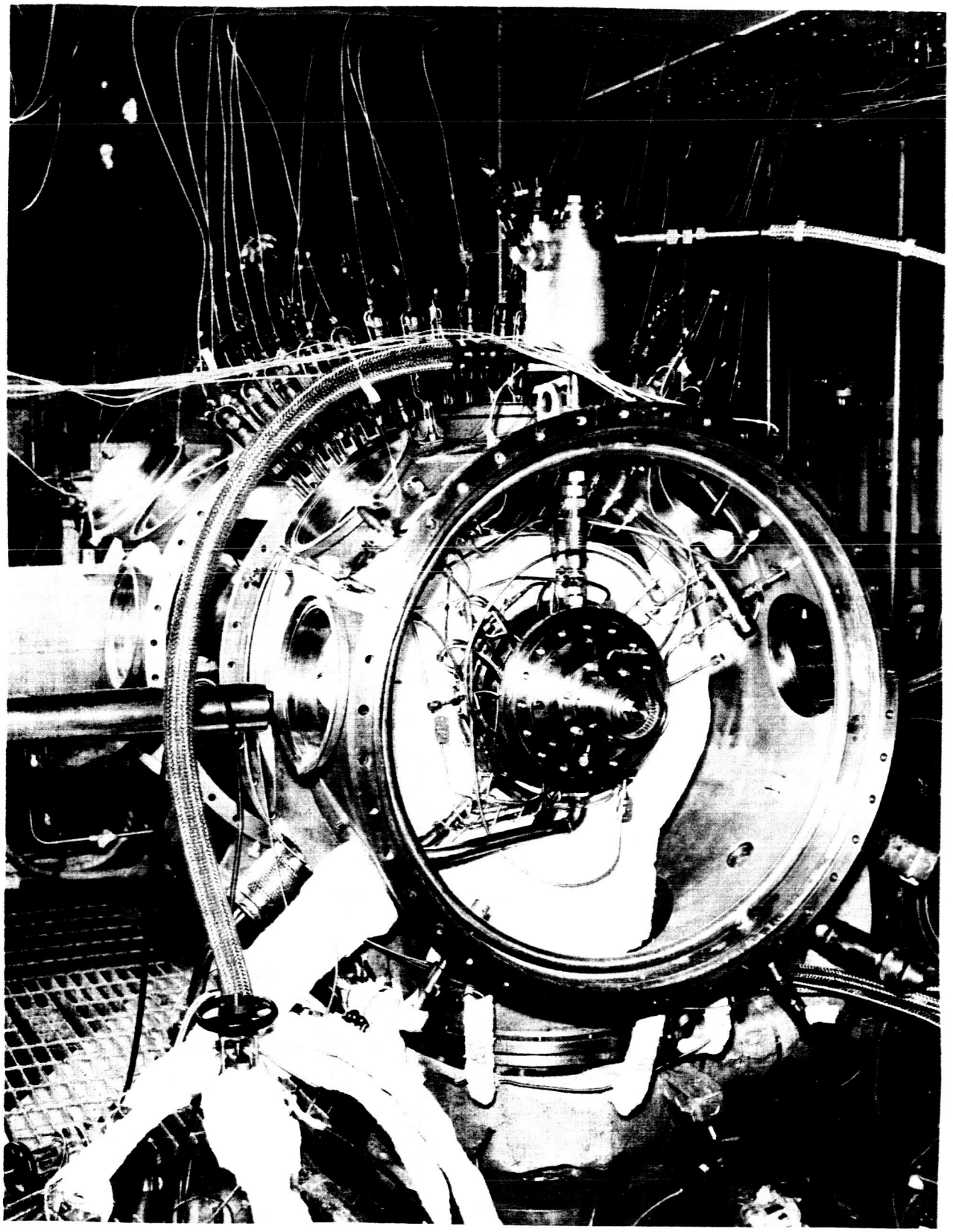

Figure 21. View Looking Forward of Turbine After Being Welded Into The 3000 KW Facility

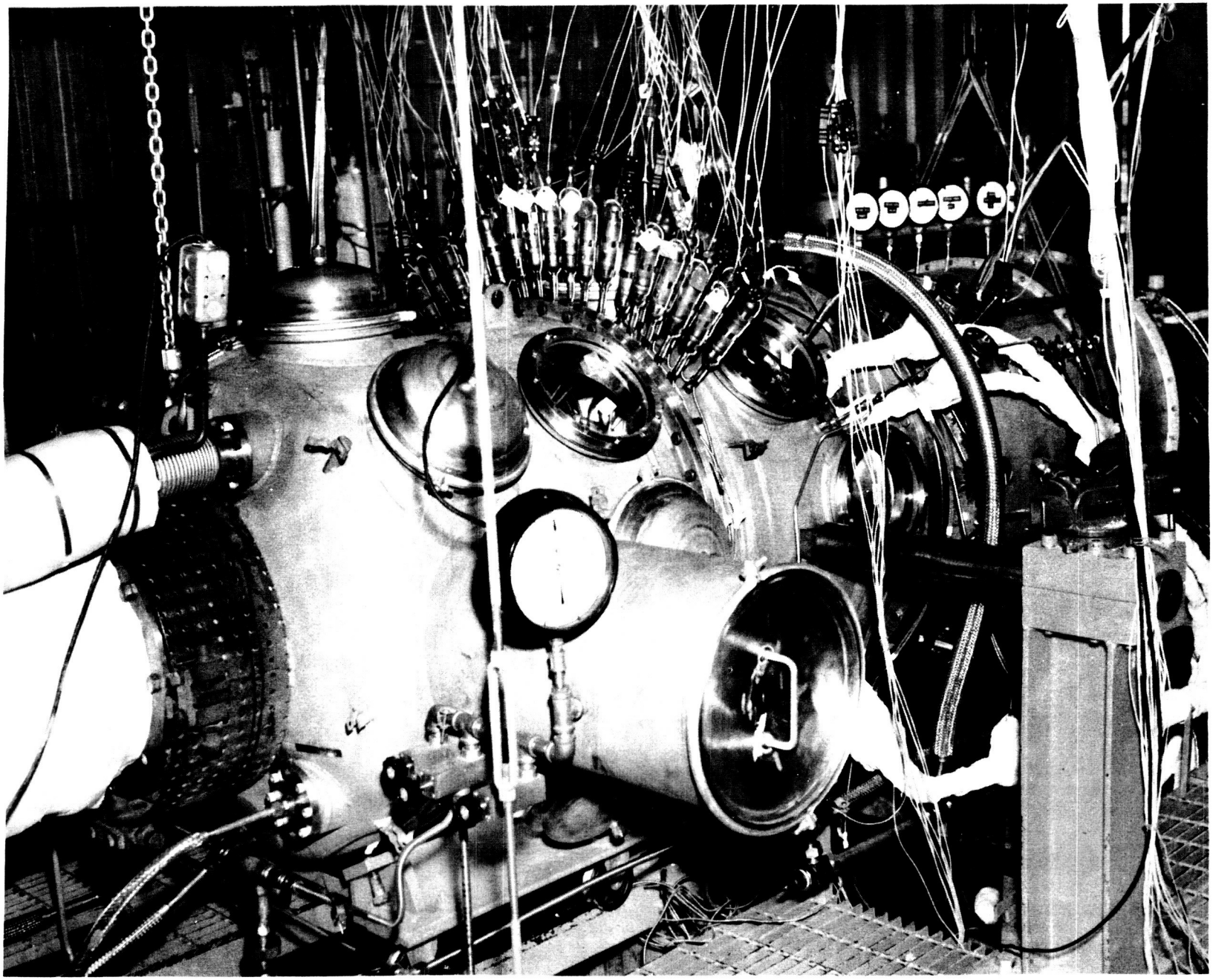

Figure 22. View Looking Aft of Completed Turbine Installation

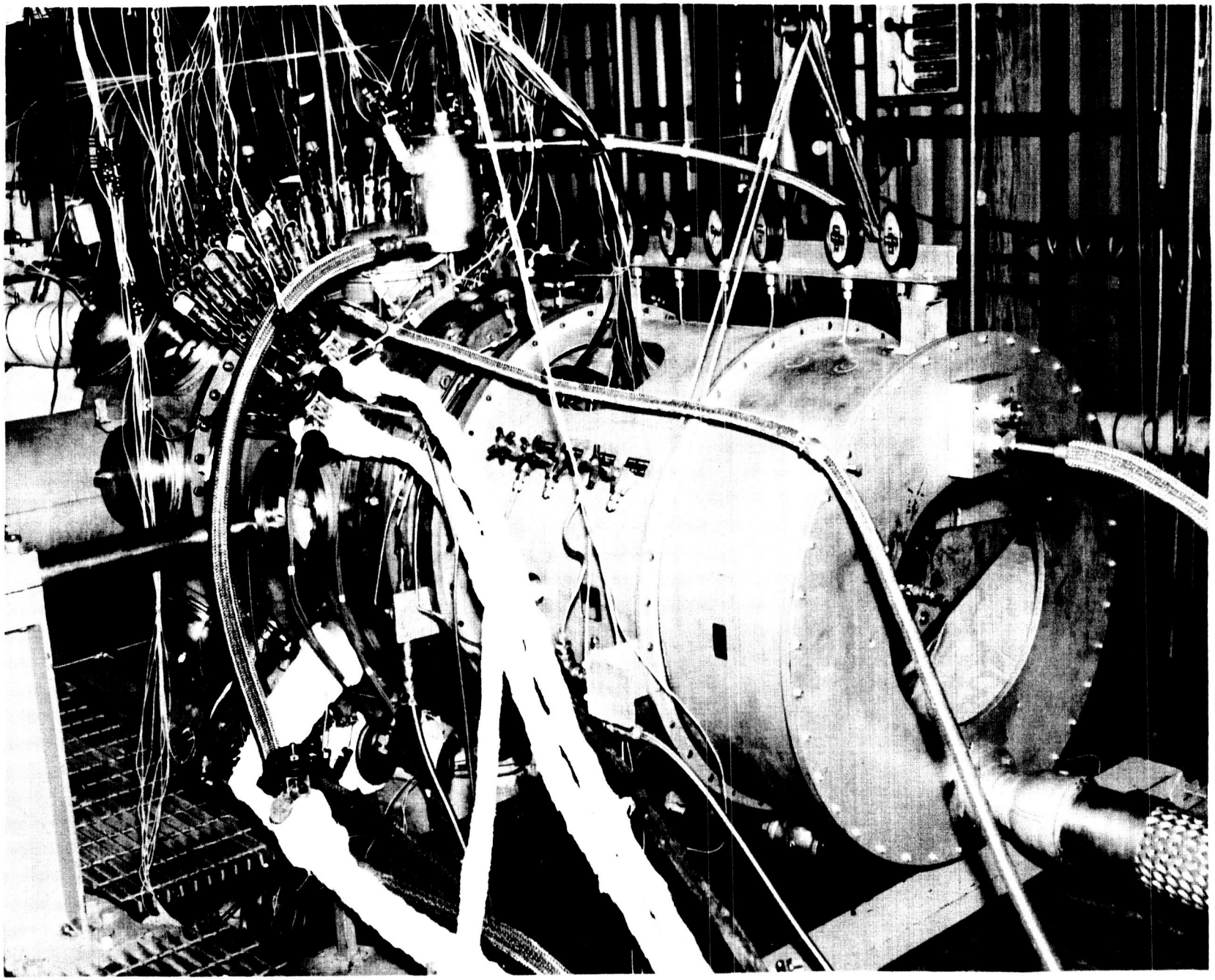

Figure 23. View Looking Forward of Completed Turbine Installation

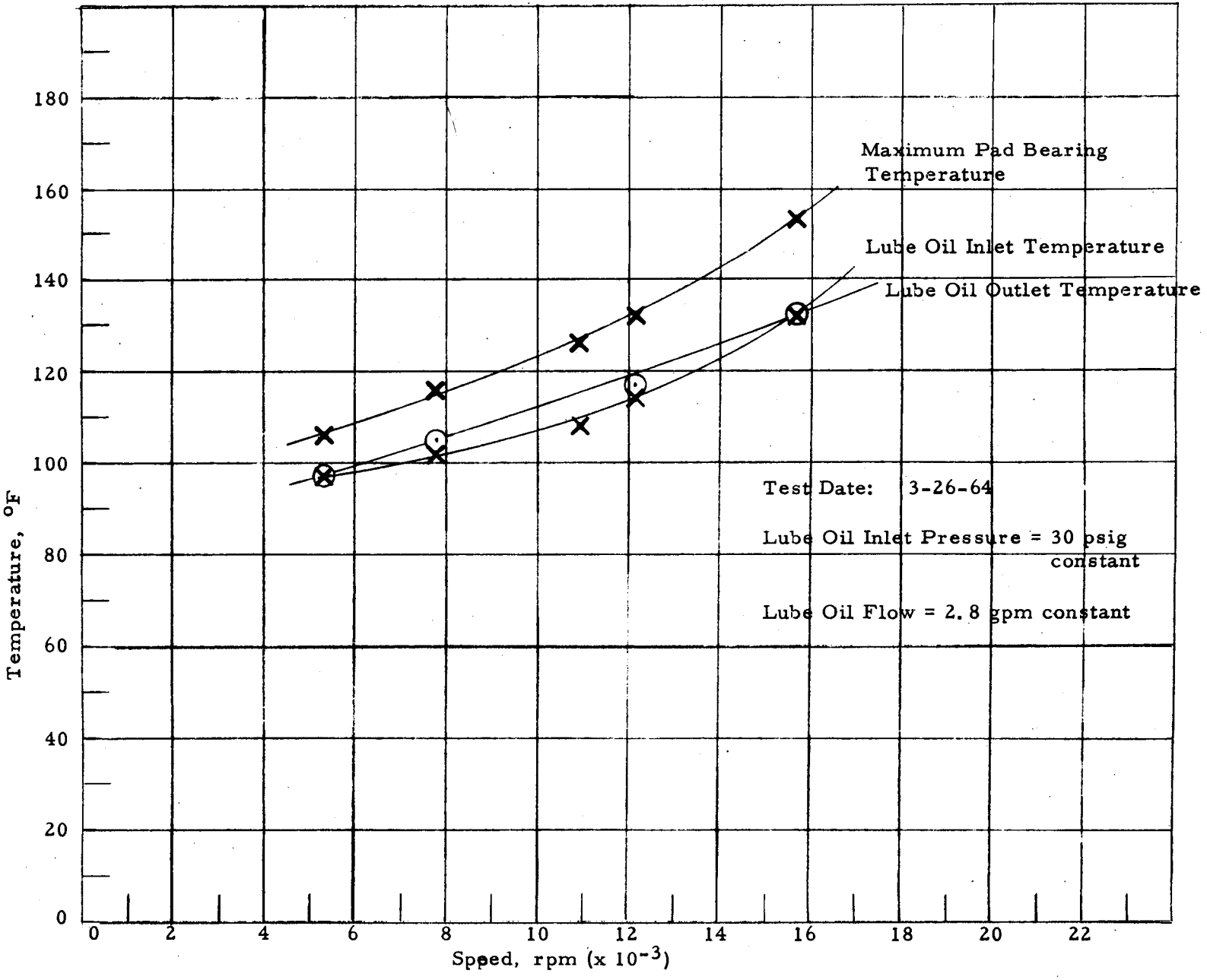

Figure 24. Pad Bearing and Lube Oil Temperature During Mechanical Check-Out Test

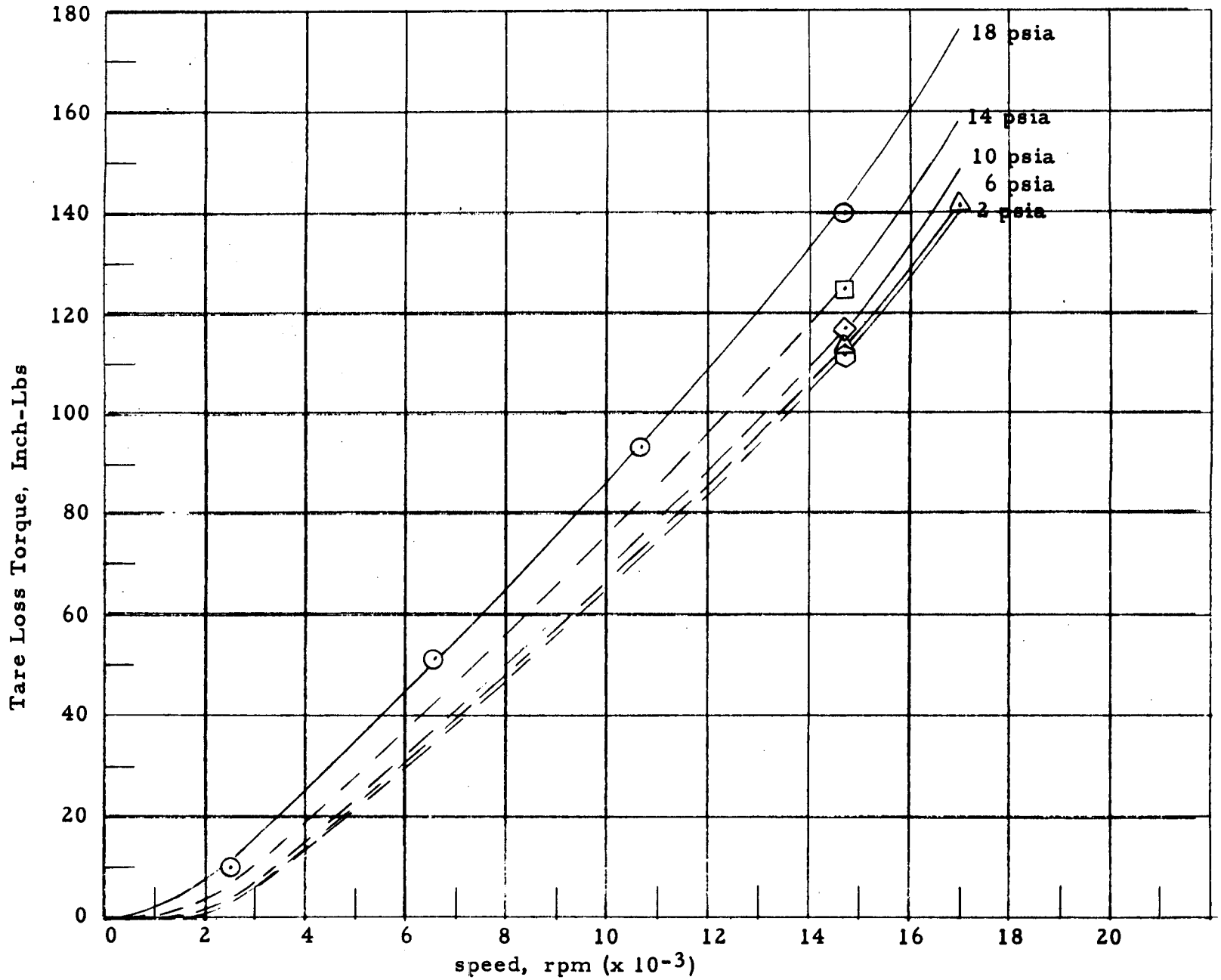

Figure 25. Torque Versus Speed for Various Values of Loop Pressure

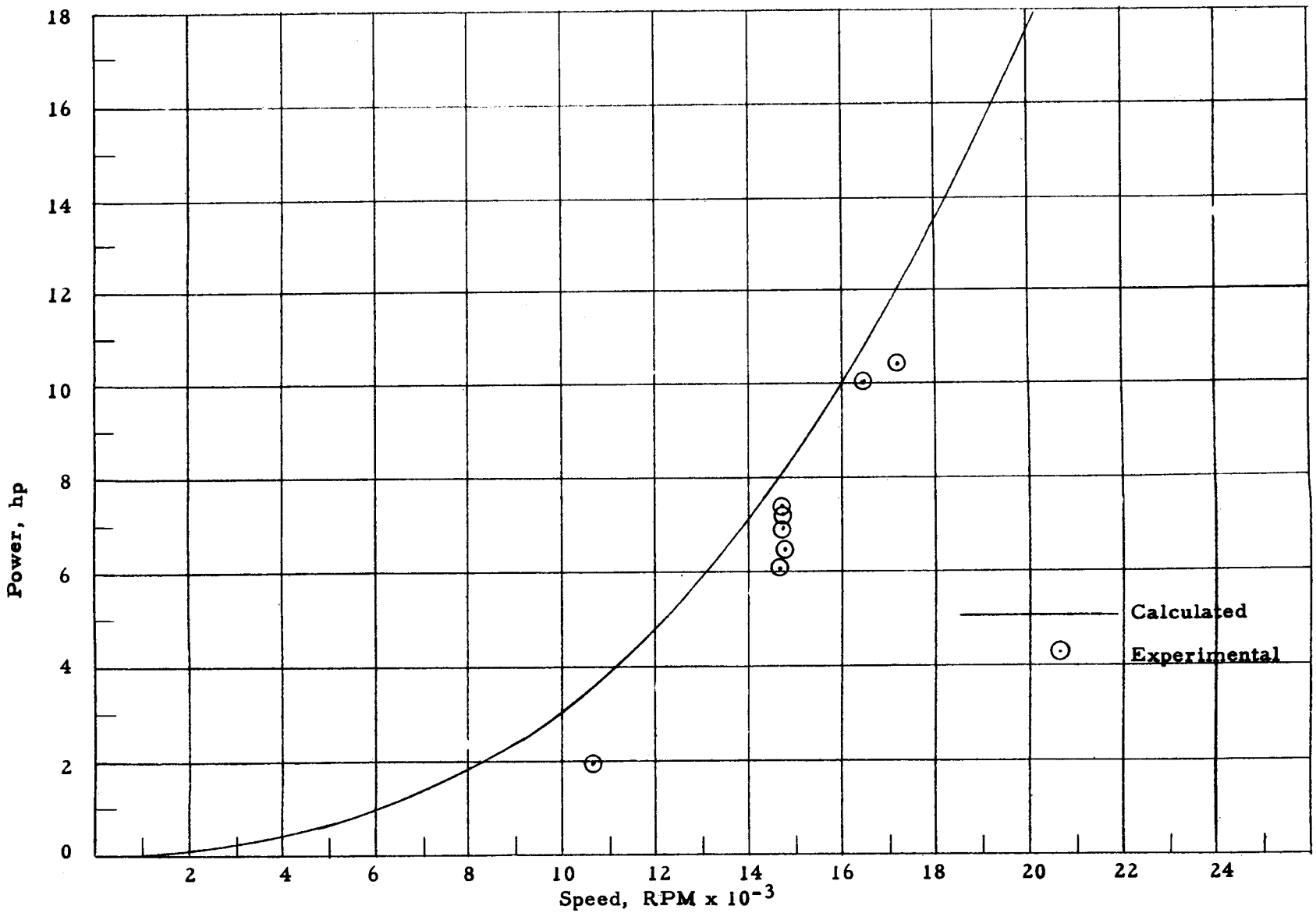

Figure 26: Hydrodynamic Seal Power Consumption Using Potassium as the Sealant

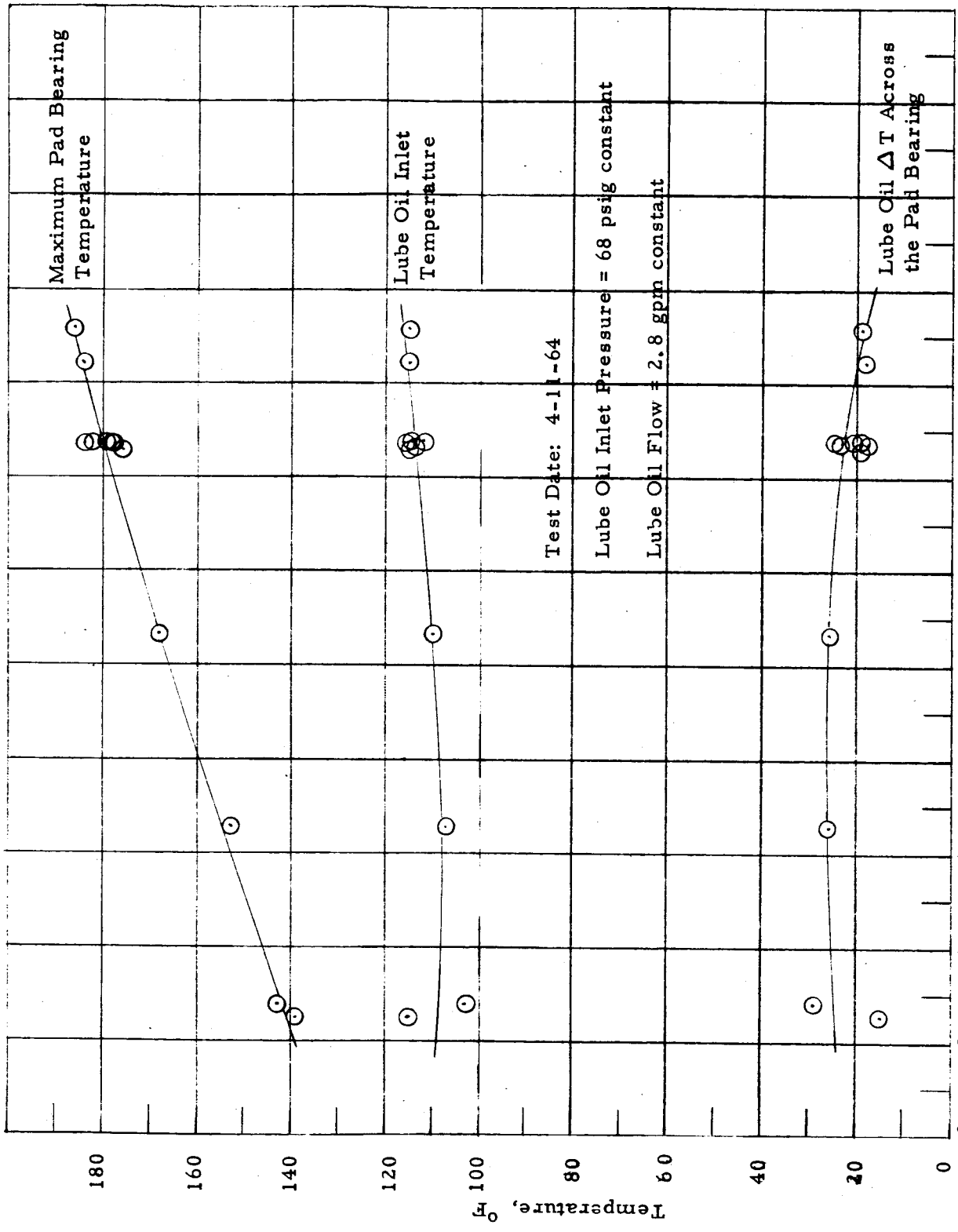

Figure 27: Pad Bearing and Lube Oil Temperature During Turbine Tare Loss Tests

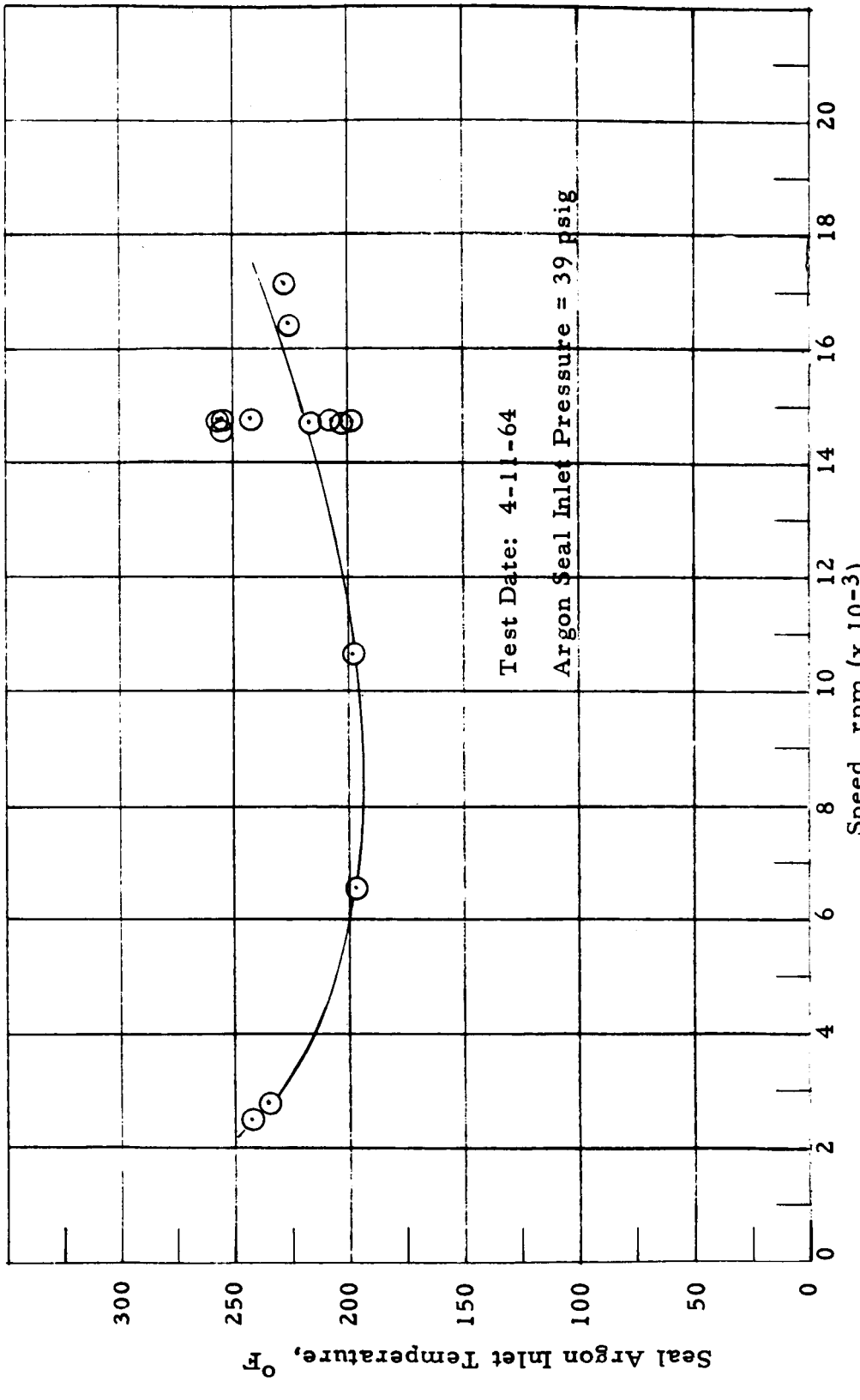

Figure 28: Argon Temperature into Buffer Seal During Turbine Tare Loss Tests

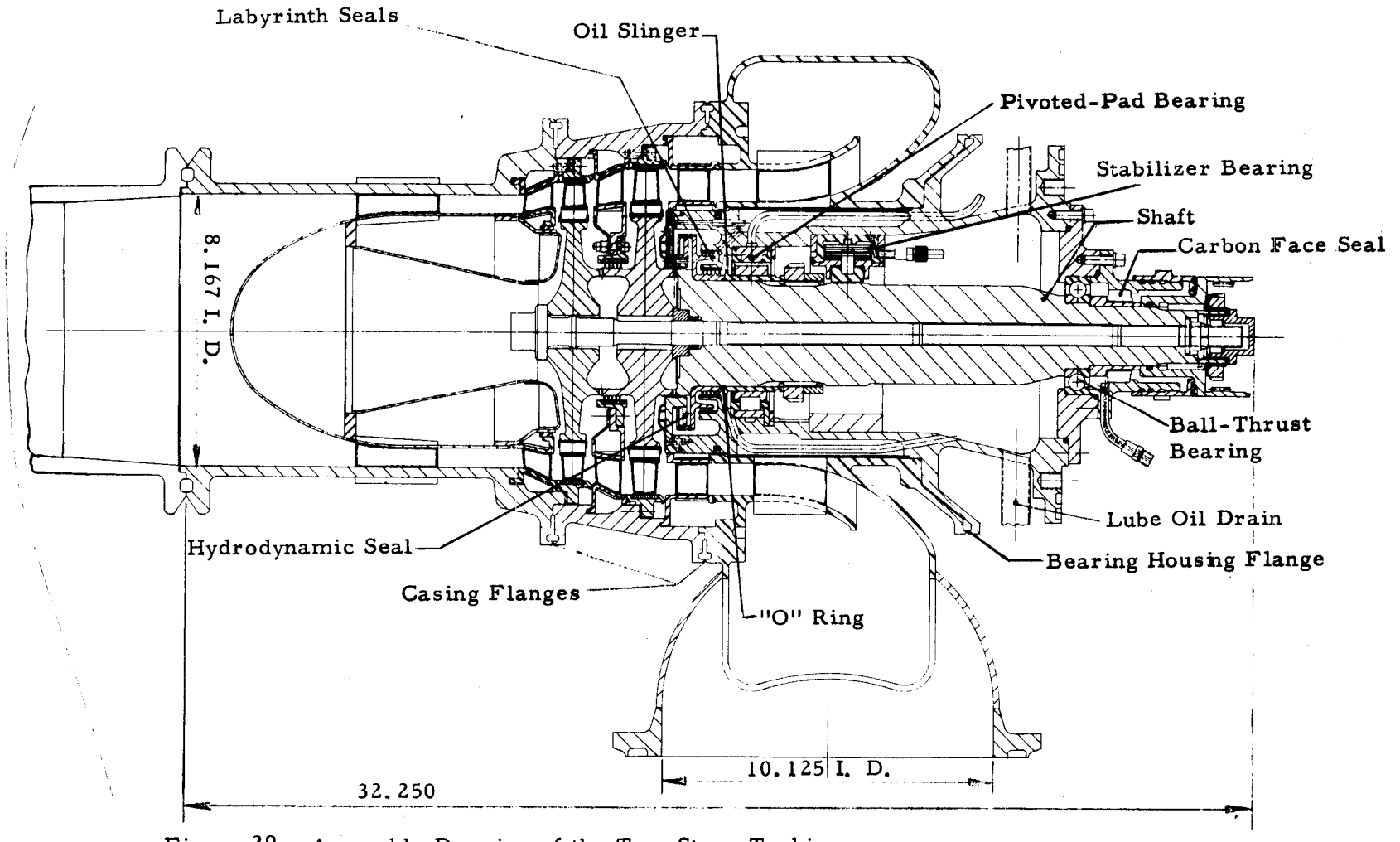

Figure 29. Assembly Drawing of the Two-Stage Turbine

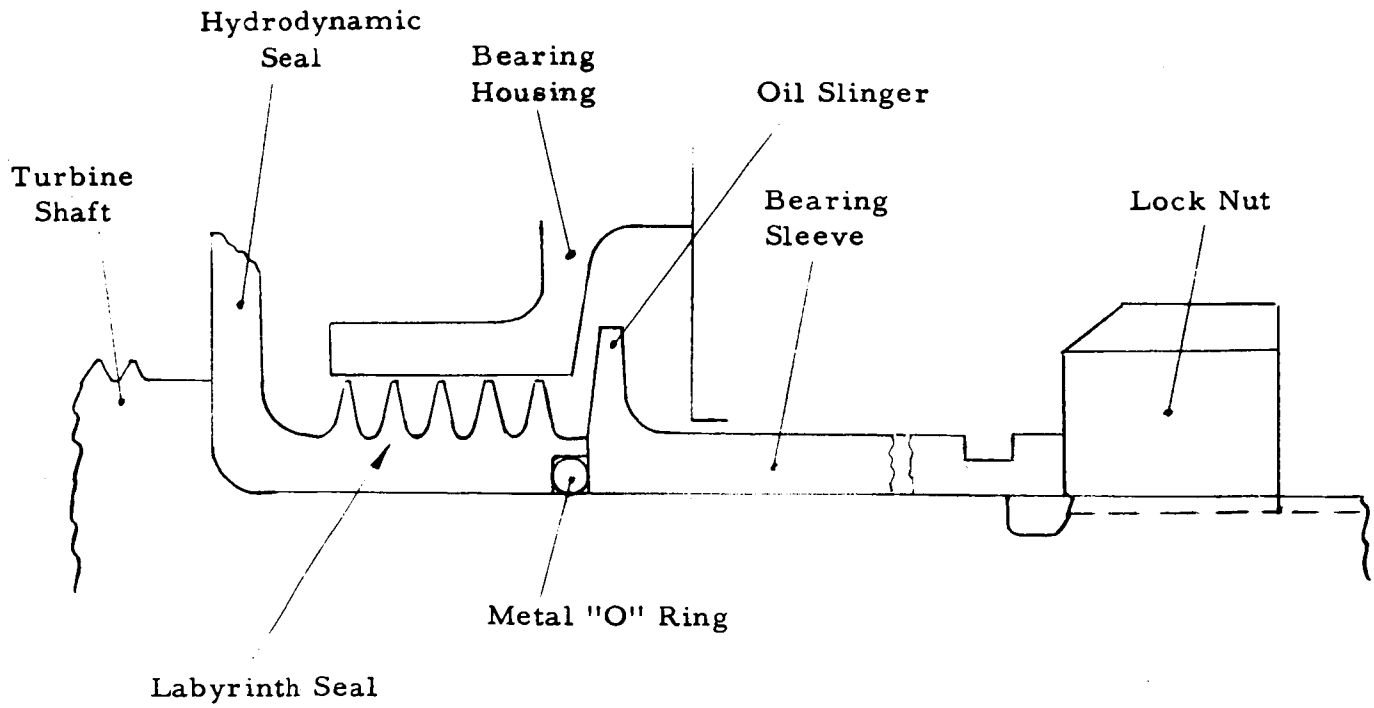

a) Sketch of the Old "O" Ring Seal Assembly

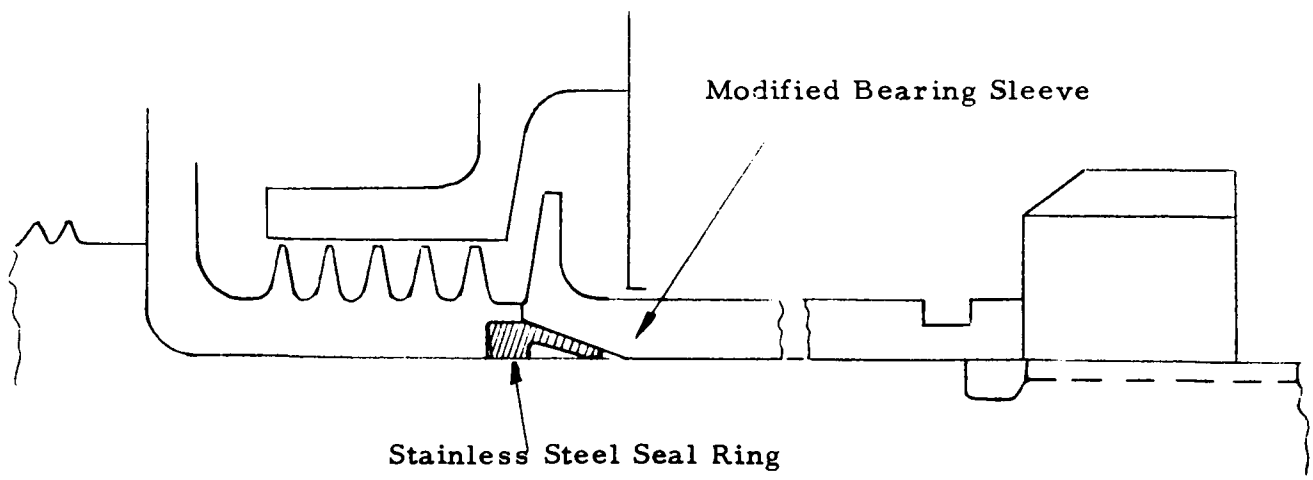

b) Sketch of the New Seal Ring Assembly

Figure 30. Original and Modified Assembly of the Lube Oil Seal Ring

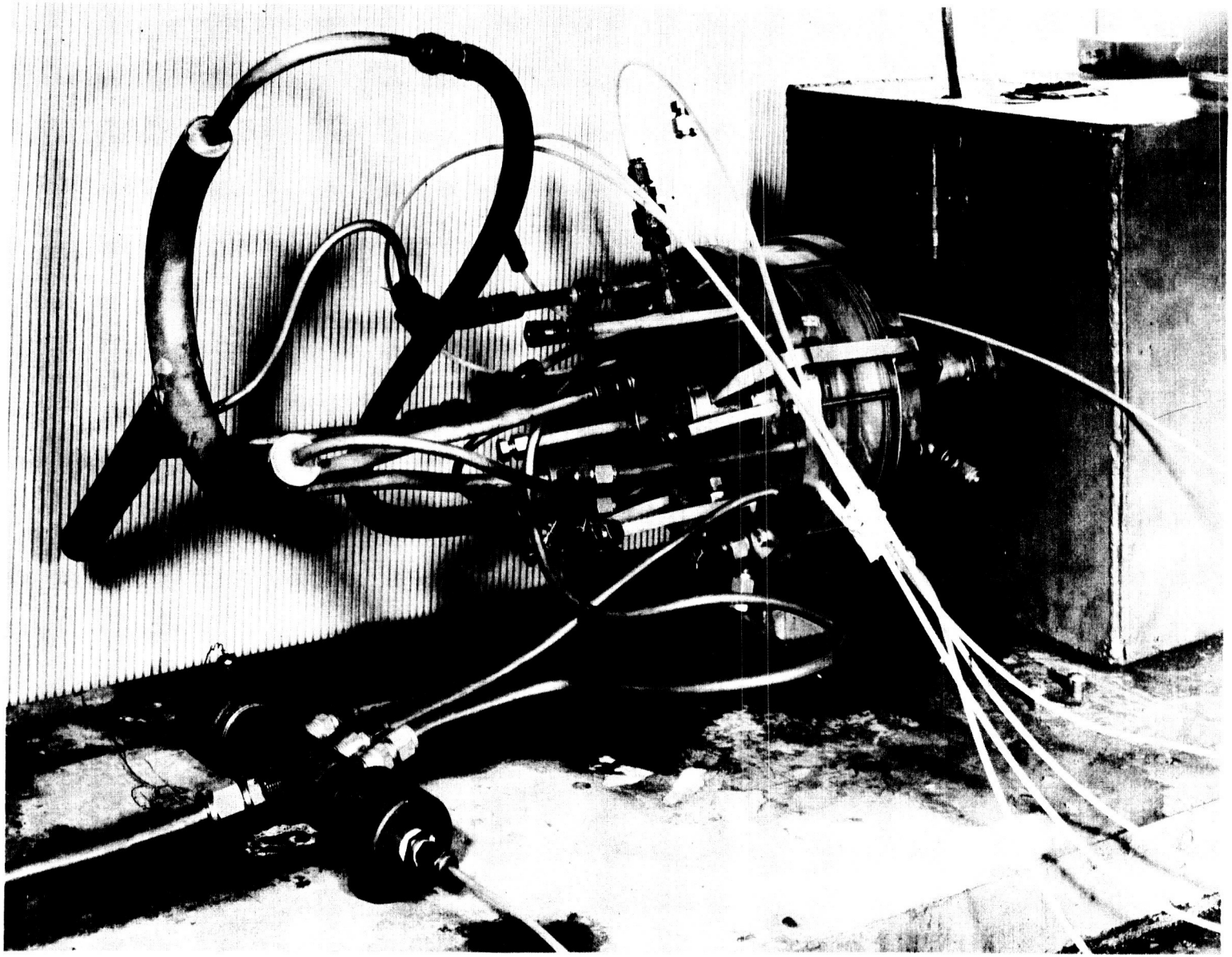

Figure 31. Hydrodynamic Seal Test Set-Up.

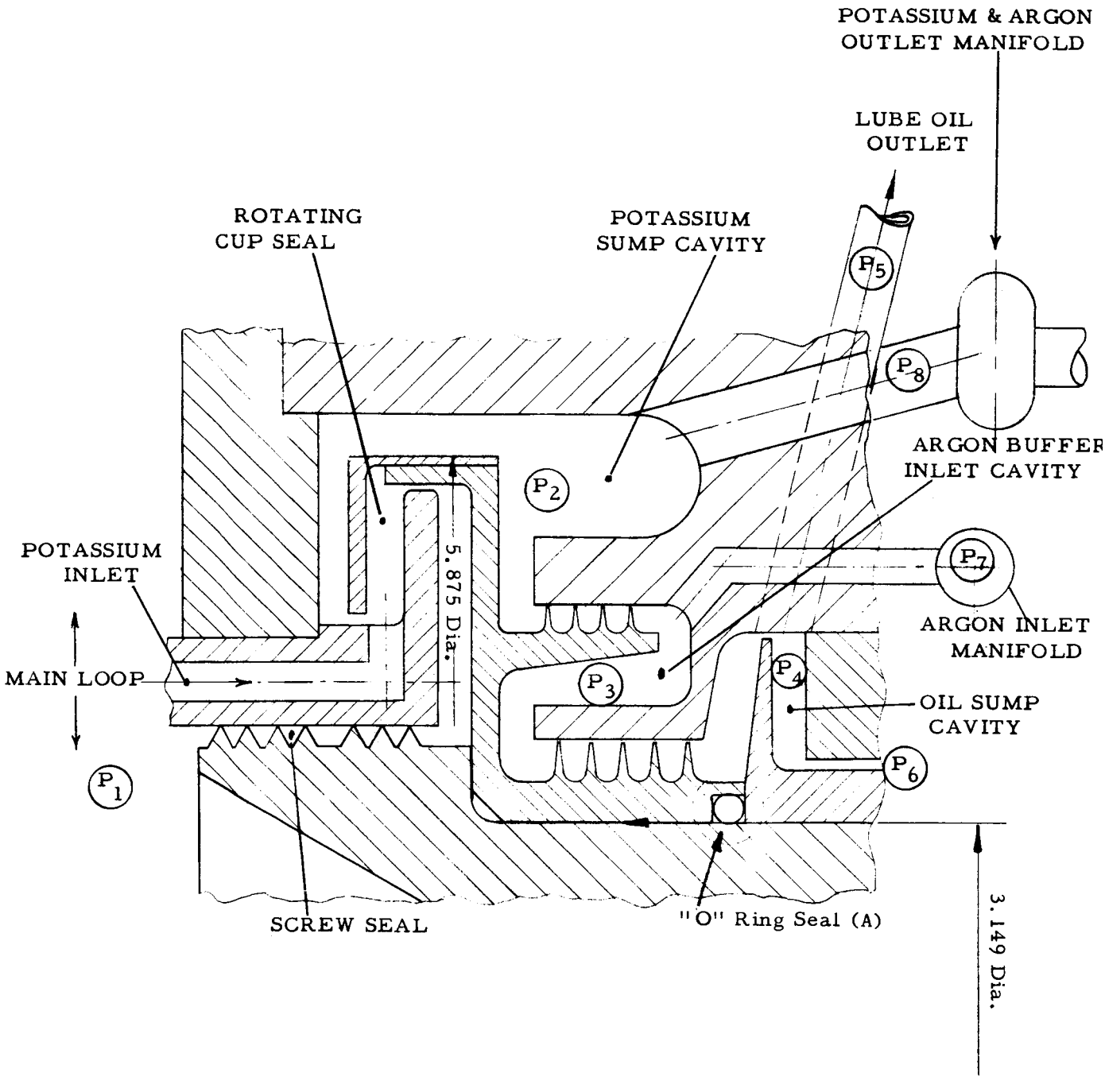

Figure 32. Sketch of Turbine Seal Assembly

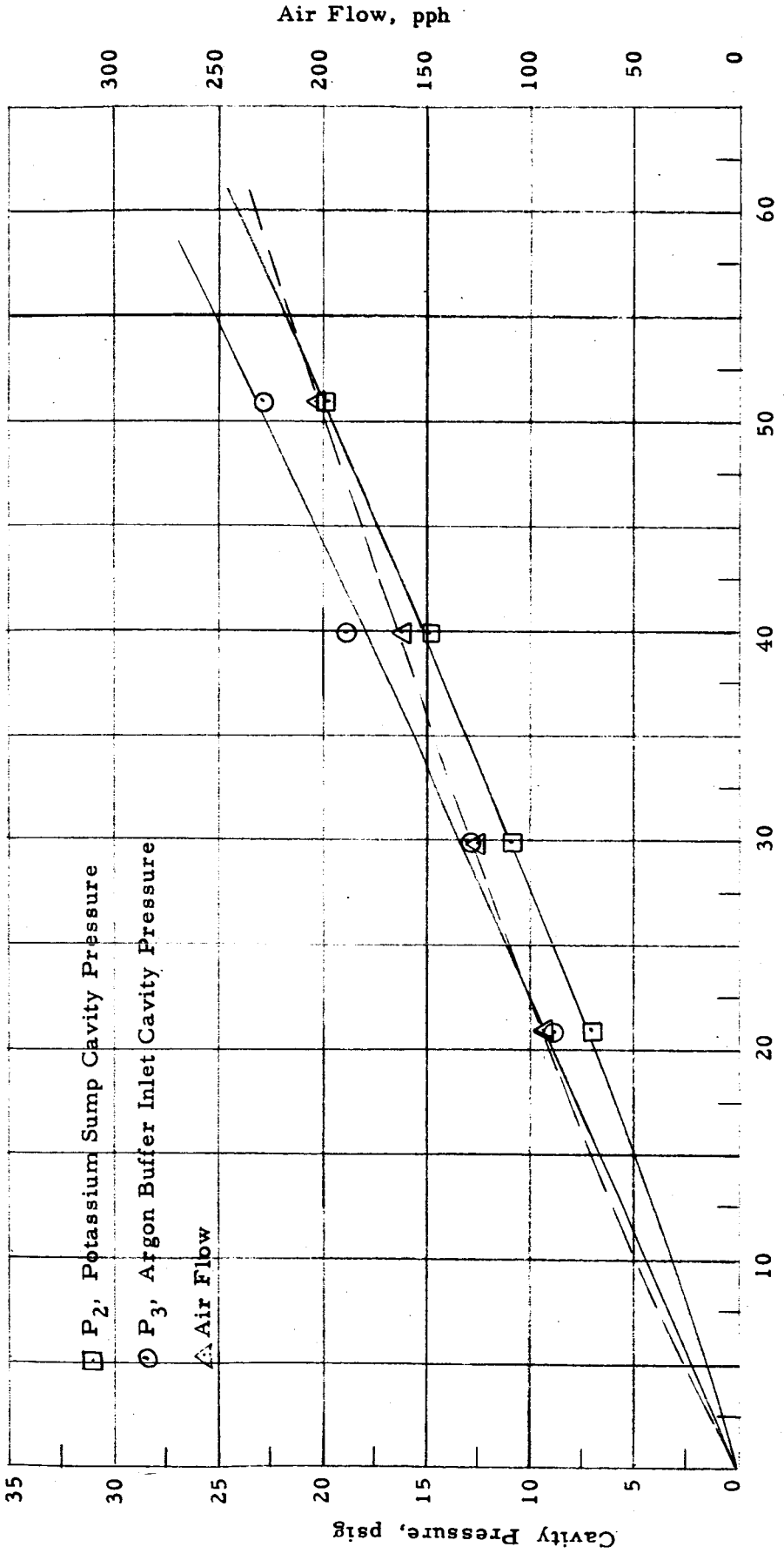

Figure 33: Turbine Seal Characteristics with All Flow Through Screw Seal. Rotative Speed, 5000 rpm, Water Flow, Zero.

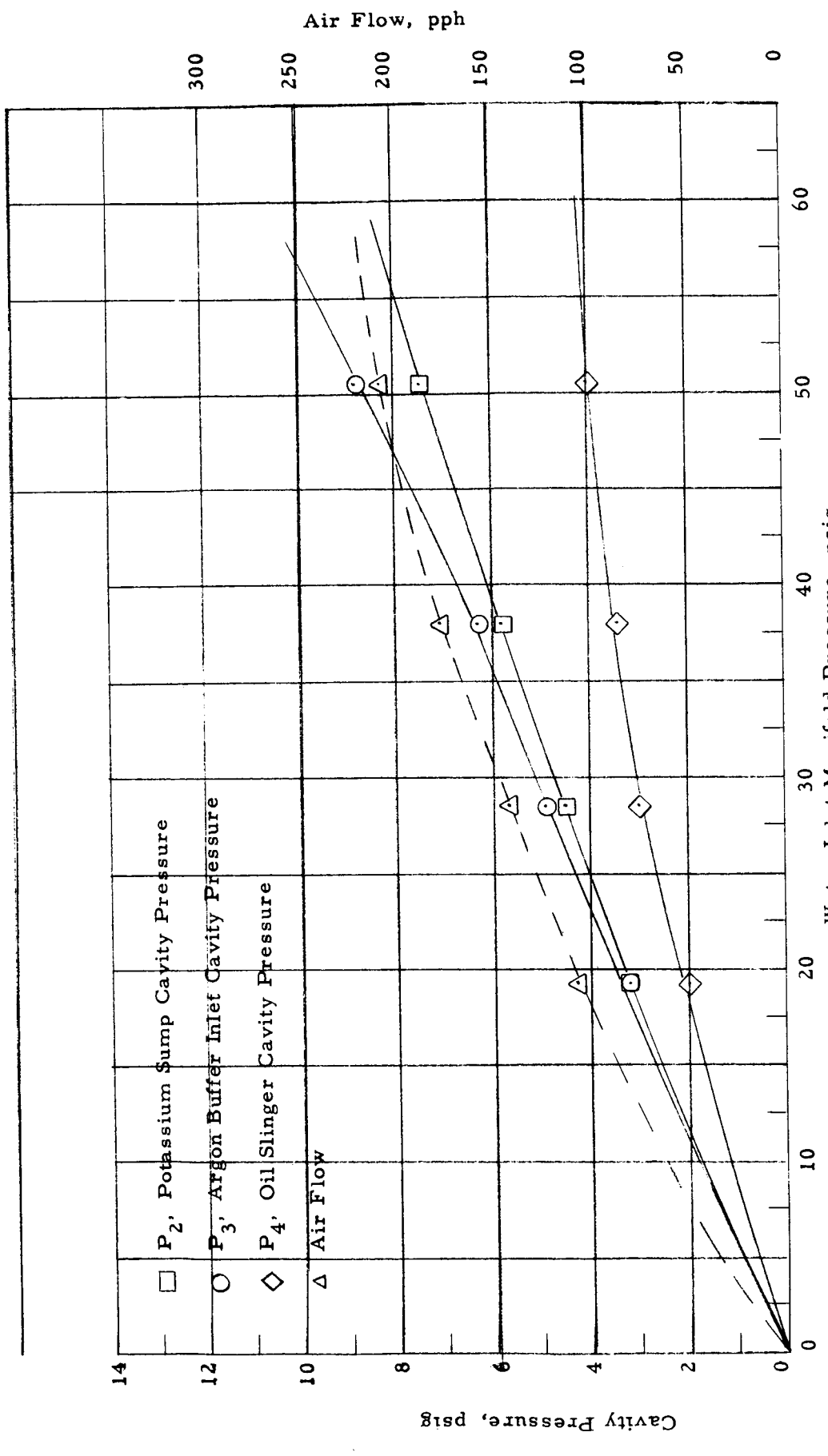

Figure 34: Turbine Seal Characteristics Showing Potassium-to-oil Sealing Capacity of Buffer Seal. Rotative Speed, 5000 rpm, Water Flow Zero.

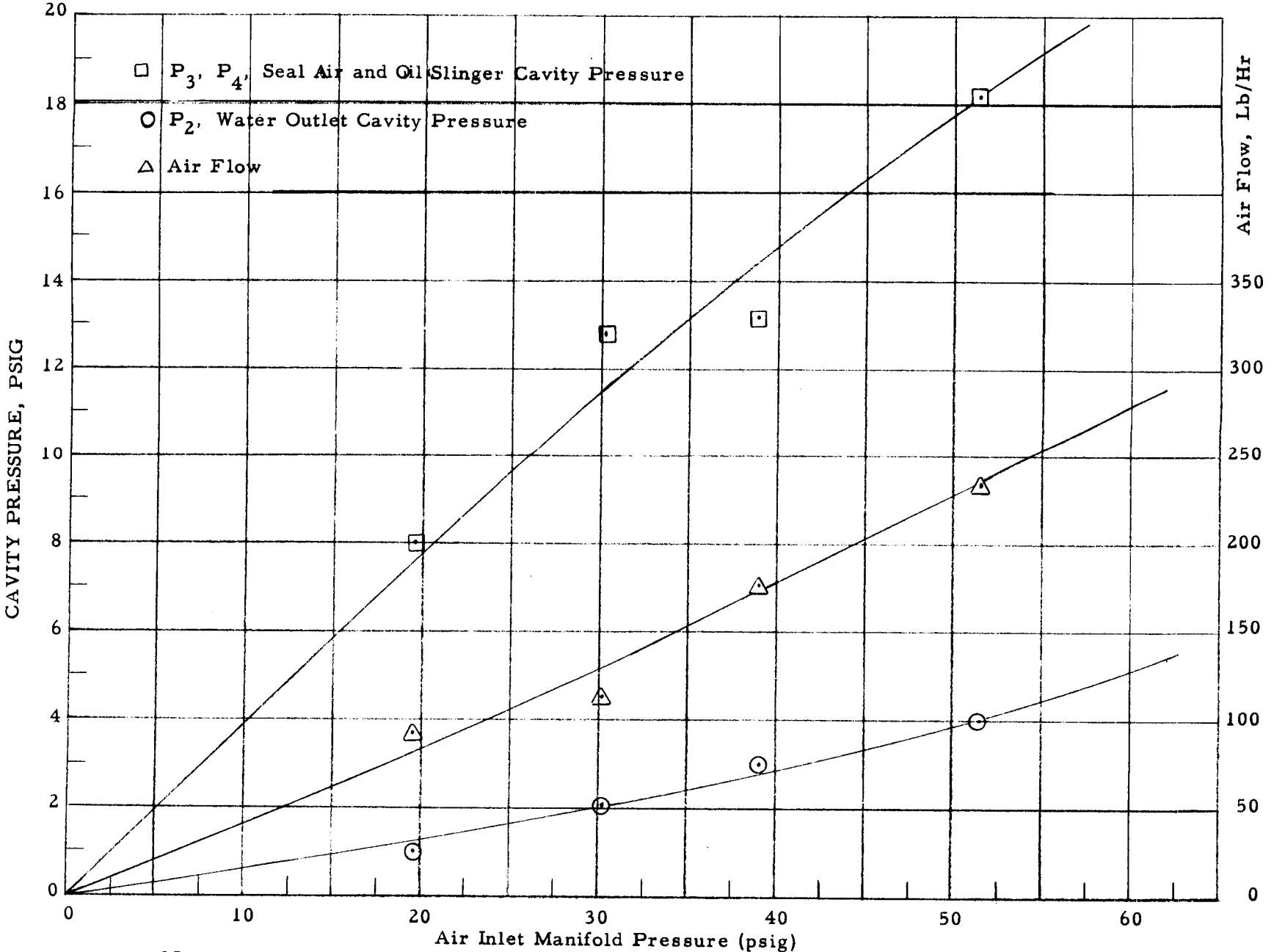

Figure 35. Turbine Seal Characteristics with Reduced Water Sump Manifold Pressure. Rotative Speed, 5000 rpm, Water Flow Zero.

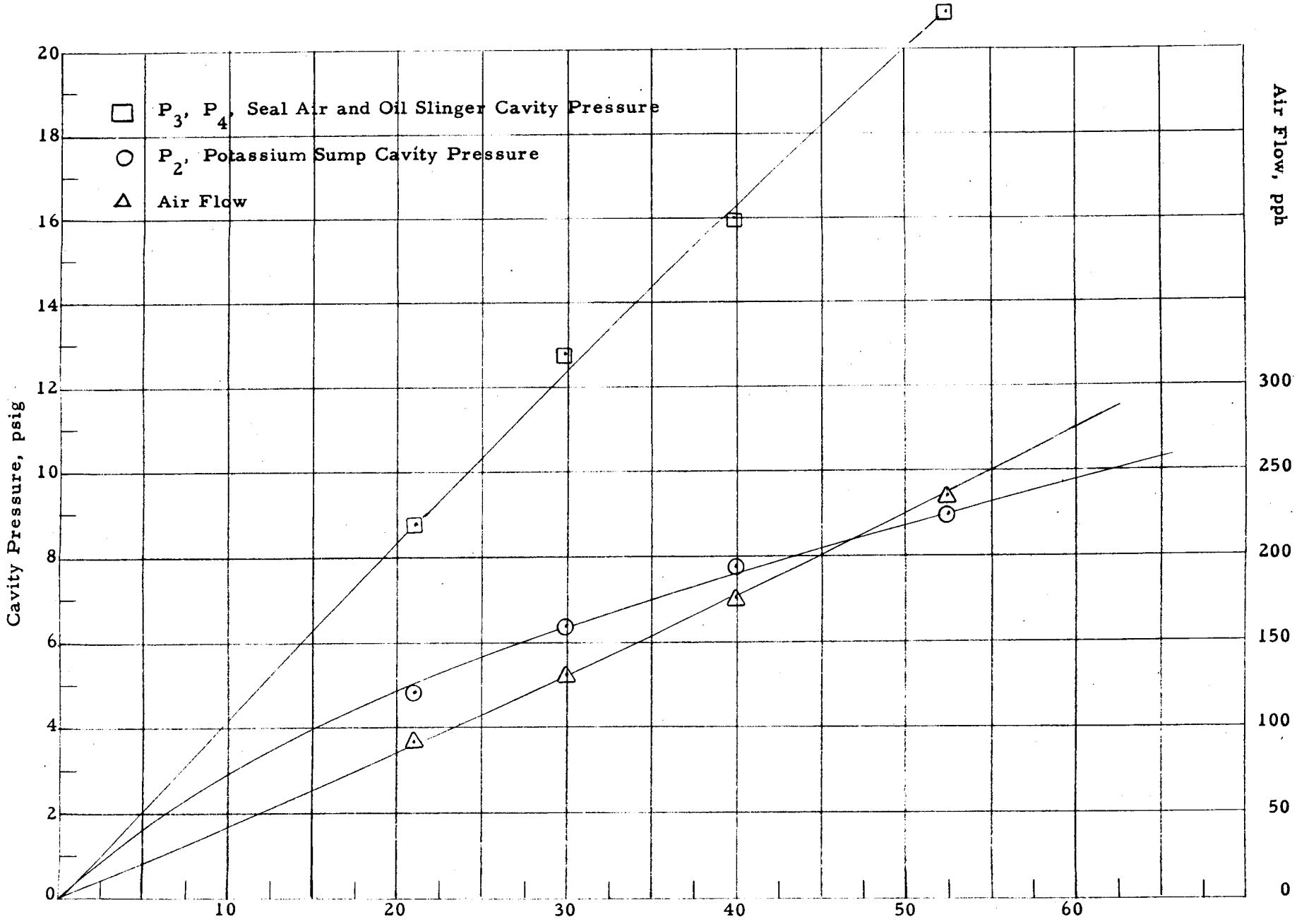

Figure 36. Turbine Seal Characteristics Showing Seal Cavity Pressure with Water Sump Outlet Manifold Pressure Relationship. Rotative Speed, 5000 rpm, Water Flow, 8.5 ppm.

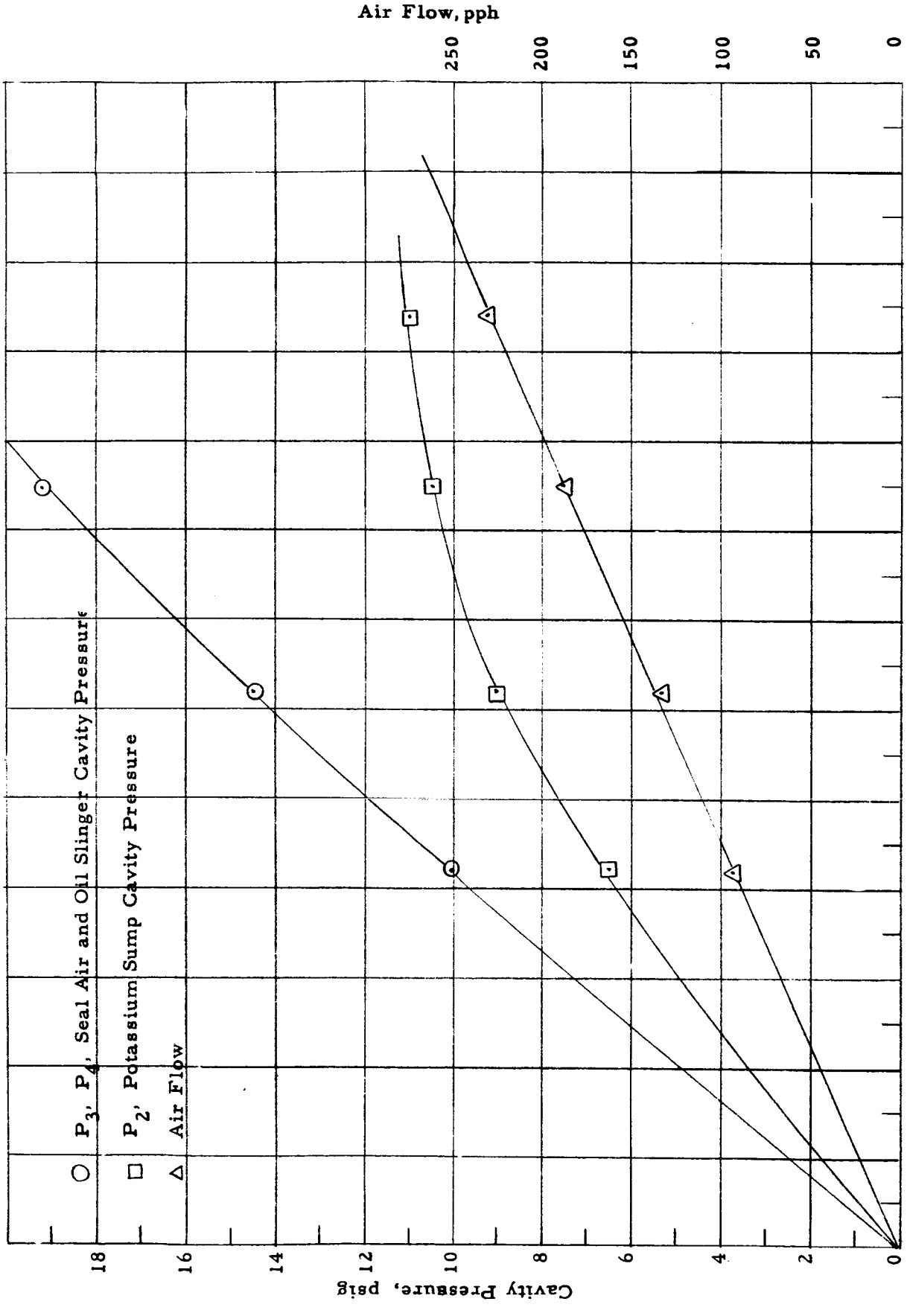

Figure 37. Turbine Seal Characteristics of the Seal Cavity Pressures and Water Sump Outlet Manifold. Rotative Speed, 5000 rpm, Water Flow, 13.5 PPM.

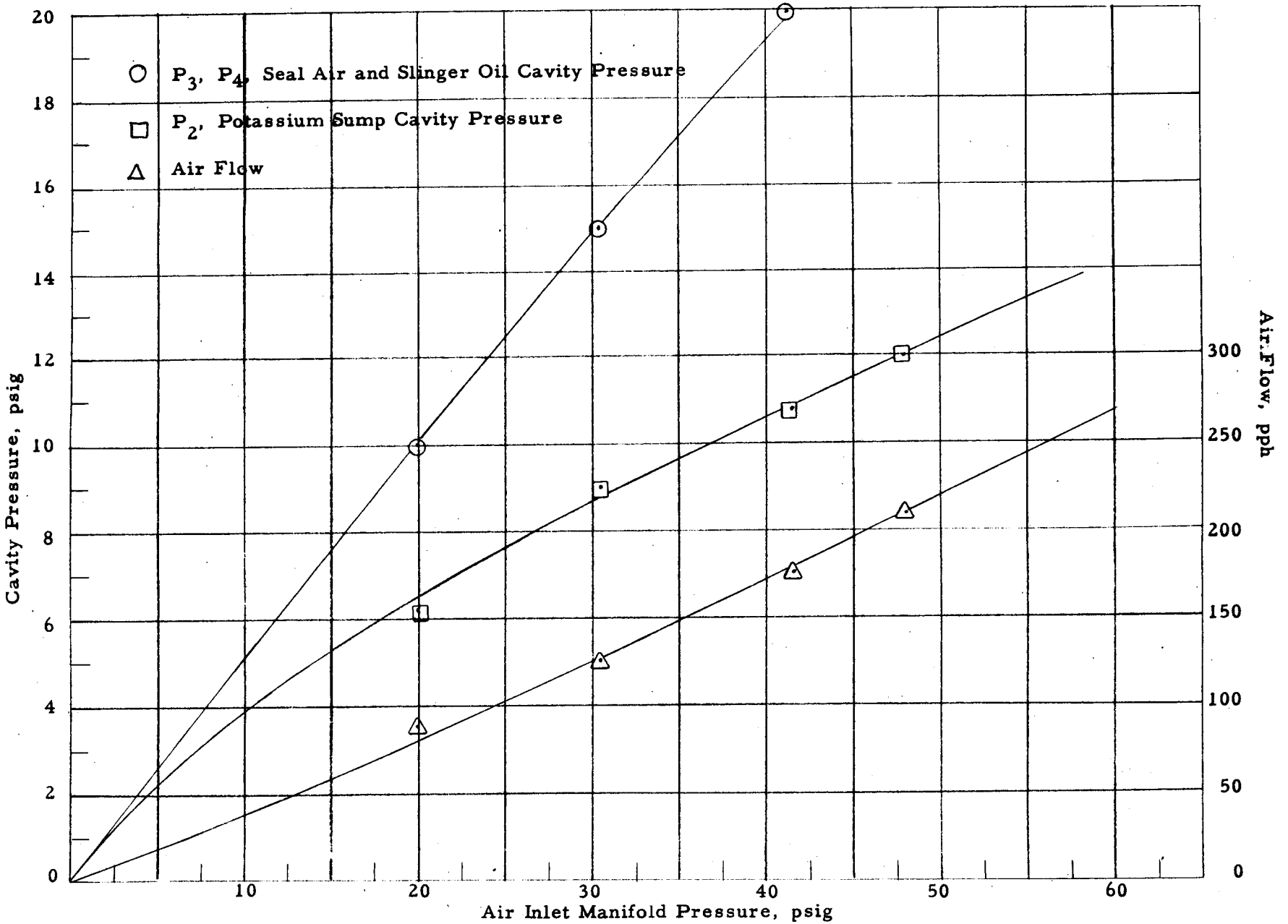

Figure 38. Turbine Seal Characteristics of the Seal Cavity and Water Sump Outlet Manifold Pressures. Rotative Speed, 5000 rpm, Water Flow, 16.2 ppm.

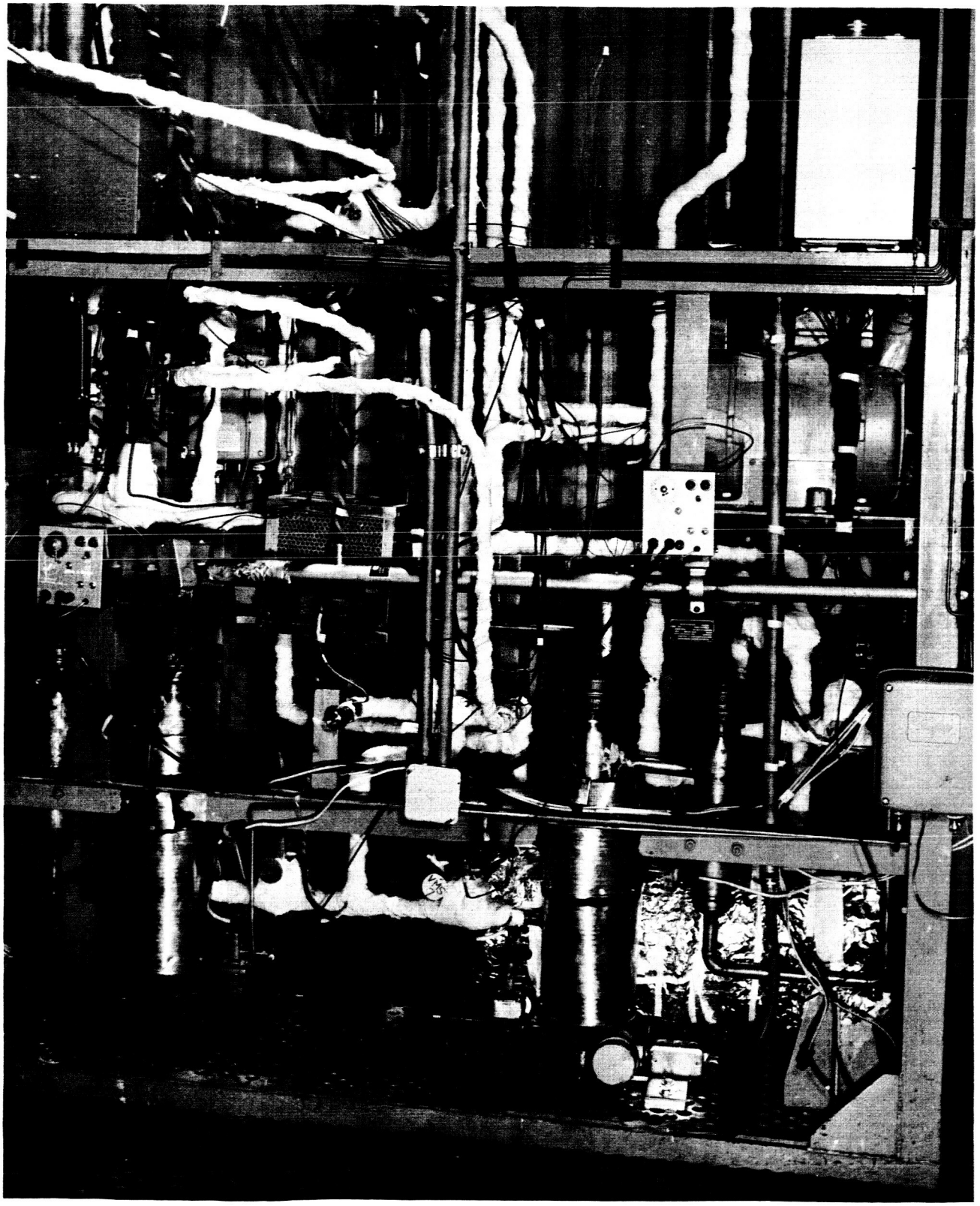

Figure 39. Hydrodynamic Seal Loop.

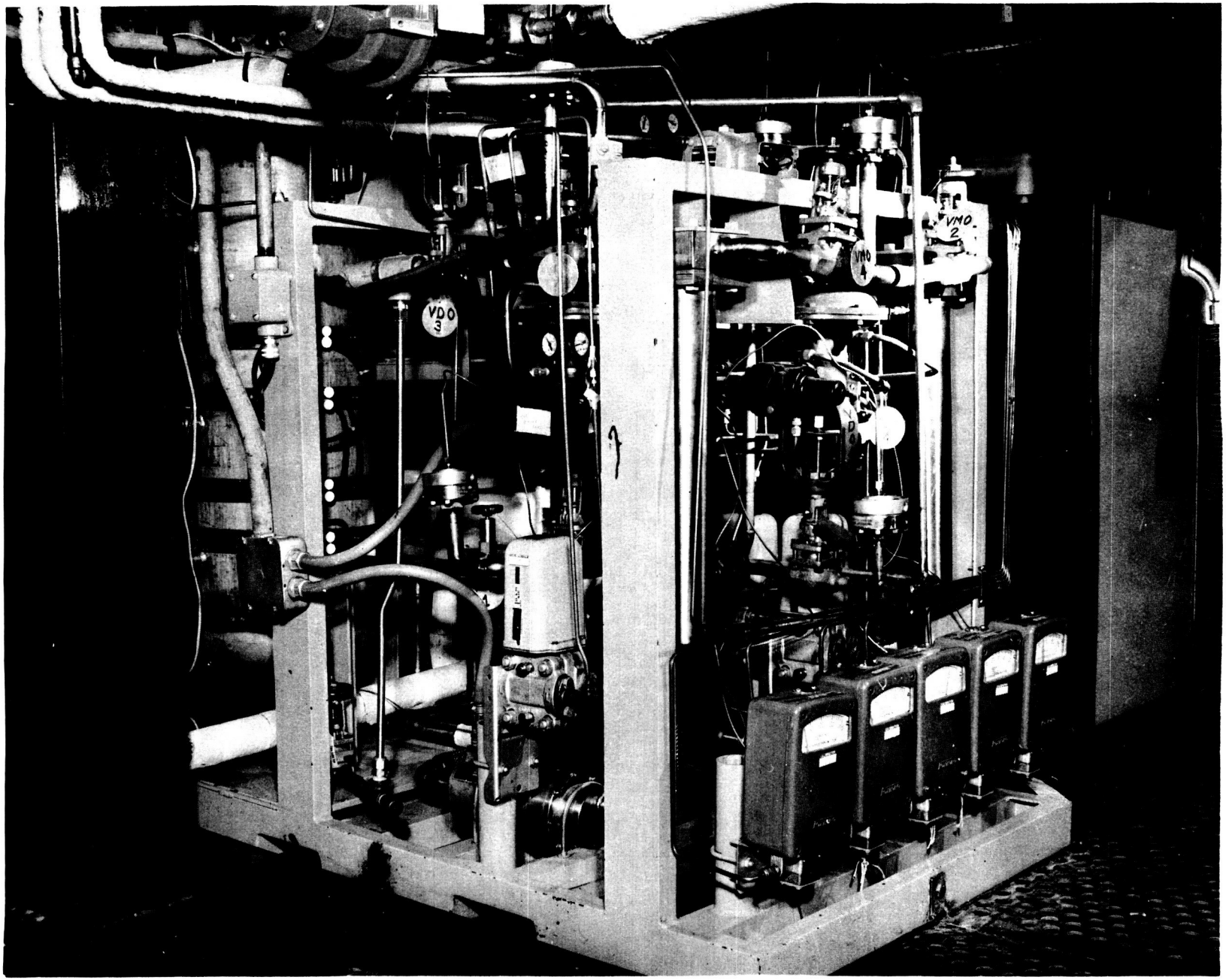

Figure 40. Potassium Turbine Main Lube System.

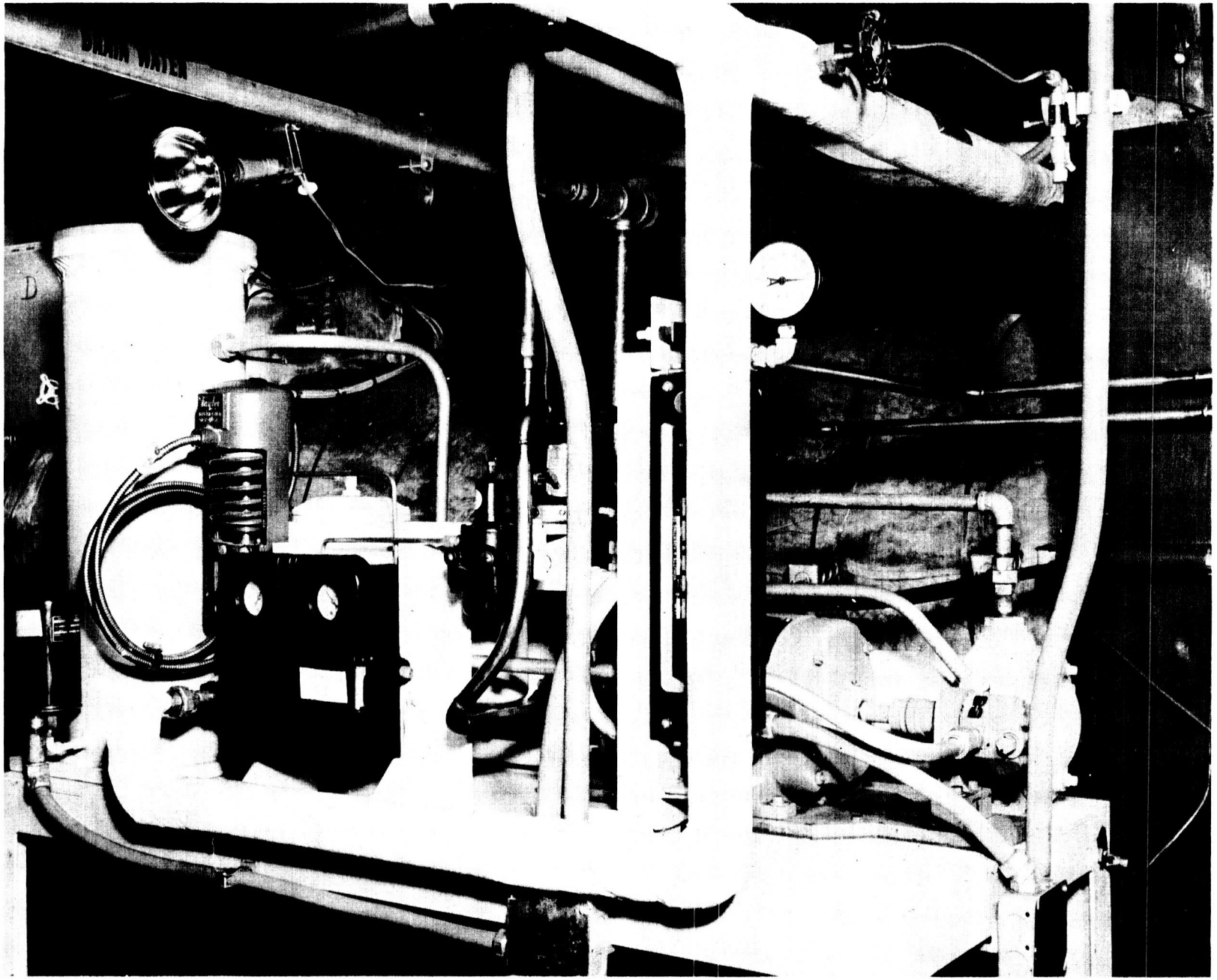

Figure 41. Starter Turbine and Water Brake Lube System.

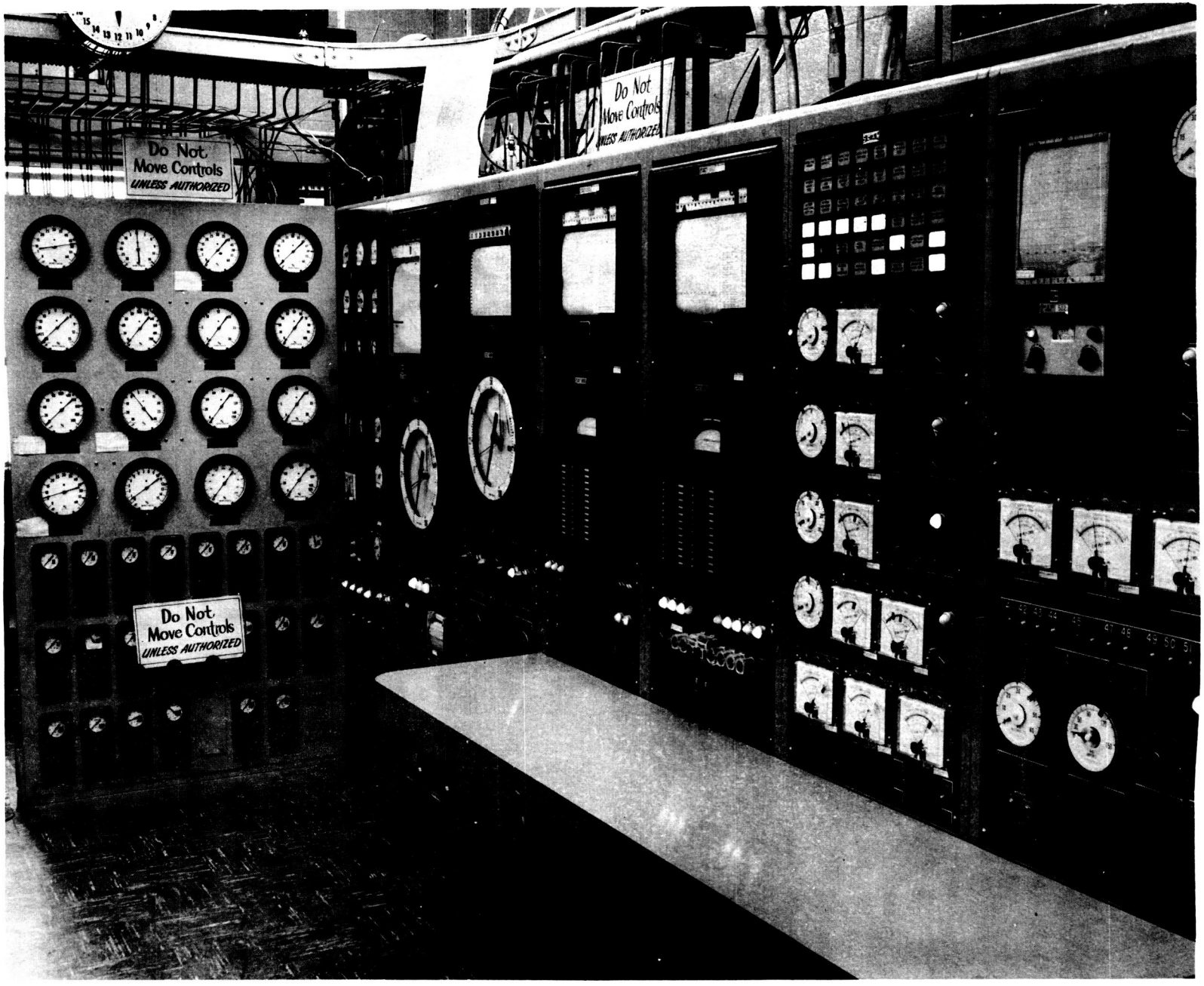

Figure 42. Control Panel

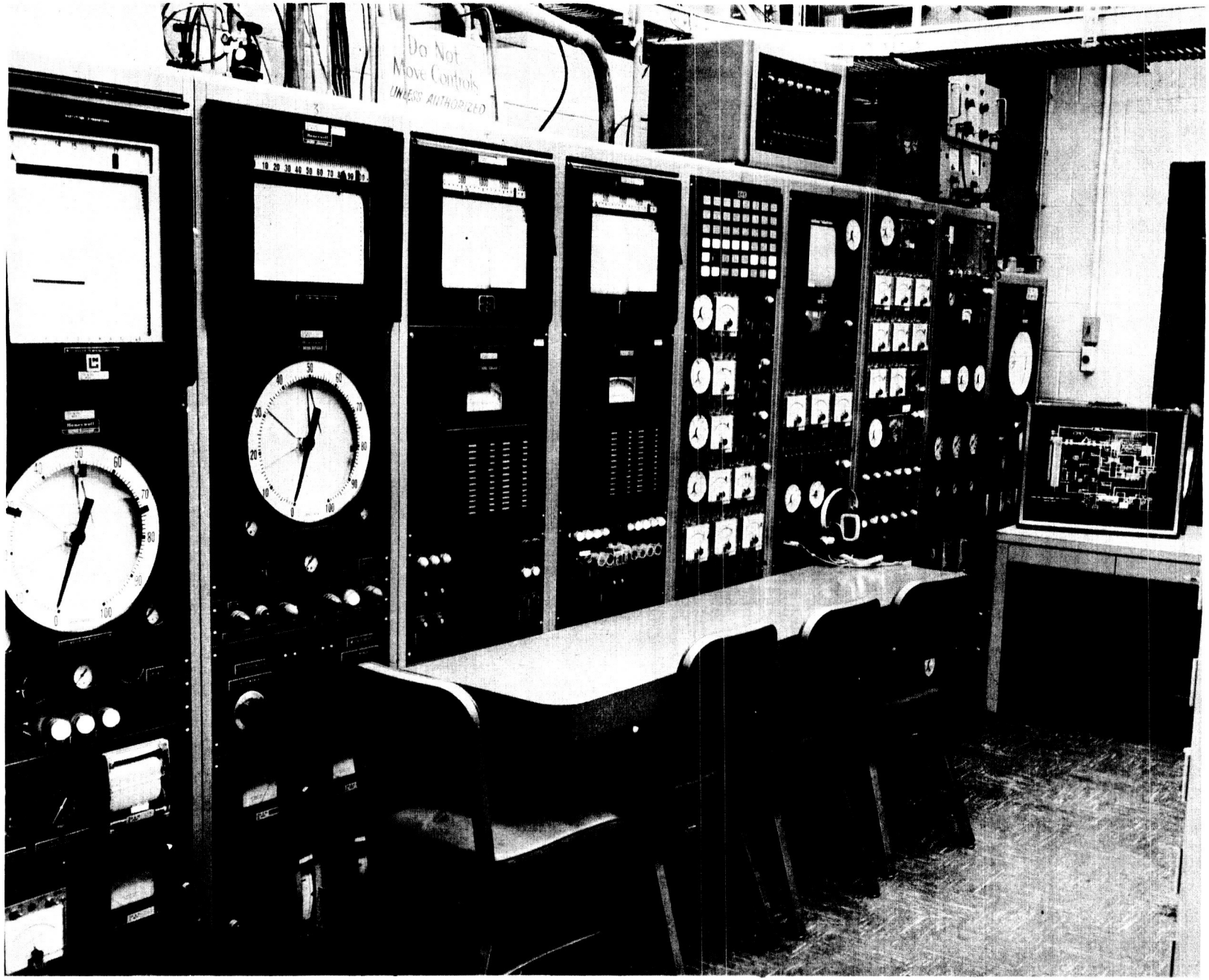

Figure 43. Control Panel

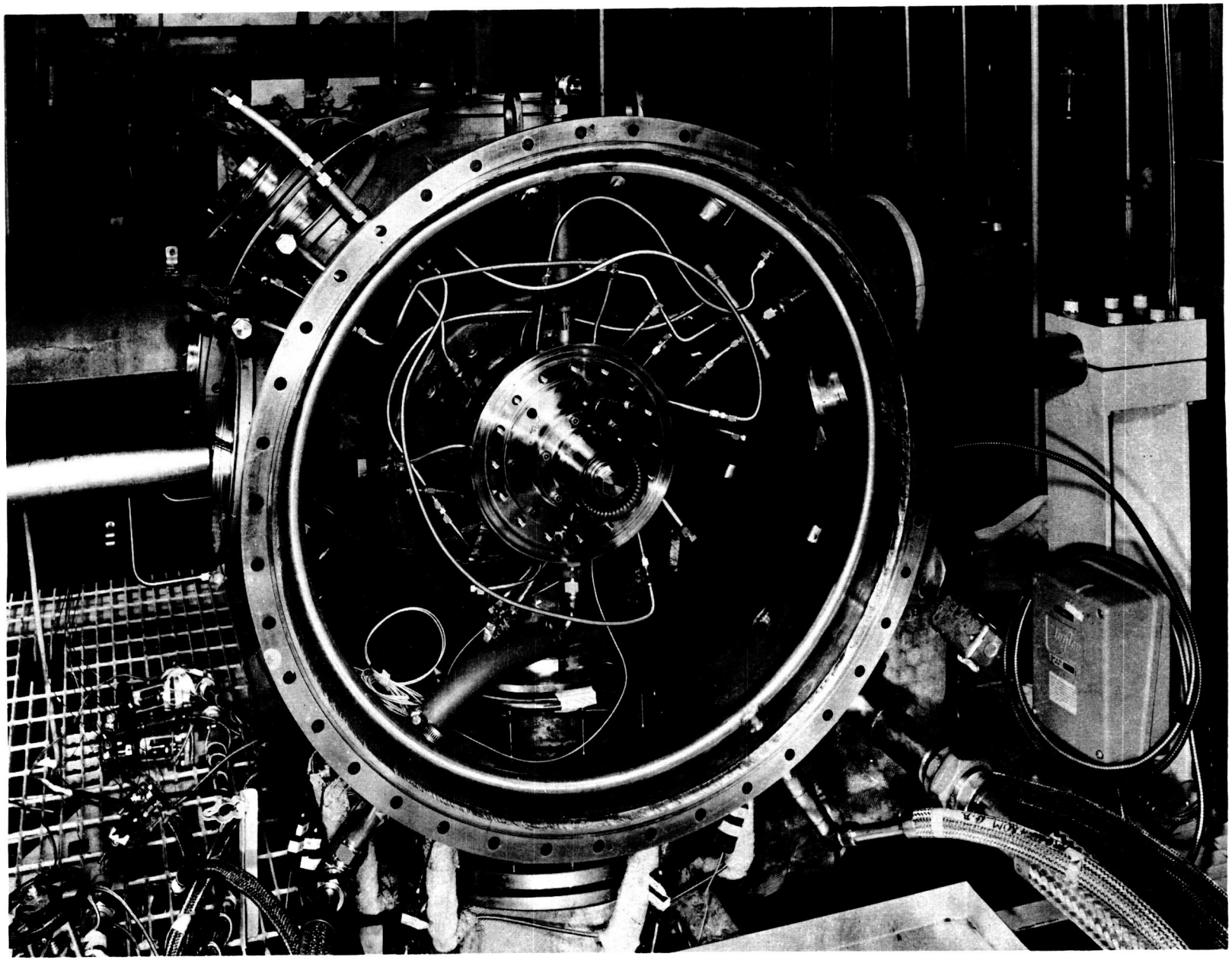

Figure 44. Turbine Installation

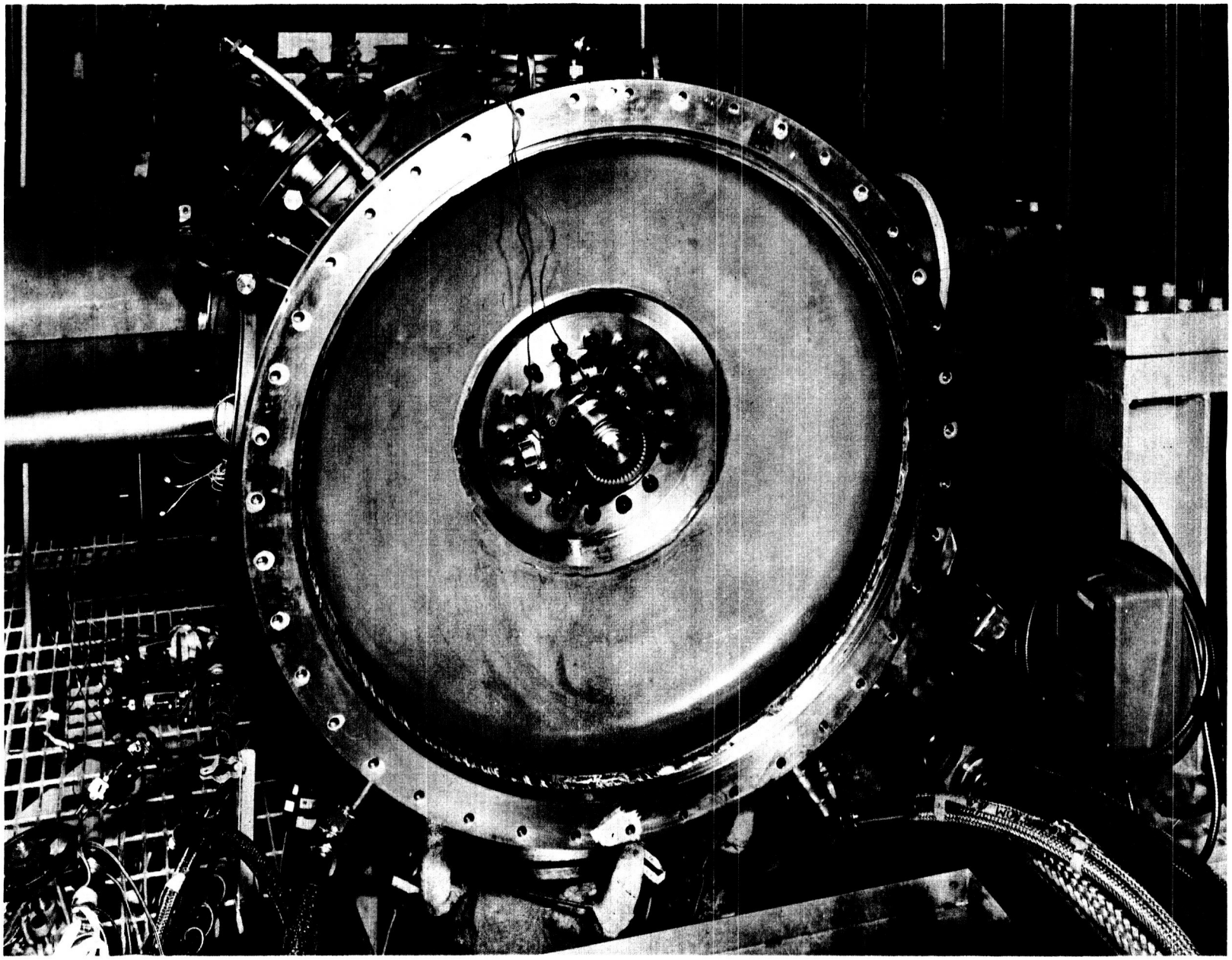

Figure 45. Dynamometer Equipment Assembly

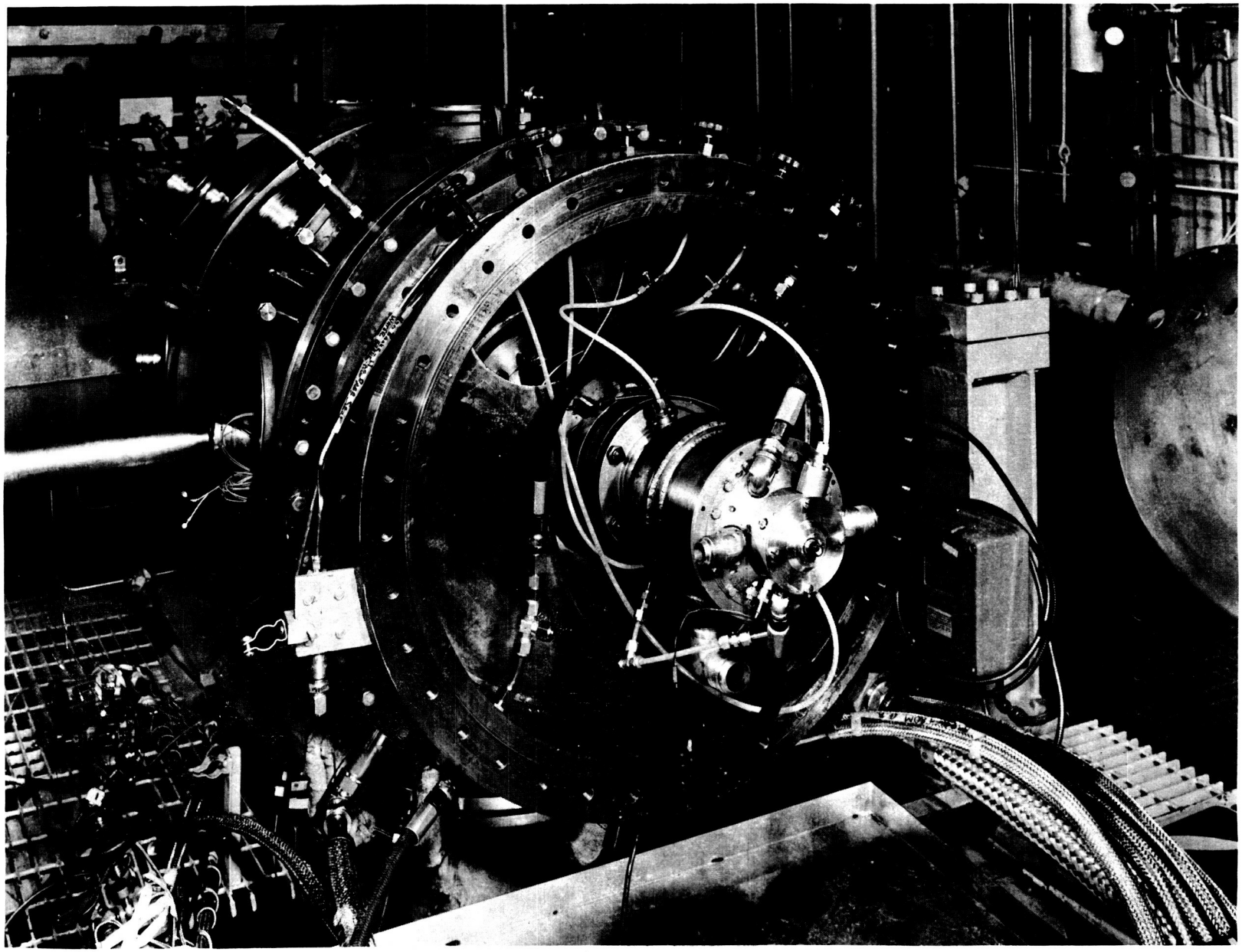

Figure 46. Dynamometer Equipment Assembly

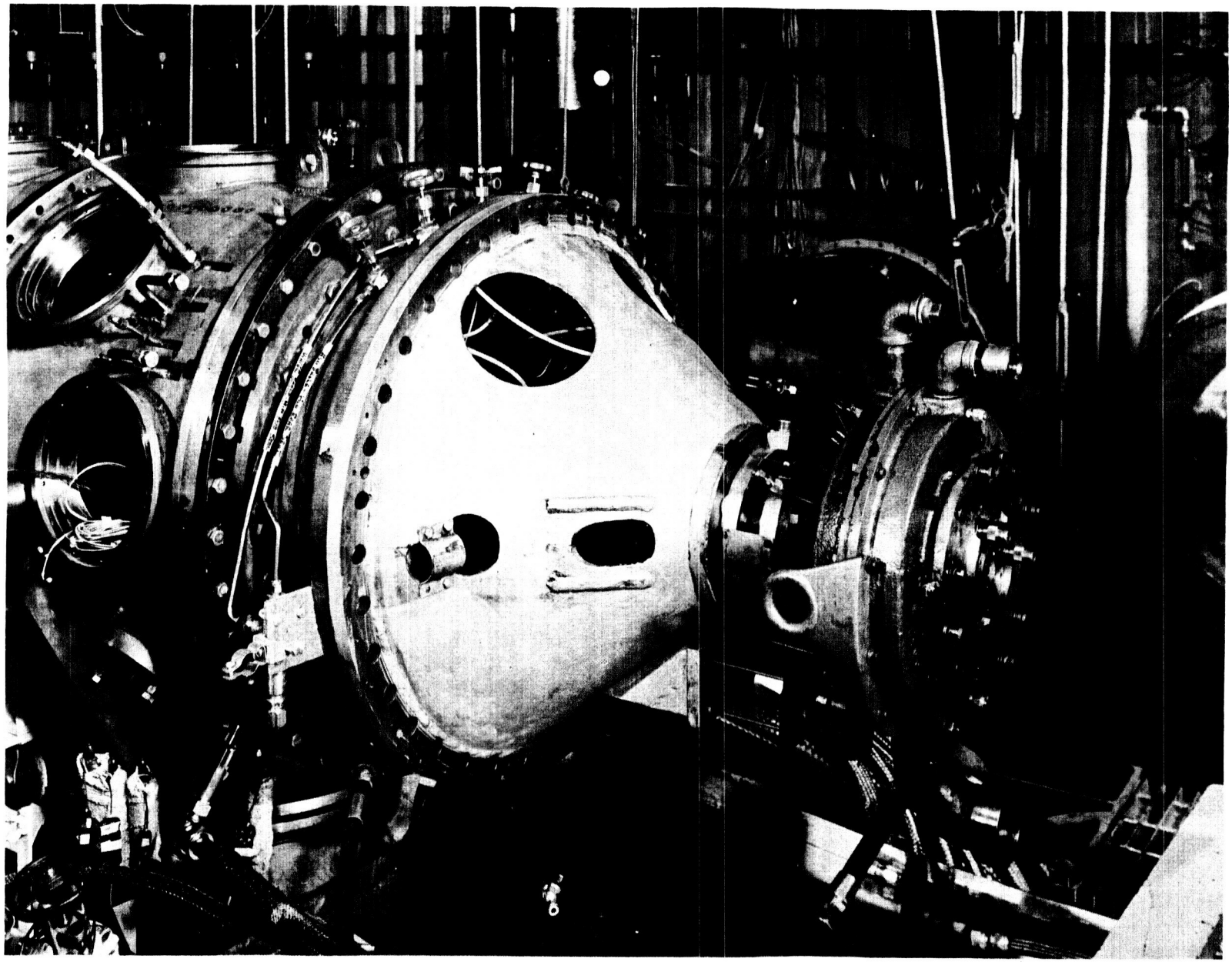

Figure 47. Dynamometer Equipment Assembly

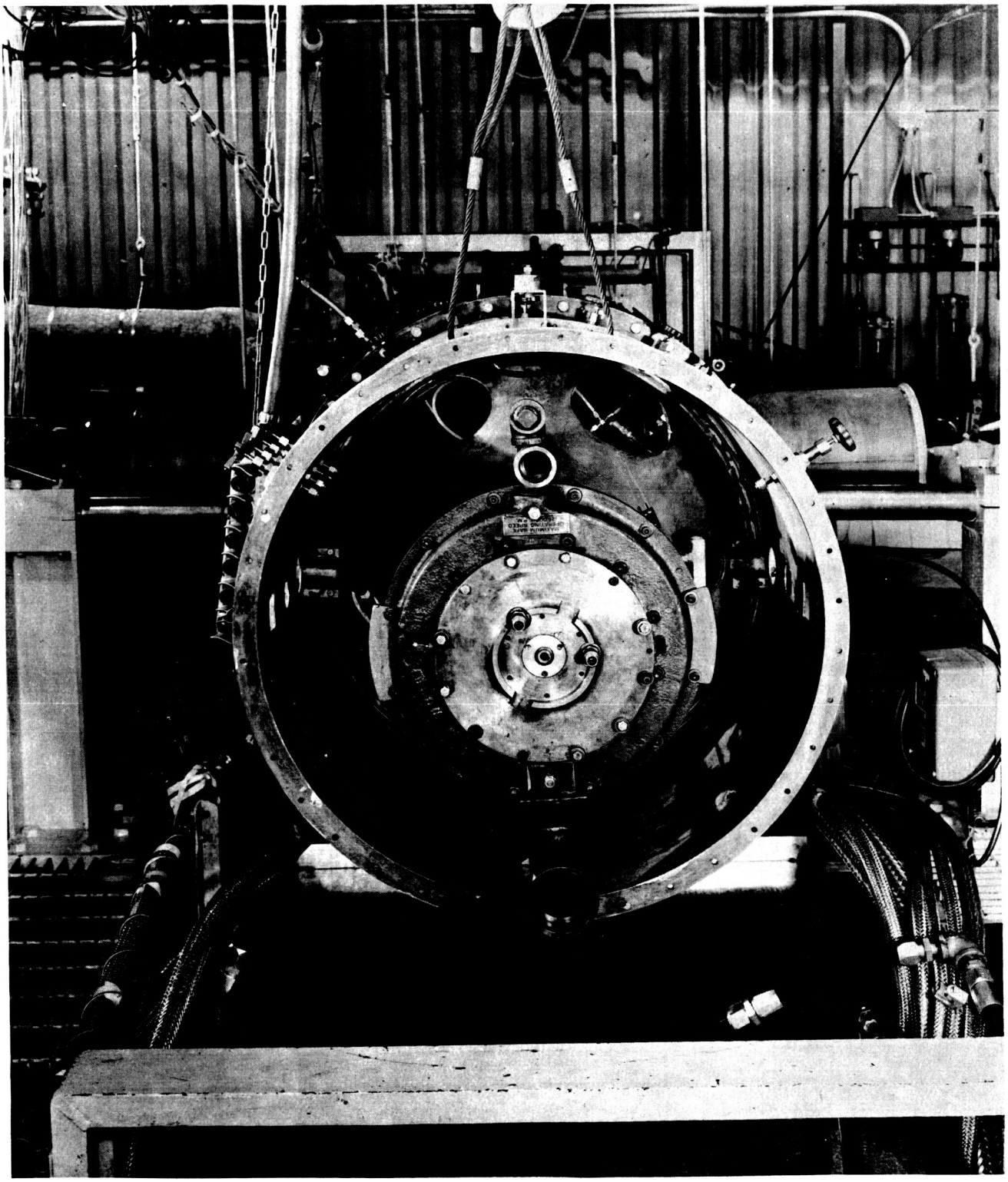

Figure 48. Dynamometer Equipment Assembly

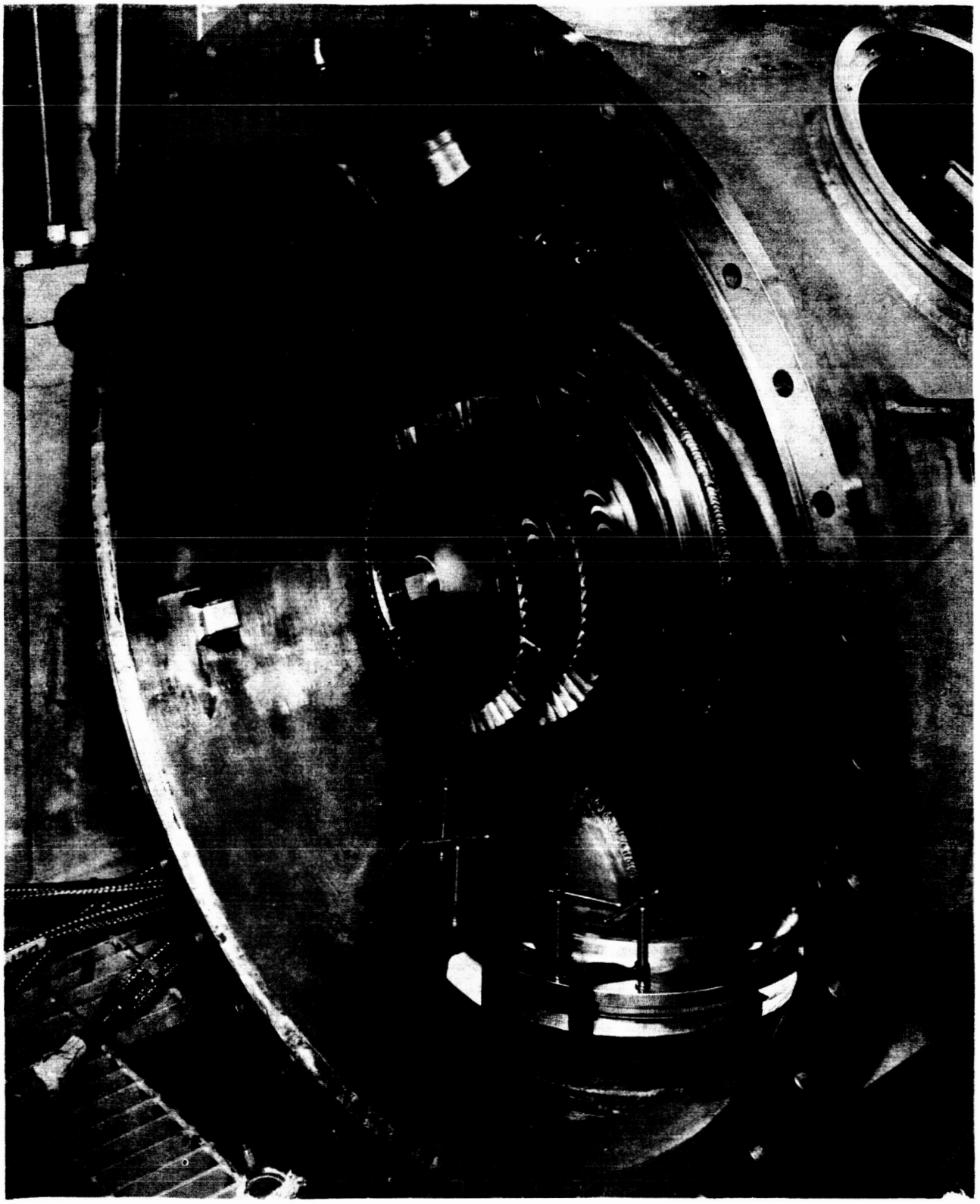

Figure 49. View of the Assembled First and Second Stage Rotor Buckets.

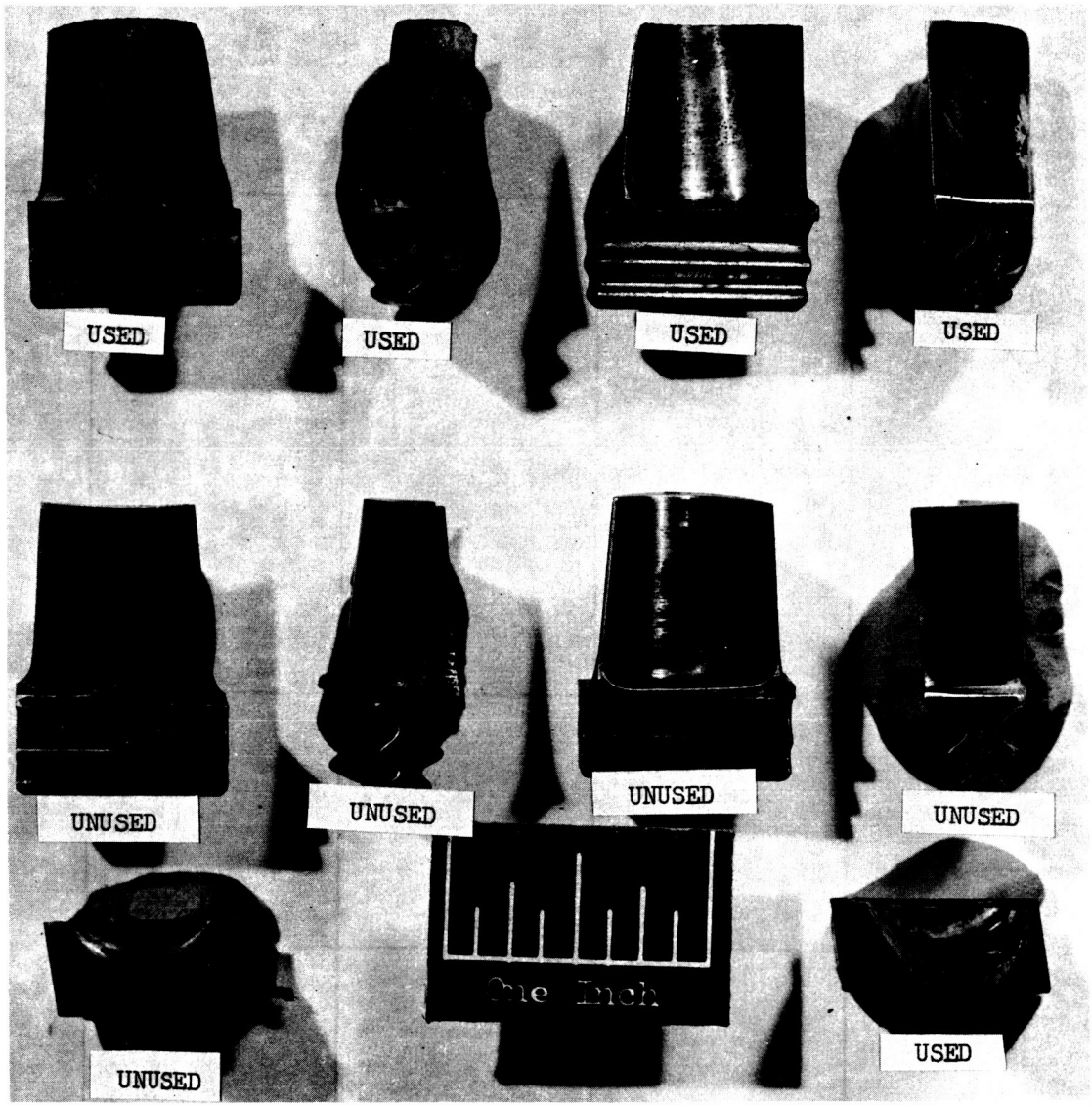

Figure 50. Cold Flow Stage 3 Turbine Buckets Compared to Unused Buckets to Show Surface Pitting and Other Damage.

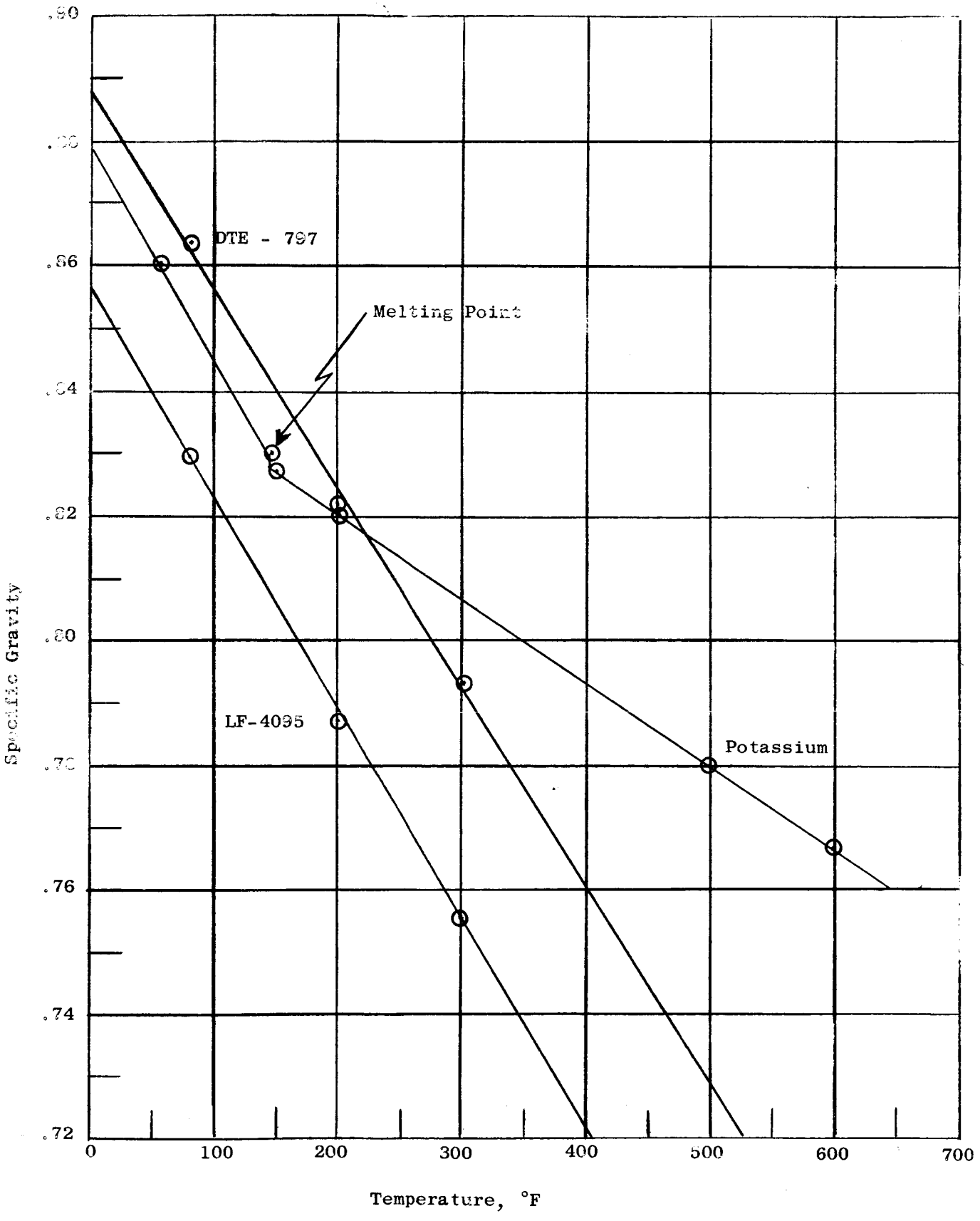

Figure 51. Comparison of the Specific Gravity of Lube Oil and Potassium as a Function of Temperature

APPENDIX A

Symbols

A^*	=	throat area, ft^2
a_{cr}	=	critical velocity of sound, fps
A_e	=	effective flow area, ft^2
C	=	constant defined by equation 22
Δh_{ideal}	=	turbine inlet to exit issentropic enthalpy drop, Btu/lb_m
Δh_{act}	=	actual turbine output work, Btu/lb_m
Δh_c	=	corrected specific work parameter, Btu/lb_m
Δh_d	=	enthalpy loss due to droplet drag, Btu/lb_m
Δh_1	=	turbine first stage work, Btu/lb_m
Δh_2	=	turbine second stage work, Btu/lb_m
EMFM	=	electromagnetic flow meter
g	=	gravitational constant, 32.174 ft/sec^2
γ	=	polytropic exponent determined from actual inlet conditions
γ_{ref}	=	polytropic exponent based on reference inlet conditions of 1600°F and 92 percent vapor quality
γ_s	=	BMI saturated vapor polytropic exponent
HP_c	=	corrected horsepower parameter, hp
h_1	=	station #1 enthalpy, Btu/lb_m
h_{fg1}	=	latent heat enthalpy based on P_{t1avg}, Btu/lb_m
h_{12}	=	liquid enthalpy based on liquid injection temperature, Btu/lb_m

h_{m3} = resulting mixture enthalpy after liquid injection, Btu/lb_m

h'_{s4} = ideal static enthalpy at first stage nozzle exit, Btu/lb_m

h'_{s5} = ideal static enthalpy at first stage rotor exit, Btu/lb_m

h'_{s6} = ideal static enthalpy at second stage nozzle exit, Btu/lb_m

h'_{s7} = turbine exit ideal static enthalpy, Btu/lb_m

h_{s11} = saturated liquid enthalpy based on P_{t1avg}, Btu/lb_m

h_{t5} = total enthalpy entering second stage nozzle, Btu/lb_m

h_{t7} = total enthalpy at turbine exit, Btu/lb_m

J = conversion, 778.2 ft-lb/Btu

KW_c = corrected kilowatt parameter, KW

η_t = turbine efficiency

N_c = corrected speed parameter, rpm

n = average polytropic exponent from inlet to throat

$\bar{n}$ = average polytropic exponent from inlet to throat to be calculated from equation 29

$\bar{N}$ = average turbine speed, rpm

P_s = static pressure, psia

P_t = inlet total pressure, psia

P_{t1avg} = average turbine inlet (station #1) total pressure, psia

$(P_s/P_t)_{12}$ = static to total pressure ratio at tap 12

$(P_s/P_t)_{th}$ = static to total pressure ratio at throat

$(P_s/P_t)_{13}$ = static to total pressure ratio at tap 13

Q_t = output torque, in-lb

RX_1 = turbine first stage hub reaction

RX_2 = turbine second stage hub reaction

T_t = inlet total temperature, ^{o}R

$\bar{T}$ = overall average torque, in-lb

$\bar{T}_t$ = tare loss torque, in-lb

$\bar{T}_m$ = average water brake torque, in-lb

$\bar{T}_s$ = average starter turbine torque, in-lb

U_{p1} = first stage rotor pitch line speed, fps

U_{p2} = second stage rotor pitch line speed, fps

v_t = turbine inlet total saturated specific volume, ft^3/lb_m

W = total nozzle flow, pps

W_c = corrected flow parameter, pps

W_{l2} = spray liquid flowmeter flow, pps

W_t = turbine flow, pps

W_{v1} = main flowmeter flow, pps

W_l = spray flow measured with spray EMFM, pps

W_v^* = critical vapor mass flow, pps

$\bar{W}_c$ = flow through inlet throttling calometer, pps

$\bar{W}_m$ = average main EMFM flow, pps

$\bar{W}_s$ = average spray EMFM flow, pps

X_{t3} = turbine inlet quality after liquid injection

X_1	=	turbine inlet vapor quality
X_2	=	turbine second stage inlet vapor quality
y	=	residual formed by subtracting the given reading from the average
z	=	number of readings